

Condition Monitoring in a Hydraulic System of an Industrial
Machine using Unscented Kalman Filter

by

Behnam Razavi

B.A.Sc., University of Saskatchewan, 2007

A THESIS SUBMITTED IN PARTIAL FULFILLMENT OF
THE REQUIREMENTS FOR THE DEGREE OF

MASTER OF APPLIED SCIENCE

in

THE FACULTY OF GRADUATE STUDIES

(Mechanical Engineering)

The University of British Columbia
(Vancouver)

September 2009

©Behnam Razavi, 2009

Abstract

The detection and isolation of faults in engineering systems is of great practical significance. The early detection of fault occurrence in a machine is critical in avoiding machine-performance degradation, and major damage to the machine itself. In the present thesis, the focus is to select and implement an appropriate modeling approach to detect and diagnose the possible faults in a complex hydraulic system of an industrial machine with on-line monitoring.

This work develops a model-based system for on-line condition monitoring of the hydraulic system of an industrial automated fish processing machine, using Unscented Kalman Filter (UKF). A requirement in implementing this technique is to develop an accurate mathematical model of the monitored system. First, a state-space model is developed and validated against simulated results. The state variables of the model are displacement and velocity of the spool valve, pressures of the two chambers of the hydraulic cylinder, and displacement and velocity of the hydraulic actuator. The unknown parameters of the state-space model are identified through direct measurement and experimentation. Results show that under normal operating conditions, the response of the machine satisfactorily matches that of the state-space model.

The developed UKF is implemented in the machine and four common hydraulic faults are artificially introduced. These faults are external leakage in the two chambers of the cylinder; internal leakage; and dry friction build up on the surface of the two moving plates (cutter carriage). Low, medium and high levels of leakage are introduced to the system. The criteria that are considered in fault diagnosing are residual moving average

of the errors, chamber pressures, and actuator characteristics. Experimental studies indicate that the developed scheme can correctly estimate the current state of the system in real time, with an acceptable residual of moving average error (MAE), thereby validating it.

Table of Contents

Abstract.....	ii
Table of Contents	iv
List of Tables	vi
List of Figures	vii
Acknowledgements	x
1 Chapter 1 Introduction.....	1
1.1 Preliminary Remarks.....	1
1.2 Motivation	4
1.3 Automated Industrial Fish Cutting Machine	6
1.4 Hydraulic Power System.....	9
1.5 Potential Faults in Hydraulic Systems	13
1.6 Research Objectives.....	17
1.7 Organization of the Thesis	18
2 Chapter 2 Experimental Set-up and Dynamic Modeling.....	20
2.1 Introduction	20
2.2 Experimental Set-up.....	21
2.3 Potential Faults Implementation	29
2.4 System Modeling	34
2.4.1 Governing Equations.....	34
2.4.2 State-Space Model	41
2.4.3 Model Validation	43
2.4.4 Experimental Results.....	44
2.4.5 Frequency Range.....	46
2.4.6 Repeatability of Experiments.....	49
3 Chapter 3 Implementation of UKF in Fault Monitoring Scheme.....	50
3.1 Introduction	50
3.2 General Techniques of Fault Monitoring.....	51
3.2.1 Model-based Fault Diagnosis Approach	52
3.2.1.1 Quantitative Approach.....	52
3.2.1.2 Qualitative Approach.....	54
3.2.2 Signal-based Fault Diagnosis Approach	55
3.3 Kalman Filtering in Fault Diagnosis.....	58
3.3.1 Fundamentals of Kalman Filter	58
3.3.2 Extended Kalman Filter.....	62
3.4 Unscented Kalman Filter.....	64
3.4.1 Unscented Transformation.....	64
3.4.2 Performance Comparison between UT and EKF.....	66

3.4.3	Unscented Kalman Filter (UKF) Algorithm.....	68
3.5	UKF Application in Hydraulic System.....	72
3.5.1	Discretised Dynamic Model	72
3.5.2	Matrix Specification.....	73
4	Chapter 4 UKF and Fault Monitoring in Hydraulic Systems.....	77
4.1	Introduction	77
4.2	Experimental Results	78
4.2.1	Actuator Leakage Faults.....	79
4.2.1.1	Actuator External Leakage at Chamber 1.....	80
4.2.1.2	Actuator External Leakage at Chamber 2.....	83
4.2.1.3	Actuator Internal Leakage	87
4.2.1.4	Dry Friction of the Cutter Table.....	91
4.3	Fault Diagnosis and Discussion.....	93
5	Chapter 5 Conclusion	99
5.1	Summary	99
5.2	Suggestions for Future Work.....	102
	References.....	104

List of Tables

Table 2.1: Dynamic Parameters of the Hydraulic System.....	41
Table 3.1: The MAE Value of the Three Measured States	74
Table 4.1: Severity Categorization of the Leakage Faults.....	79
Table 4.2: External Leakage at Chamber 1 and the Change in MAEs.....	83
Table 4.3: External Leakage at Chamber 2 and the Change in MAEs.....	86
Table 4.4: Internal Leakage and the Change in MAEs	90
Table 4.5: Dry Friction Build-up and the Change in MAEs.....	93
Table 4.6: Summary of the Increase in MAEs due to Fault Occurrence.....	94

List of Figures

Figure 1.1: Schematic Drawing of the “Iron Butcher” Machine	7
Figure 1.2: The Hydraulic-Actuation Positioning System in One Axis.....	8
Figure 1.3: Pneumatic Cutter System.....	9
Figure 1.4: General Failure Rate of Common Hydraulic Elements.....	15
Figure 2.1: Schematic Diagram of the Basic Planar Manipulator	22
Figure 2.2 : Diagram of Monitoring Components	23
Figure 2.3: Control System Block Diagram	23
Figure 2.4: Waveguide Interaction.....	29
Figure 2.5: Schematic Diagram of the Potential Faults in the Hydraulic Actuator	30
Figure 2.6: Experimental Hydraulic Setup with Working Sensors.....	31
Figure 2.7: System Characteristics – (a) Actuator Reference Signal, (b) Actuator Displacement, (c) Pressure in Chamber 1, (d) Pressure in Chamber 2	33
Figure 2.8: Slip Friction Experimental Result	40
Figure 2.9: (a) Characteristic Plots for Simulated versus Measured Pressure in Chamber 1, (b) Plot of MAE between Simulated and Measured Pressures	45
Figure 2.10: (a) Characteristic Plots for Simulated versus Measured Pressure in Chamber 2, (b) Plot of MAE between Simulated and Measured Pressures	45
Figure 2.11: (a) Characteristic Plots of Actuator Displacement- Simulated and Measured Results, (b) Plot of MAE between Simulated and Measured Results.....	46
Figure 2.12: Error in Chamber 1 Pressure between Measured and Simulated Signals....	47
Figure 2.13: Error in Chamber 2 Pressure between Measured and Simulated Signals.....	47

Figure 2.14: Error in Displacement between Measured and Simulated Signals.....	48
Figure 2.15: Pressure Repeatability Data for Chamber 1	49
Figure 3.1: Block Diagram of Working Kalman Filter [4].....	62
Figure 3.2: Unscented Transformation Scheme.....	65
Figure 3.3: Comparison between UT and EKF	67
Figure 3.4: Schematic Block Diagram of UKF	71
Figure 3.5: System Estimation Error for (a) Pressure in Chamber 1, (b) Pressure in Chamber 2, (c) Actuator Position.....	76
Figure 4.1: Actuator Displacement with Moderate External Leakage at Chamber 1	80
Figure 4.2: Residual Error for Low Leakage at Chamber 1; (a) Actuator Displacement (b) Pressure in Chamber 1; (c) Pressure in Chamber 2.....	81
Figure 4.3:Residual Error for Moderate Leakage at Chamber 1; (a) Actuator Displacement (b) Pressure in Chamber 1; (c) Pressure in Chamber 2	82
Figure 4.4: Residual Error for High Leakage at Chamber 1; (a) Actuator Displacement (b) Pressure in Chamber 1; (c) Pressure in Chamber 2.....	82
Figure 4.5: Actuator Displacement with Moderate External Leakage at Chamber 2	84
Figure 4.6: Residual Error for Low Leakage at Chamber 2; (a) Actuator Displacement (b) Pressure in Chamber 1; (c) Pressure in Chamber 2.....	85
Figure 4.7: Residual Error for Moderate Level Leakage at Chamber 2; (a) Actuator Displacement (b) Pressure in Chamber 1; (c) Pressure in Chamber 2	85
Figure 4.8: Residual Error for High Leakage at Chamber 2; (a) Actuator Displacement (b) Pressure in Chamber 1; (c) Pressure in Chamber 2.....	86
Figure 4.9: Actuator Displacement with Moderate Internal Leakage	88

Figure 4.10: Residual Error for Low Internal Leakage; (a) Actuator Displacement (b) Pressure in Chamber 1; (c) Pressure in Chamber 2..... 89

Figure 4.11: Residual Error for Moderate Internal Leakage; (a) Actuator Displacement (b) Pressure in Chamber 1; (c) Pressure in Chamber 2 89

Figure 4.12: Residual Error for High Internal Leakage; (a) Actuator Displacement (b) Pressure in Chamber 1; (c) Pressure in Chamber 2..... 90

Figure 4.13: Actuator Displacement with Dry Friction Build-up..... 92

Figure 4.14: Residual Error for Dry Friction Build-up; (a) Actuator Displacement (b) Pressure in Chamber 1; (c) Pressure in Chamber 2..... 92

Figure 4.15: Chambers Pressure Characteristics under High Internal Leakage; a) Pressure in Chamber 1, and b) Pressure in Chamber 2 97

Figure 4.16: Chambers Pressure Characteristics under Dry Friction; a) Pressure in Chamber 1, and b) Pressure in Chamber 2 97

Figure 4.17: Zoomed-in Chamber Pressure Characteristics Plot under Dry Friction; a) Pressure in Chamber 1, and b) Pressure in Chamber 2 98

Acknowledgements

This research project would not have been possible without the support of many people.

First and foremost, I offer my sincerest gratitude to my supervisor, Professor Clarence W. de Silva, who has supported me throughout my thesis with his patience and knowledge as well as his encouragement, guidance, unconditional help and effort. As well, the financial support provided by him in the form of a Research Assistantship and also the necessary equipment and resources for carrying out my research, which is primarily of experimental nature, is greatly appreciated.

Special thank goes to all my colleagues at Industrial Automation Laboratory (IAL) for their friendship and invaluable assistance in the last two years, notably Ramon, Guan-Lu, Srini, Gamini, Tahir, Arun, Ying, and Roland. A very special thanks goes to my very good friends: Mohammad Sepasi and Ehsan Azadi for their assistance and input throughout the completion of this work. Additionally, I would like to thank Dr. Farbod Khoshnoud and Dr. Lalith Gamage, who are research affiliates of our lab, for their helpful instructions and advice.

I would also like to acknowledge the sources of financial support for this research, namely: Tier 1 Canada Research Chair (CRC), Canada Foundation for Innovation (CFI), British Columbia Knowledge Development Fund (BCKDF), and the Discovery Grant of the Natural Sciences and Engineering Research Council (NSERC) of Canada.

I cannot end without thanking my family, on whose constant encouragement and love I have relied throughout my time finishing the work. A special gratitude goes to my father who is the source of my motivation and inspiration and my mother who is the source of

all greatness. Finally I would like to thank my brother and sisters; Behrad and Behnaz, for their everyday supportive call, and my late sister, Bahareh, whose thought will always be in my mind.

Chapter 1

Introduction

1.1 Preliminary Remarks

Hydraulic actuator systems are used in industrial machines and tools, which use fluid power to carry out mechanical tasks. Heavy equipment is a common example category. In this type of machinery, high pressure hydraulic fluid is transmitted throughout the machine to various hydraulic motors and hydraulic cylinders. The fluid may be controlled manually or automatically by control valves and distributed through hoses and tubes. The popularity of hydraulic machinery may be attributed to the high levels of power that can be transferred through small tubes and flexible hoses, the high power density, low risk of hazards (compared to potential electric fire), and the ability of multiple and small-size actuators that can make use of a common power source. The hydraulic fluid must flow into the actuator or hydraulic motor in a controlled manner and then return to a reservoir. The fluid is then filtered, pressurized through a pump, and used again. Corresponding to the path taken by the hydraulic fluid there is a hydraulic circuit, analogous to an electric circuit through which current flows, of which there are several types. Open center circuits use pumps which supply a continuous flow. The flow is returned to the reservoir tank through the open center of the control valve; that is, when the control valve is centered, it provides an open return path to the tank and the fluid is not pumped to a high pressure. On the other hand, if the control valve is actuated, it

routes fluid to and from the actuator and the tank. The fluid pressure will increase to meet any resistance, since the pump has a constant output. If the pressure rises too high, the fluid returns to the tank through a pressure relief valve. Multiple control valves may be stacked in series. This type of circuit can use inexpensive, constant-displacement pumps. Closed center circuits supply full pressure to the control valves, regardless of whether any valves are actuated or not. The pumps vary their flow rate, pumping very little hydraulic fluid until the operator actuates a valve. The valve spool therefore does not need an open center return path to the tank. Multiple valves can be connected in a parallel where the system pressure is equal for all valves.

The increasing amount of power available to man that requires control and the high demand of modern control systems have focused attention on the theory, design and application of control systems. Hydraulics, the science of liquid flow, is an old engineering discipline which has commanded new interest in recent years, especially in the area of hydraulic control. There are many unique features of hydraulic systems compared to other type of systems. As mentioned in [1] and [7], some of the relatively important advantages of such systems are as follows:

1. Heat generated by internal losses is a basic limitation of any machine.
Lubricants deteriorate, mechanical parts seize, and insulation breaks down as the temperature increases. Hydraulic components are superior to others in this respect since the fluid carries away the heat generated to a convenient heat exchanger. This feature permits smaller and lighter components.
2. Hydraulic fluid also acts as a lubricant thereby prolonging the component life.

3. There is no phenomenon in hydraulic components comparable to the saturation and losses in magnetic materials of electrical machines. The torque developed by an electric motor is proportional to the current and is limited by magnetic saturation. The torque developed by hydraulic actuators (i.e., motor and pistons) is proportional to pressure difference and is limited only by safe stress levels. Therefore, hydraulic actuators are able to generate relatively large torques for comparatively small devices.
4. Hydraulic actuators have a higher speed of response enabling fast starts, stops and speed reversals. Also Torque to inertia ratios is large with resulting high acceleration capability.
5. Hydraulic systems have long operating lives even if employed in harsh environments.
6. Open and closed loop control of hydraulic actuators is relatively simple using valves and pumps.
7. The same fluid power source may be employed with distributed multiple actuator elements of low size (again with high power density).
8. Concerns of electric hazards (compared to arcing in electric motors) are minimal.

Although, there are a number of these advantages associated with hydraulic power systems, as mention in [1] and [7], there exist several disadvantages which tend to limit their use. They are as listed below:

1. Hydraulic power is not as readily available as the electrical power.
2. Small allowable tolerances results in high costs of hydraulic components.

3. The hydraulic fluid imposes an upper temperature limit.
4. Hydraulic systems can become messy because it is difficult to maintain a system free from leaks and there is always the possibility of complete loss of fluid if a rupture in the system occurs.
5. Hydraulic systems are nonlinear.
6. They can be more expensive than comparable electric actuators.
7. Hydraulic power systems can be more noisy than electric actuators.

As mentioned, despite of the hydraulic systems pros and cons compared to other power sources, hydraulic systems have many unique features. In particular they are more compact and can supply high levels of power, which can greatly improves the performance of a machine. In addition, hydraulic actuator systems are unavoidable for jobs requiring high levels of power for mobilization. They can be found in many mobile, airborne and stationary applications. Due to the mentioned reasons, there has been an extensive research activity in this area [2].

1.2 Motivation

The detection and isolation of faults and malfunctions in engineering systems is of great practical significance. These systems encompass a variety of machinery including:

1. Industrial production facilities; e.g., power plants, chemical plants, and oil refineries
2. Transportation vehicles; e.g., ships, automobiles, and airplanes,
3. Household appliances; e.g., air conditioning equipment, refrigerators, and washing machines.

The early detection of fault occurrence is critical in avoiding product deterioration, performance degradation, major damage to the machinery itself, and damage to human health or even loss of life. The quick and correct diagnosis of the faulty component facilitates the decisions on corrective actions or repairs.

As stated in [3], the traditional approaches to fault detection and diagnosis involve the limit checking of some variables or the application of redundant sensors. More advanced methods rely on the spectral analysis of signals measured from the machinery or on the comparison of the actual plant behavior to what is expected under normal operating conditions, typically based on a mathematical model. The latter approach includes methods which are more deterministic, such as observers, and those formulated more on a statistical basis, such as Kalman filter and parameter estimation.

The development of approaches for fault detection and diagnosis in automated systems such as hydraulic machinery has been an important focus area of researchers in engineering. A successful performance of real-time fault detection and diagnosis in large and complex hydraulic systems is seldom achieved and reported. The lack of an effective method for handling temporal data is seen as one of the key problem in this area [4]. Thus the main objective of the present thesis is to develop, implement, and study a suitable model-based approach for detection and diagnosis of possible faults in a complex hydraulic system. Real time application with on-line system monitoring is treated. The industrial hydraulic manipulator chosen in the present research for experimental investigation of fault detection and isolation (FDI) is a planar electro- hydraulic actuation system which is an integral part of an automated industrial fish processing machine.

1.3 Automated Industrial Fish Cutting Machine

The traditional "Iron Butcher," which is commonly used in the fish-processing industry for head cutting of fish, is known to be somewhat inefficient and wasteful, and the resulting product quality may be unacceptable for high-end markets. Fish processing involves head removal/cutting of fish at the position of the collarbone, with the objective of optimizing the quality and yield of the product. The challenges include, accurate positioning of cutter blades and smooth cutting of fish. The assessment of the quality of processed fish is dependent on the skillful but subjective evaluation by experienced plant operators. In recent years, the fish processing machine has been automated with respect to the machine operation, quality control, and on-line monitoring of the state of the machine. Some of the components of the automated Iron Butcher, which is available in our laboratory, are as follows:

1. Hydraulic actuators for cutter positioning
2. Pneumatic actuator for fish cutting
3. Various electronic sensors (accelerometers, position sensors, pressure sensors, etc.)
4. Fish conveyor with the associated transmission, drive system, and induction motor

The main purpose of this machine is to automate the fish cutting process and also to reduce the meat wastage by guiding the cutter to the optimum location for cutting. As shown in Figure 1.1, first the fish is placed on the conveyer system, which moves the fish into the cutting zone. A camera takes an image of the fish, and by processing the image, the control computer identifies the location of the gill and the best location for the cut.

This information is then sent to the controllers of the two axes of the positioning system. On receiving these drive commands at the servo valves the operation of the hydraulic manipulator begins, thereby positioning the carriage of the cutting blade to the desired coordinates. The cutting table (cutter carriage) is simply a Cartesian feed system empowered by two hydraulic actuators which can move independently in orthogonal X and Y directions. Once the table is accurately positioned, a pneumatic cutter with axial vertical motion, which gets its power from an air compressor, performs the cut. After the separation, the head slides down the ramp and the rest of the body exits the machine from the end of conveyor for further processing. A second camera obtains an image of the processed fish for further analysis to determine the cutting quality.

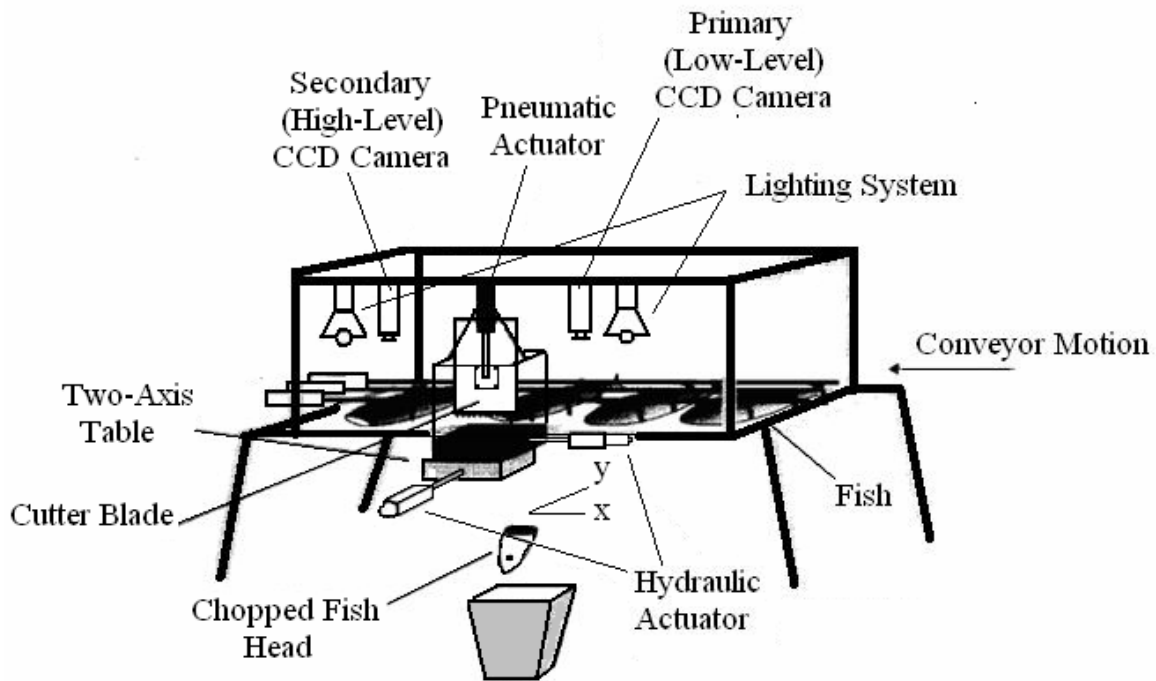


Figure 1.1: Schematic Drawing of the “Iron Butcher” Machine

As shown in Figure 1.2, to control the X motion, a position transducer is mounted at the head of the hydraulic cylinder. Two gage-pressure transducers are installed on the

head and rod sides of the cylinder to measure the fluid pressures P_1 and P_2 in the corresponding chambers.

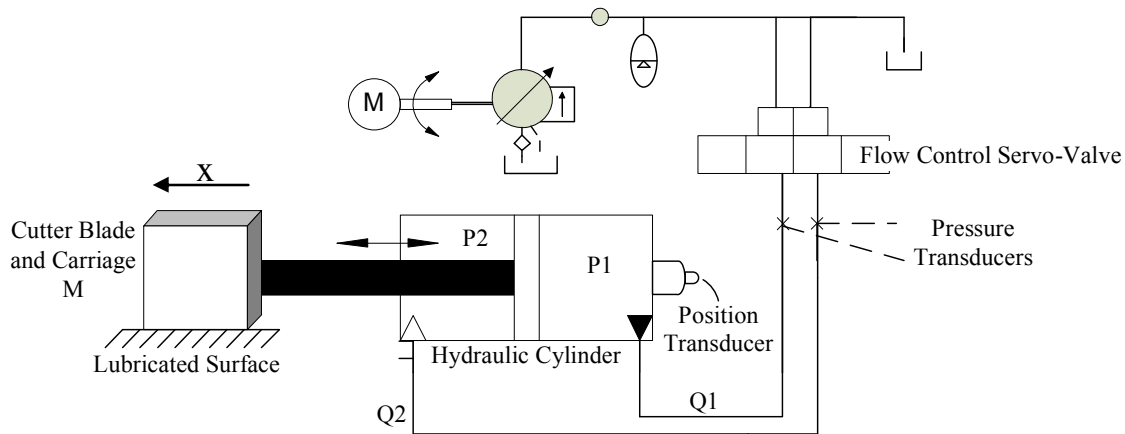


Figure 1.2: The Hydraulic-Actuation Positioning System in One Axis

The industrial sector is in a quest for becoming more productive, efficient, and cost effective through the replacement of human workers with enhanced technology including automation and machine control. In the present example, using on-line monitoring of the “Iran Butcher”, it is expected to predict impending faults and diagnose them. This method can add to the cost effectiveness of the machine because it can prevent the costly and time consuming approach of going through all the machine parts using traditional machine health checks and visual inspection, for possible repair or replacement.

Another main component of the Iron Butcher is the pneumatic actuator. Pneumatic actuators are widely employed in position and speed control applications where cheap, clean, simple and safe operating conditions are required. In recent years low cost pneumatic components have become available in the market which has made it possible to adopt more sophisticated control strategies in pneumatic system control.

Figure 1.3 shows the cutter pneumatic system that is employed in our industrial fish cutting machine.

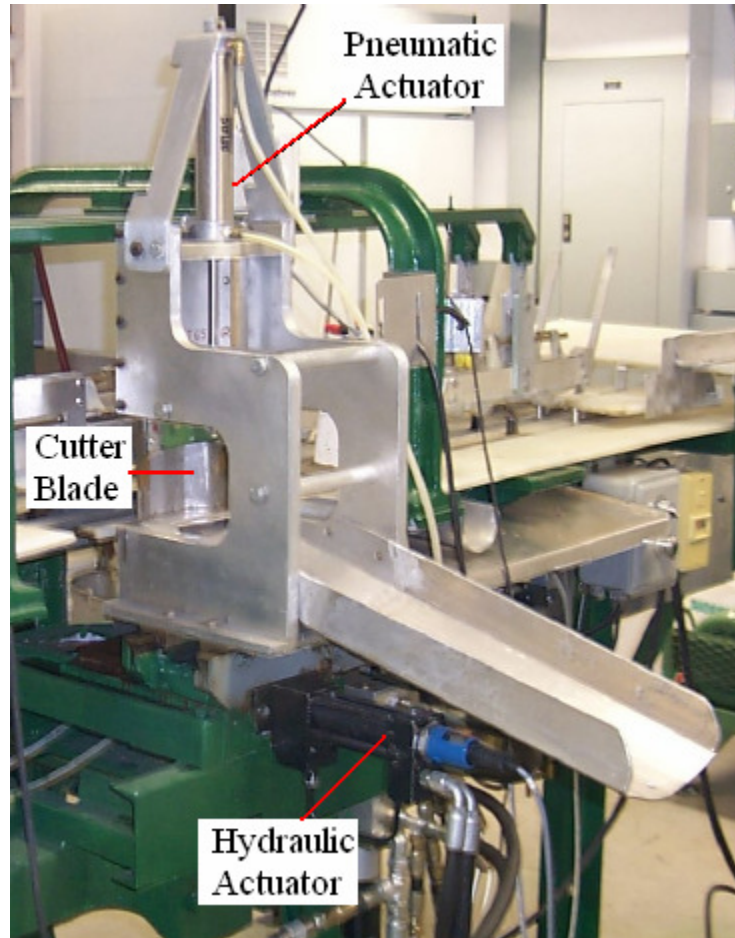


Figure 1.3: Pneumatic Cutter System.

1.4 Hydraulic Power System

There appears to be a resurgence of interest within the universities and hydraulic industries regarding fluid power control systems [5]. Modern hydraulic fluid systems are developed in order to better control and accurately transmit fluid power. Components such as hydraulic actuators, servo valves, sensors, and controllers are essential for these systems. The main components of a hydraulic servo system are outlined next.

Actuator

Actuator is the mechanism that is responsible for delivering force and motion to the external load of a given application. In the present machine (Iron Butcher) it is the cutting table. The Iron Butcher uses linear actuators, which are hydraulic cylinders, to generate the translational motion of the cutting table. A hydraulic cylinder has a piston sliding through it. The two sides of the piston are alternately pressurized and depressurized to achieve precisely controlled linear displacement of the piston and the load connected to it. A familiar example of a manually operated hydraulic actuator is a hydraulic car jack. Typically, a "hydraulic actuator" is controlled by a servo valve or a hydraulic pump.

Hydraulic Control Valve

Hydraulic control valves are used commonly within hydraulic control systems for accurate modulation and control of the entire system. The valve provides the interface between the hydraulic power element (the pump) and the hydraulic output device (actuator). This valve receives the feedback from the operator or the control source and adjusts the system output accordingly. Commonly, the feedback signal is generated by taking the difference between the actual state of motion of the actuator (i.e., velocity or position) and the reference signal sent to the control valve. Hydraulic control valves can be classified in a number of ways; however, they are mostly based on the number of flow lines connected to the valve. For instance, a two-way valve has a single input and a single output. A three-way valve has three flow lines given by a supply line, an output line and a return line back to the reservoir.

Electrohydraulic Servo Valves

Electrohydraulic systems use low-power electrical signals for precisely controlling the movements of high-power hydraulic pistons and motors. The interface between the electrical (control) equipment and the hydraulic (power) equipment is the so-called electrohydraulic servo-valve [6]. These valves are used on systems which must respond both quickly and accurately. Consider the position of an actuator in open-loop operation. The position response steadily grows and displays an unstable behavior in the presence of a slightest disturbance. Furthermore the speed of response must be good enough for proper performance. Therefore, as mentioned before, it is essential to include feedback control into the system [7]. The servo valves are manufactured in different configurations which include single-stage, two-stage and three-stage models each of which consists of a spool valve that is used extensively in hydraulic servo systems. The moving part is called the spool rod along with one or more expanded regions called lands. By applying an input displacement to the spool rod and using a torque motor, it regulates the flow rate.

Pump

A hydraulic pump is a pump that is used in hydraulic drive systems. Hydraulic pumps can be hydrostatic or hydrodynamic. Hydrostatic pumps are positive displacement pumps. A positive displacement pump causes a fluid to move by trapping a fixed amount of it and then forcing (displacing) that trapped volume into a discharge pipe. The periodic fluid displacement results in a direct increase in pressure. Hydrostatic pumps can be fixed displacement pumps, in which the displacement (flow through the

pump per rotation of the pump) cannot be adjusted or variable displacement pumps, which have a more complicated construction that allows the displacement to be adjusted. Hydrodynamic pumps for non-positive-displacement. A non-positive-displacement pump produces a continuous flow. However, because it does not provide a positive internal seal against slippage, its output varies considerably as pressure varies.

Additional Hydraulic Components

In order to complete the hydraulic system, other components are required in addition to the ones discussed above. Examples of these components are sensors, hydraulic hoses and valves. Each of these requires proper installation in the appropriate location in the hydraulic circuit for accurate measurement of the required data and for avoiding system malfunction. As mentioned, some of these data are required for system control. For instance, in a closed-loop hydraulic control system, sensors send required measurements to the controller using feedback, which generates input signals to the servo-valve system based on the received information and the existing system condition.

Based on the application, different valves are employed to control the hydraulic flow, fluid pressure and the direction of flow in the circuit. These valves are manufactured in different sizes based on their applications and the pressure of the hydraulic pump supplied to the hoses.

To minimize losses in hydraulic systems it is important to reduce pressure losses in high power valves and outer components as much as possible. In particular, long hydraulic hoses can have a major effect on the pressure drop of the system. At the same time, depending on the circumstances, the choice of permanent or reusable hoses for the

replacement assemblies can have a considerable impact on the system cost. A comparison of reusable and permanent couplings should be based on cost and convenience [8].

1.5 Potential Faults in Hydraulic Systems

Modern hydraulic systems have become highly sophisticated and increasingly complex, operating at much higher power and speed with greater accuracy. They can be applied in many fields of modern engineering. The failure of these systems can result in serious problems, however. When the system is out of order and stops operation, there will be loss in production and revenue. A system may develop various types of faults and malfunctions which will need periodic and routine maintenance. An older system may even need reconditioning. In order to prevent operational losses, machinists should take up various maintenance and repair measures. In a hydraulic system, detecting a fault alone is not enough. Fault diagnosis is important because correcting the problem will depend on the diagnosis. A component malfunction can arise and, if ignored and left uncorrected, it can damage the entire system. As an example, replacing a faulty pump with a new one may correct the problem but the new pump may also fail if the cause of the initial fault is not diagnosed and corrected. This fault may not be obvious and more careful analysis and study of the system as a whole may be needed to isolate the primary cause from the secondary effects. It is mostly the technicians' job to understand the overall behavior of the system. A thorough knowledge of the hydraulic circuit diagram along with its control system will be important in the context of maintenance, troubleshooting, and reconditioning of the hydraulic oil system.

Before going for repair or reconditioning of a hydraulic system, it is essential to know the type and nature of the faults commonly found in these systems. According to Majumdar [8], the most common type of defects are as follows:

- Reduced speed of travel of machine elements
- Sharp noise in the system
- Steep rise in the oil temperature
- Non-uniform or jerky movement of the tables, carriage, especially at low feed rates
- Slow response to control
- Excessive leakage in the system
- Excessive loss of system pressure
- Cavitation of the pump
- No supply or low supply from the pump
- High rate of seal failure
- High contamination level of the system media and poor oil life

Figure 1.4 shows comparative failure rates of some of the common hydraulic elements listed above.

It should be noted that these faults may be caused by many interrelated factors. Once the causes are established, correcting action becomes easy during breakdown maintenance or system reconditioning. The decision to recondition a system will depend on the individual condition of the system components (subsystems), their interrelated behavioral patterns, and hydraulic performance of the system as a whole.

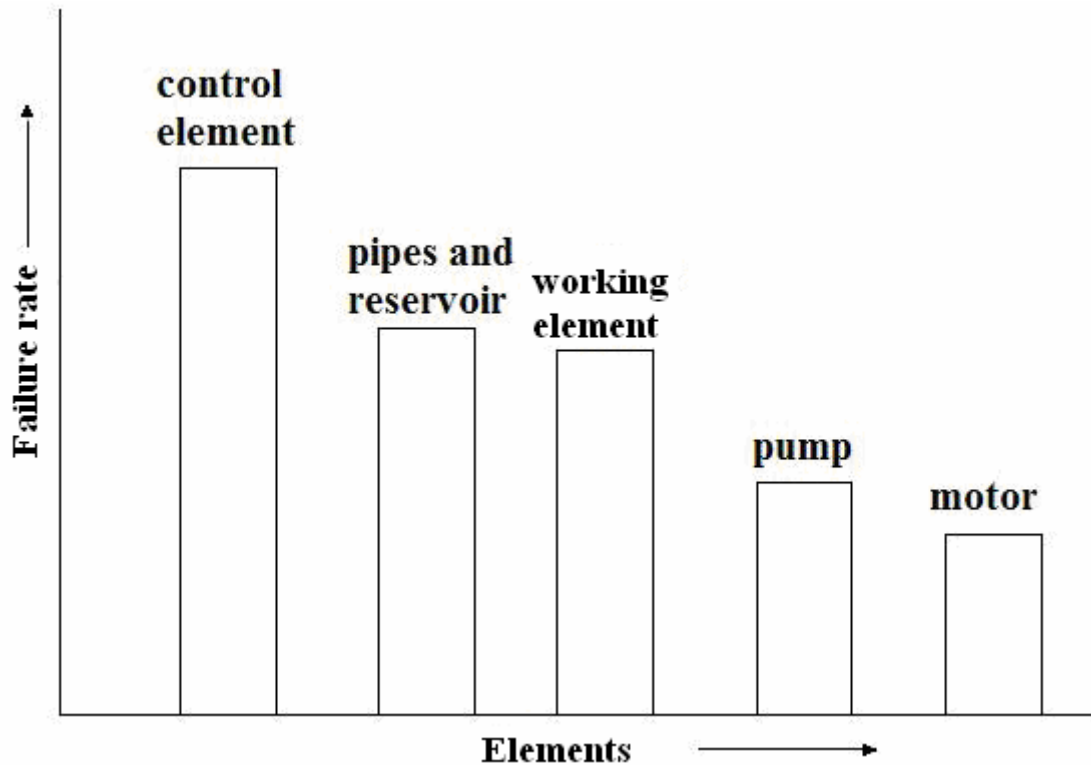


Figure 1.4: General Failure Rate of Common Hydraulic Elements

As mentioned before, leakage is one of the common faults occurring in hydraulic systems. Due to leakage in our hydraulic system, we may experience extensive drop in pressure, thereby reducing the moving force required to do the work. Some other problems that we may experience include the reduced system efficiency, the cost of replacing the oil lost due to leakage, and machine component wear. We may categorize the leakages into two classes: internal leakage and external leakage.

While the achievements of technology are significant, we still have not fully resolved one of the most widespread hydraulic problems. In 1987, Henke Russ [9] proposed that many leakage problems can be traced to improper installation and inadequate in-service monitoring. Solutions to these problems lie at their source - in the area of adequate training of field and plant personnel and a more realistic attitude on the

part of operating management as to requirements for more satisfactory performance. In recognition of these deficiencies in 'practice' the fluid power industry has been moving in the direction of more leak-resistant products.

In 2008, An and Sepehri [10] developed an experimental evaluation of a leakage fault detector in hydraulic actuator based on Extended Kalman Filtering (EKF). Identification of external leakage at either side of the actuator as well as the internal leakage between the two chambers was examined. Their work was built upon their previous work reported in [11] and incorporated a significant improvement in that the new scheme was capable of detecting leakage faults for actuators that were also subject to unknown loading and/or significant friction.

Werlefors and Medvedev [12] developed a nonlinear observer with static feedback for leakage detection in hydraulic servo systems. Two issues, namely fast dynamics reduction and elimination of multiple stationary points in the estimation error dynamics, were treated. In their work it was shown that leakage detection performance was not degraded by the use of a reduced plant model, and that static feedback offered enough degrees of freedom to leave one and only one stable stationary point of the error dynamics, at the origin.

Fang [13] and his colleagues introduced a method based on back-propagation (BP) neural-networks for the leakage fault diagnosis of a hydraulic system. This method analyses the transient procedure of the pressure of the hydraulic system. After adding noise on the learning patterns of the BP neural networks, the anti-noise ability was improved over what is possible with conventional BP networks. They concluded that this method of leakage fault diagnosis was more reliable, widely applicable, and less costly

than the traditional method. In addition to this work, in 2006 El-Betar [14] and colleagues proposed another idea of using Artificial Neural Networks (ANN) which dealt with the problem of fault detection, isolation and identification of a hydraulic power system. They employed a feed-forward neural network to diagnose actuator internal leakage and valve spool blockage. They trained their ANN with sufficient data of the faults obtained from the system. They have concluded that the trained network had the capability to detect and identify various levels of faults.

1.6 Research Objectives

As discussed in the previous sections, in the operation of hydraulic actuators, we may encounter problems and faults due to factors such as wear in instruments and accessories wear, excess improper use of the equipment, and ignoring of on-schedule maintenance. It is essential to identify, detect and deal with these potential faults before they occur as they can result in a major catastrophic failure in the system. In order to achieve this, researchers have introduced many different techniques which include the use of sensor fusion and signal processing techniques, adaptive control, and implementing intelligent control systems that make the system autonomous.

For the purpose of the present research, the main focus is on the existing industrial fish cutting machine. Specifically, the hydraulic actuator system, which is used to move the cutter table in the X and Y directions, is considered. We expect to emulate hydraulic faults in the system and then detect and diagnose them in real time using the model-based approach developed in the thesis. Specifically, Unscented Kalman Filter (UKF) technique is employed. The UKF uses a deterministic sampling approach which

estimates the states recursively. The state distribution is approximated and represented using a minimal set of carefully chosen sample points. This means it only requires the measurement from the current state and the estimated state from the previous time step to compute the current state.

There are many common faults in hydraulic systems. Due to project constraints, only the following four faults are studied in this thesis:

1. Internal leakage of the actuator
2. External leakage of the actuator through the connecting hose of chamber 1
3. External leakage of the actuator through the connecting hose of chamber 2
4. Effect of dry friction build-up on the moving table of the fish cutting machine

It is hoped that through the present work, we are able to develop a feasible and robust method for on-line monitoring and fault diagnosis of the existing industrial machine. The subsequent chapters will present development, implementation, and evaluation of the approach.

1.7 Organization of the Thesis

The organization of the thesis is given now. In Chapter 1 a typical industrial machine, which is studied in the present research, and its application have been introduced. The hydraulic system which is one of the main components of the machine is brought into the forefront and its essential components are discussed. Some of the common faults that occur in hydraulic systems are also introduced. Finally, the main objectives of the current research are outlined.

In Chapter 2, the experimental setup and its components are thoroughly introduced. The mathematical state-space model is developed, and discussed. Unknown model parameters are indicated and an appropriate method for finding them is proposed. At the end, a set of tests are carried out to validate the developed state-space model.

In Chapter 3, general approaches of fault diagnosis are introduced and common roadmaps to these approaches are discussed. A literature survey is done to justify the methodology chosen for the project. Kalman filtering in general and Unscented Kalman filter in particular are discussed. The steps of applying the fault monitoring scheme to the hydraulic test rig in our laboratory is developed. Results are shown to confirm the satisfactory operation of the developed technique.

In Chapter 4, the developed condition monitoring technique is implemented in the industrial machine and the employed faults are investigated. Results for on-line monitoring and state estimation in real time are shown, followed by a discussion on the related fault diagnosis.

In Chapter 5, conclusions are drawn based on both simulated data and experimental results of the present work. Recommendations are made on possible future work for improvement of the developed technique.

Chapter 2

Experimental Set-up and Dynamic Modeling

2.1 Introduction

This chapter describes the experimental set-up using which the implementation and experimentation of the present research are carried out. As indicated in the previous chapter, an industrial fish cutting machine, which is available in our laboratory (Industrial Automation Laboratory), is used in our work. This is an automated machine which has developed for the fish processing industry for the operation of head removal of fish. It consists of many components. The main focus in this work is the hydraulic system which is used to position the cutting table (cutter carriage) for accurately positioning the fish head for the cutting operation so as to minimize the meat waste and also improve the cutting quality. The main components of this hydraulic system are the servo-valves, hydraulic pump, hydraulic actuators, needle valves, and hydraulic filter. A mathematical model (dynamic model) of the system is developed after carefully studying each of these components. Control and Graphical User Interface (GUI) software module has been developed, using LabViewTM, to control and interact with the system and to analyze the monitored data received from the sensors of the system. Data from on-line system monitoring is analyzed to perform fault detection and diagnosis.

In section 2.2, the experimental test rig and the components of its hydraulic system are indicated and system operation is explained.

In section 2.3, the state-space model of the experimental system is derived. The unknown parameters of the model are introduced and the method of parameter estimation is explained.

In Section 2.4, the actual data obtained from the experimental setup is compared with that of the results from simulations in order to verify and validate the developed state-space model.

2.2 Experimental Set-up

A schematic diagram of the experimental set-up (Iron Butcher) is shown in Figure 2.1. The cutter module of the machine is divided into two subsystems: hydraulic and pneumatic subsystems. The main focus For the purpose of the present project is the hydraulic subsystem of the machine.

The hydraulic subsystem consists of two hydraulic actuators each working independently to adjust the cutter table in two orthogonal directions on a horizontal plane (X and Y). The two hydraulic actuators are able to correctly position the approaching fish and stabilize it in place during the cutting operation. These actuators are powered by a hydraulic pump which supplies a maximum supply pressure of 3000 psi. A hydraulic actuator has an asymmetric cylinder with effective difference in cross-sectional area. Accordingly, a cylinder consists of two chambers: chamber 1 and chamber 2, which are connected to a four-way five-ported solenoid servo valve with the following specifications:

- System pressure: 2.1 bar = 30.4 psi
- Voltage: 48 Vdc, 5.3 W
- Frequency: 60 Hz at 100-120 V or 50 Hz at 200-240V

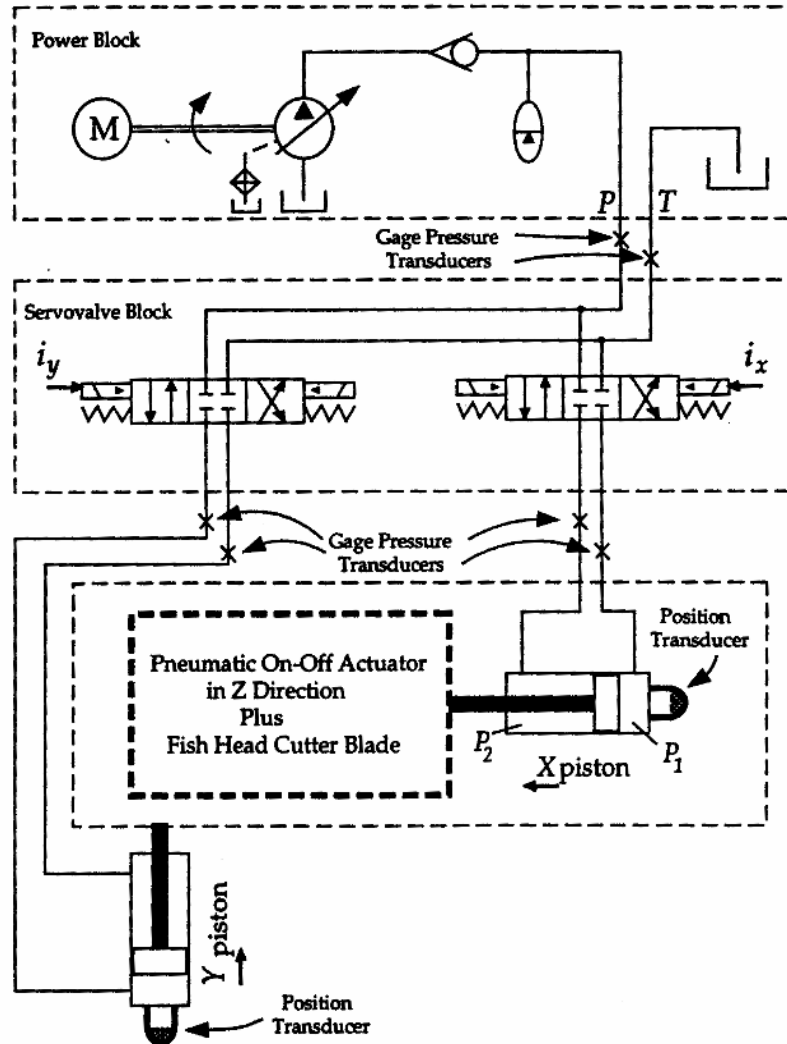


Figure 2.1: Schematic Diagram of the Basic Planar Manipulator

For each cylinder-valve unit here are three sensors, which are used to measure the required states. Specifically, two pressure transducers and a Temposonics Linear Displacement Transducer (LDT) are employed. The pressure transducers are installed on each side of the cylinder actuator to measure the pressures in the chambers 1 and 2. The linear displacement transducer (LDT) is installed in the cylinder to measure the actuator (piston) displacement. The signals from these sensors are transmitted to a PC via a data acquisition (DAQ) board for further analysis. A 2-conductor 26-AWG gauge microphone

stereo cable is used to connect all the sensors to the BNC DAQ board. For this cable, the maximum frequency for 100% skin depth for solid conductor copper is 107 kHz. In particular, the band width of the cable is 107 kHz when it carries approximately 0.361 Amps. A complete monitoring diagram of the working system is shown in Figure 2.2 and a system control block diagram as given in Figure 2.3.

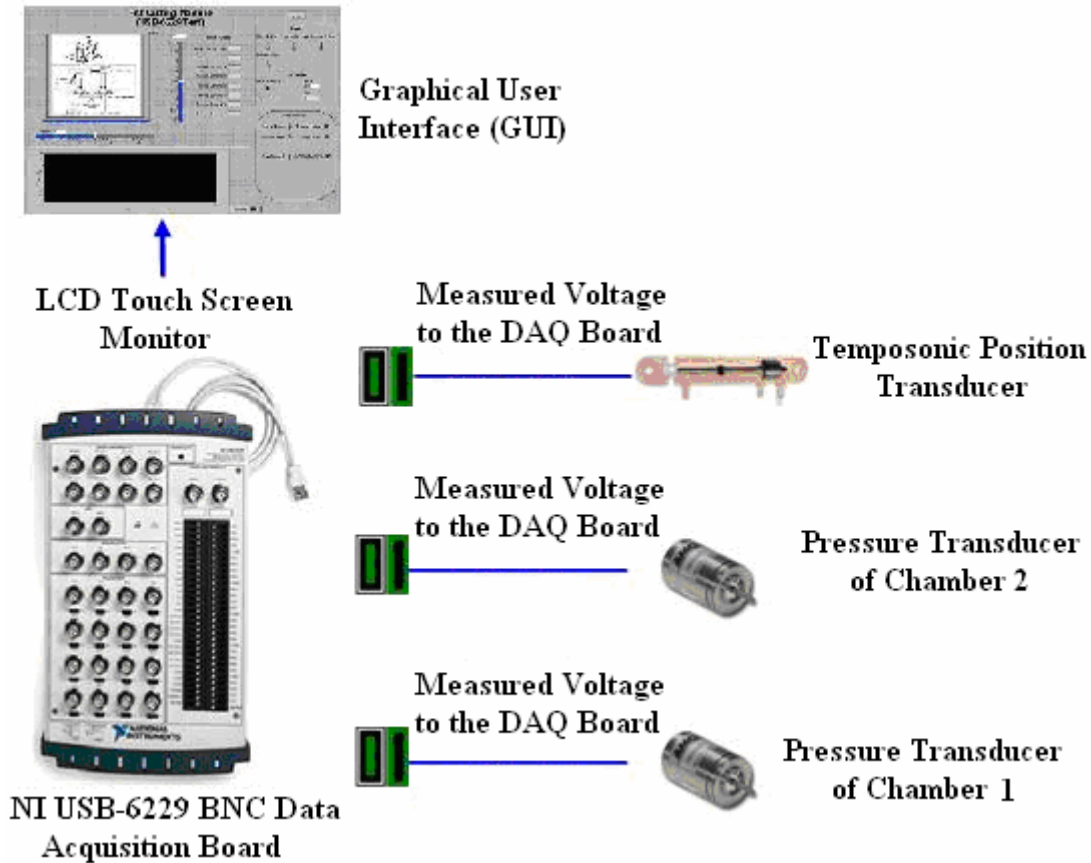


Figure 2.2 : Diagram of Monitoring Components

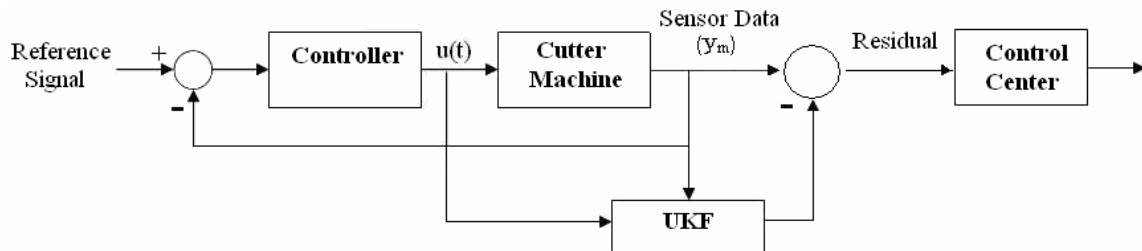


Figure 2.3: Control System Block Diagram

1) Data Acquisition Board

Supplied by Omega, the data acquisition system is used to collect information to analyze the state of the system. As technology has progressed, DAQ units have been simplified and made more accurate, versatile, and reliable. Some useful terminology in data acquisition is given below:

- **Analog-to-digital converter (A/D)**

An electronic device that converts analog signals to an equivalent digital form.

The analog-to-digital converter is the heart of a data acquisition system.

- **Digital-to-Analog Converter (D/A)**

An electronic component which produces an analog output signal corresponding to an incoming stream of digital data.

- **Differential Input**

Refers to the way a signal is wired, with respect to another signal or condition (reference) in a data acquisition device. Differential inputs have a unique high and unique low connection for each channel. Data acquisition devices have either single-ended or differential inputs, and many devices support both configurations.

- **General Purpose Interface Bus (GPIB)**

Synonymous with HPIB (for Hewlett-Packard), this is the standard bus used for integrating electronic instruments with a computer. This is also called IEEE 488 with reference to ANSI/IEEE standards.

- **Resolution**

The smallest signal increment that can be detected by data acquisition system. Resolution can be expressed in bits, in proportions, or as a percentage of the full scale. For example, a system with 12-bit resolution has a corresponding resolution of one part in 4,096 or 0.0244 % of full scale.

- **Sample Rate**

This is the speed at which a data acquisition system collects data. The speed is normally expressed in samples per second (S/s). For multi-channel data acquisition devices the sample rate is typically given as the speed of the analog-to-digital converter (A/D). To obtain individual channel sample rate, it is necessary to divide the speed of the A/D by the number of channels being sampled.

The Universal Serial Bus (USB) is a new standard for connecting PCs to peripheral devices such as printers, monitors, modems and data acquisition devices. USB offers several advantages over conventional serial and parallel connections. These include higher bandwidth (up to 12 Mbits/s) and the ability to provide power to a peripheral device. USB is ideal for data acquisition applications. Since USB connections supply power, only one cable is required to link the data acquisition device to the computer (PC), which most likely has at least one USB port. A National Instrument (NI) USB-6229 BNC with the following specifications is chosen for the present project:

- 16 differential BNC analog inputs (16-bit, 250 kS/s)

- 4 BNC analog outputs (16-bit, 833 kS/s), 48 digital I/O (32 clocked, 8 BNC), and 32-bit counters
- NI Signal Streaming for sustained high-speed data streams over USB; OEM version available
- Compatible with LabVIEW, ANSI C/C++, C#, Visual Basic .NET and Visual Basic 6.0
- NI-DAQmx driver software and NI LabVIEW SignalExpress LE interactive data-logging software

The National Instruments USB-6229 BNC is a USB high-performance M Series multifunction data acquisition (DAQ) module optimized for high accuracy at fast sampling rates. The NI USB-6229 BNC is suitable for applications such as data-logging and bench-top sensor measurements. The National Instruments USB-6229 BNC is designed for mobile or space-constrained applications. Plug-and-play installation reduces the configuration and setup time, while direct screw-terminal connectivity helps keep costs down and simplifies the signal connections. This module also features the new NI Signal Streaming technology which allows for DMA-like bidirectional high-speed streaming of data across the USB bus. NI-DAQmx driver and measurement services software provides easy-to-use configuration and programming interfaces with features such as DAQ Assistant to help reduce development time.

2) Pressure Transducer

A pressure sensor measures fluid pressure, expressed in force per unit area. Typically, the sensor output is an electrical signal, but optical, visual, and auditory

signals are available as well. Pressure sensors can also be used to indirectly measure other variables such as fluid flow rate, liquid level, and altitude. Pressure sensors are also variously called pressure transducers, pressure transmitters, and pressure indicators. Pressure sensors can be classified with respect to the pressure ranges they measure, temperature ranges of operation, and most importantly the type of pressure they measure. In terms of the pressure type, pressure sensors can be divided into five categories:

- **Absolute pressure sensor**

This sensor measures the pressure relative to the perfect vacuum pressure (0 psi or no pressure). Atmospheric pressure is 101.325 kPa (14.7 psi) at sea level with reference to vacuum.

- **Gauge pressure sensor**

This sensor is used in different applications because it can be calibrated to measure the pressure relative to a given atmospheric pressure at a given location. A tire pressure gauge is an example of gauge pressure indication. When the tire pressure gauge reads 0 psi, there is really 14.7 psi (atmospheric pressure) in the tire.

A SENSOTEC pressure transducer (model LV/2359-12) is chosen and installed on our experimental machine to measure the pressure of the hydraulic fluid at different stages. It has an amplified DC output (voltage) with pressure capacity of 3000 psig, accuracy of 0.5% and output voltage range of 0-5VDC. Its pressure port is 1/4 – 18NPT female with a supply voltage of ± 15 VDC. This pressure transducer is an all-welded stainless steel sensor built for rugged industrial applications that require high accuracy and measurement stability. The gage Model LV/2359-12 is a strain gage based

transducer. This design references the primary pressure sensing diaphragm to the atmosphere, and provides a stable zero regardless of the transducer environment. These sensors connect to the BNC DAQ board using 2-conductor shielded microphone stereo cable (#21188).

3) Linear Displacement Transducer (LDT)

A linear actuator is a device that develops force and motion, from an available energy source, in a rectilinear manner, as opposed to rotational (angular) motion and torque like in an electric motor. There are various methods of achieving this linear motion. In hydraulic actuators or hydraulic cylinders they typically involve a hollow cylinder having a piston within it. The two sides of the piston are alternately pressurized and de-pressurized to achieve a controlled linear displacement of the piston and in turn the load connected to the piston. The linear displacement exists only along the axis of the piston/cylinder. In the present project, a Temposonics II Linear Displacement Transducer (LDT) model TTRCU0020 with a stroke of 2.0 inches (0.05 meter) is installed on the hydraulic actuator. The origin of actuator cylinder is located at the point where the ram is fully retracted. It draws a maximum current of 100 mA and a minimum of 25 mA for the required voltage of ± 15 Vdc. The output range of the sensor is from -15 to +15 V. It can operate at pressures up to 3000 psi.

The Temposonics II Linear Displacement Transducer senses the position of an external magnet to measure displacement with a high degree of resolution. The system measures the time interval between an interrogation pulse and a return pulse. As shown in Figure 2.4, the interrogation pulse travels the length of the transducer by a conducting wire threaded through the hollow waveguide. The waveguide is spring loaded within the

transducer rod and exhibits the physical property of magnetostriction. When the magnetic field of the interrogation pulse interacts with the stationary magnetic field of the external magnet, a torsional strain pulse is produced. This strain pulse travels in both directions, away from the magnet and at the end of the rod, the strain pulse is damped. At the head of the transducer, two magnetically coupled sensing coils are attached to strain sensitive tapes. The tapes translate the strain pulse through coils to an electrical "return pulse." The coil voltage is then amplified in the head electronics before it is sent to a measuring device as the conditioned "return pulse."

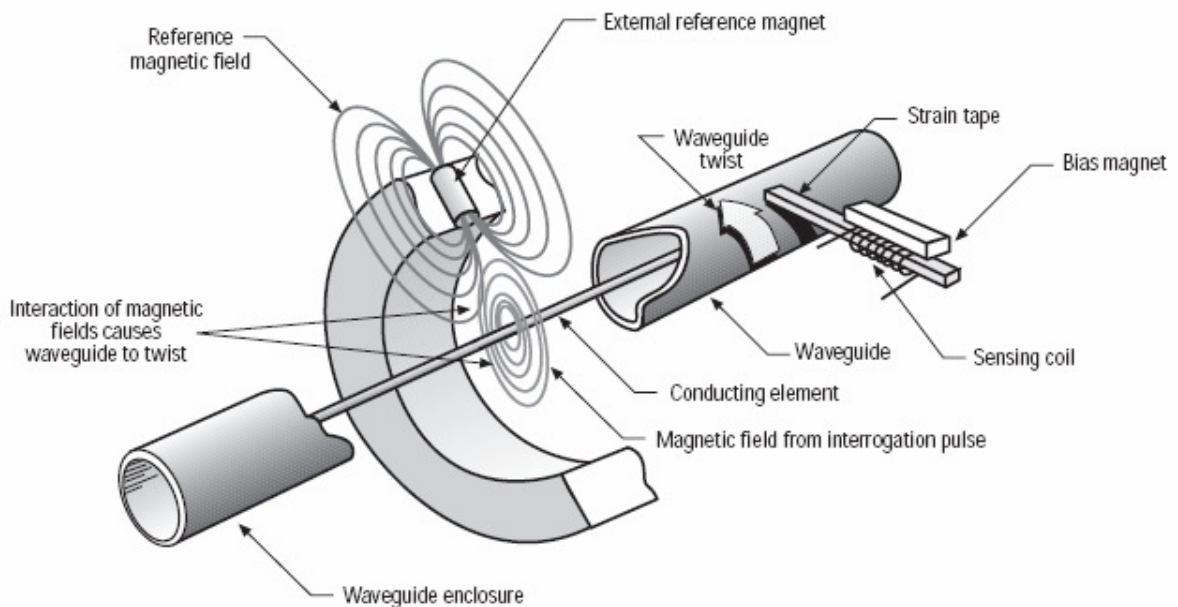


Figure 2.4: Waveguide Interaction

2.3 Potential Faults Implementation

As mentioned in section 1.6 and illustrated in Figure 2.5, internal and external leakages as well as friction build-up on the sliding surface of the cutter table are the main faults that are studied in this research. The friction build-up acts as an external force

which restrains the actuator movement (in the y-direction, in the present exercise) and thus can be considered as an external force.

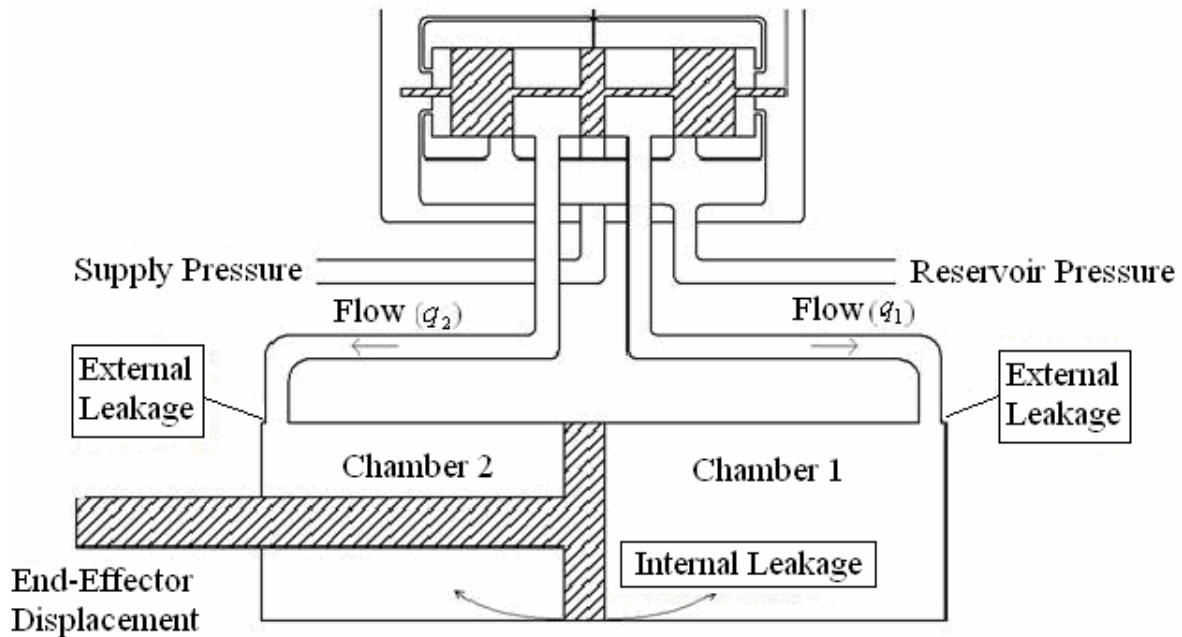


Figure 2.5: Schematic Diagram of the Potential Faults in the Hydraulic Actuator

Under normal operating conditions, the hydraulic flows q_1 and q_2 entering chamber 1 and chamber 2, respectively. They are regulated by adjusting the input current to the servo-valve. However, under some conditions, due to wear, rapture or insufficient lubrication, hydraulic faults will occur. In external leakage, the hydraulic hosing can undergo fatigue or rapture which will result in loss of hydraulic fluids. Then less flow will reach the chambers and as a result the chamber pressure will drop as well. In the case of internal leakage, due to the wear and tear of piston material or sealing defects, the hydraulic fluid escapes from one chamber into the other. As in external leakages, this defect causes a drop in chamber pressure, thereby reducing the driving force of the actuator.

In the present work, needle valves and hydraulic hosing are used to implement specific faults in the system, as shown in Figure 2.6.

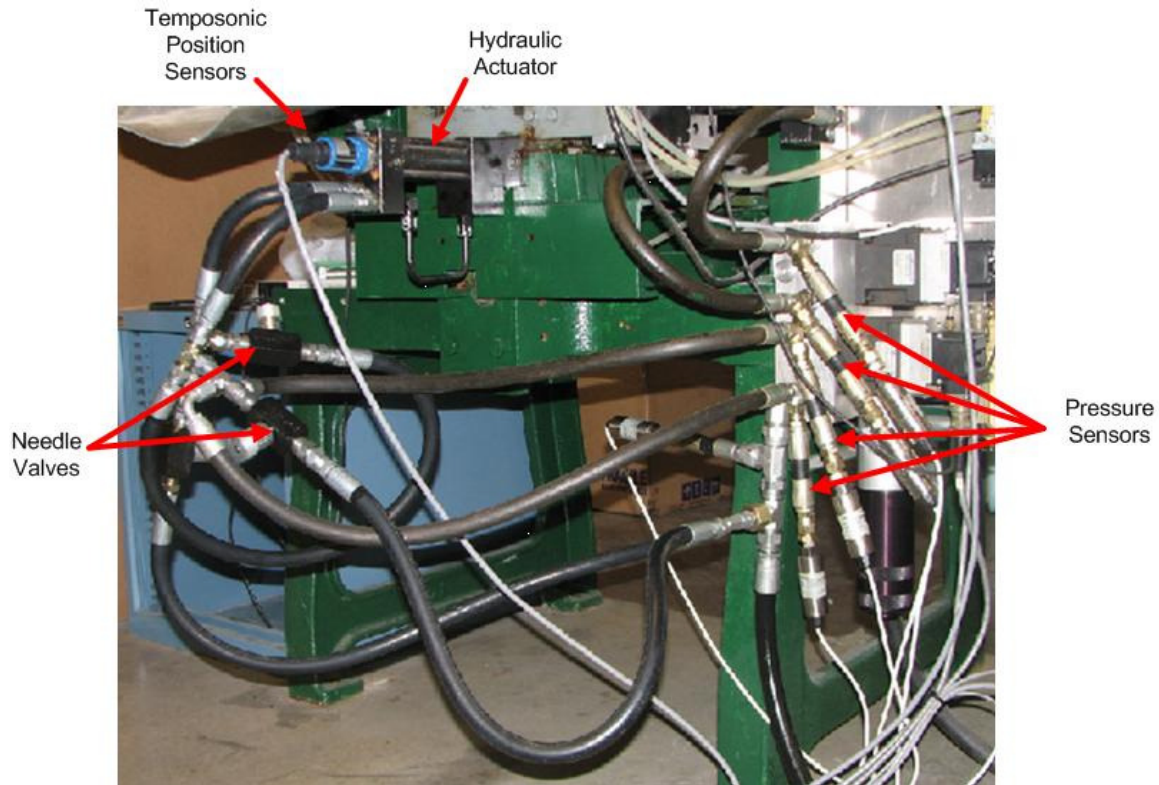


Figure 2.6: Experimental Hydraulic Setup with Working Sensors

Three needle valves are used in total to emulate the internal and external leakages. One valve is required to connect the two chambers of the cylinder for emulating an internal leakage. The other two valves are used to redirect the hydraulic oil back to the tank before it could enter the two chambers. The required pressure drop in each chamber is achieved and the external leakage in chambers one and two is emulated in this manner. The severity of the leakage in the system can be decided by simply adjusting the knob of each of the needle valves. For the purpose of this study, three conditions of leakage: low, medium (moderate), and high are considered. For emulating the fourth type of fault in the system, the lubrication of the moving table is removed and dried in order to restrict

and slow down the table movement by creating more friction on the sliding surface of the table. This force resists the piston displacement during both retraction and extension.

As shown in Figure 2.3, a closed loop controller is used to regulate the behavior of the hydraulic system. After closing all the needle valves, the set-up is excited with a sinusoidal reference signal in order to study the performance of the system. A low frequency reference signal of $r = 0.025 + 0.0125 \sin(0.4 \pi t)$ m is applied in the present research for a period of 30 seconds. A sampling time of 50 ms is chosen for sensor measurements, considering the limits on the data computation and the processing time required by the computer and the hardware. As shown in Figure 2.7, parts (a) and (b), there is about $\pi/4$ phase difference and 0.004 meter (10%) amplitude difference between the actuator displacement and the reference signal. Additionally, in parts (c) and (d), it is observed that the pressure in chamber 2 is higher than that of chamber 1 with a difference of about 2 MPa. This difference in pressure is due to the difference in the effective areas of the chambers. In other words, since the hydraulic cylinder is asymmetric and the reference signal is symmetric around the origin, chamber 2 tolerates higher pressure due to the smaller effective area.

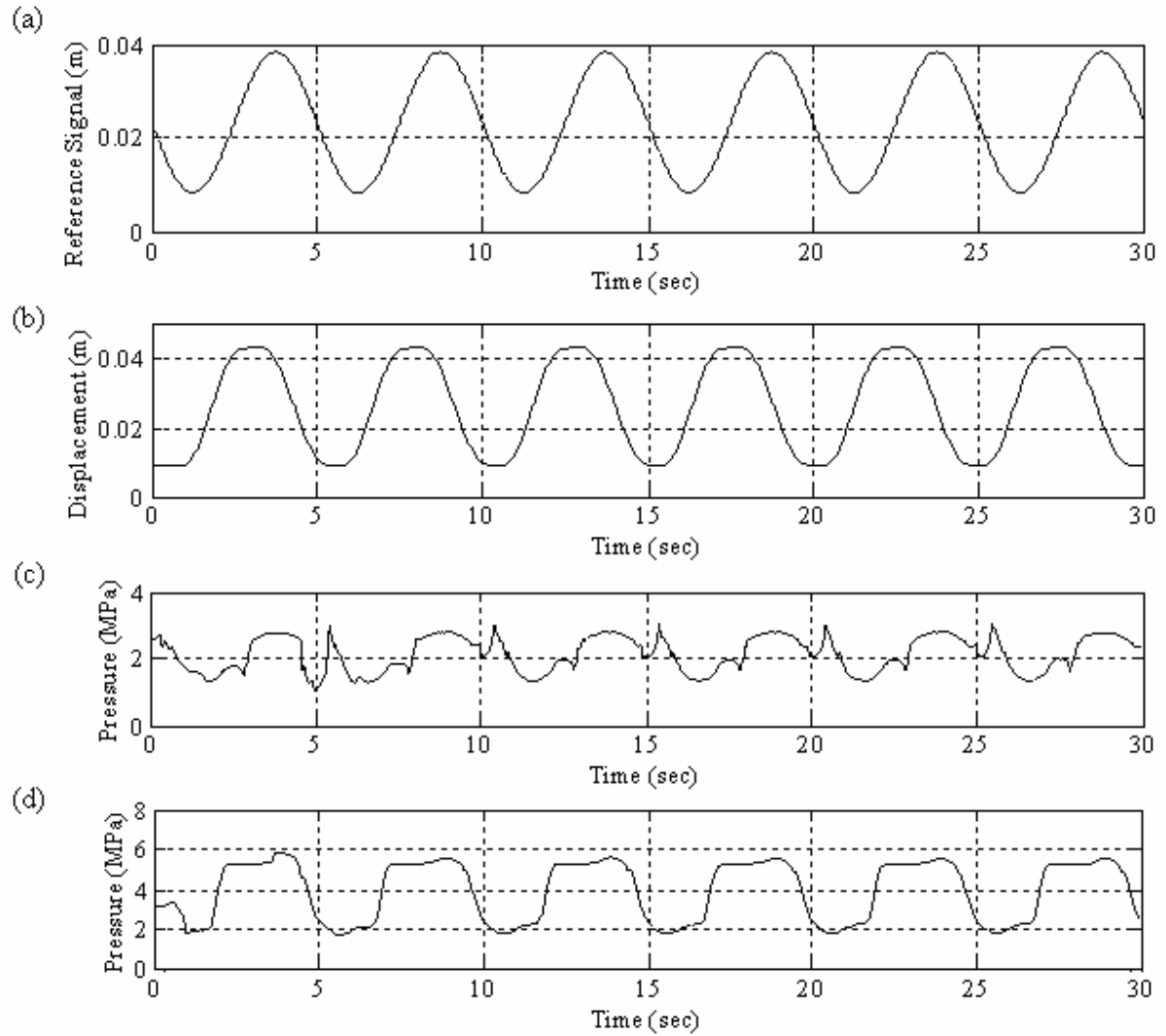


Figure 2.7: System Characteristics – (a) Actuator Reference Signal, (b) Actuator Displacement, (c) Pressure in Chamber 1, (d) Pressure in Chamber 2

2.4 System Modeling

2.4.1 Governing Equations

Knowing the system behavior and knowledge of the fundamental laws of physics is essential for correctly describing the system dynamics as presented in [1] and [7]. This modeling will take into account the nonlinear nature of the actuator dynamics. There are two types of common nonlinearity exist in the hydraulic servo-valve systems, as given by the basic flow equation through an orifice and the flow forces on the valve spools [15].

What causes a change in the position of the piston is the displacement of the valve spool from the null position, resulting in a pressure difference across the single-rod hydraulic actuator. This creates a force that is applied to the external load by the actuator and can be expressed in the form:

$$\sum F = P_1 A_1 - P_2 A_2 = M \ddot{x} + f_f \quad (2.4-1)$$

Where:

p_1, p_2 : Pressures in chamber 1 and chamber 2

A_1, A_2 : Effective piston areas of chamber 1 and chamber 2

M : Equivalent moving mass in Y direction

f_f : Opposing frictional force of the actuator

x : Piston displacement in Y Direction

Hydraulic fluid flows from the servo-valve to the head-side and the rod-side of the cylinder (chamber 1 and chamber 2) and it is a function of both the square root of the cylinder pressure difference across the port, and the spool valve displacement. The

orifice area depends on the valve geometry and changes linearly with the valve stroke. The rate of change of orifice area with stroke is called the “*opening*” or “*area gradient*” of the valve. By applying a linear orifice area gradient, the flow equations of the servo-valve are obtained as follows:

$$\begin{cases}
 Q_1 = -C_d A_{orifice} x_v \left(\sqrt{\frac{2}{\rho} (p_1 - P_r)} \right) \text{sign}(p_1 - P_r) \\
 Q_2 = C_d A_{orifice} x_v \left(\sqrt{\frac{2}{\rho} (P_s - p_2)} \right) \text{sign}(P_s - p_2)
 \end{cases}
 \quad x_v \geq 0$$

$$\begin{cases}
 Q_1 = -C_d A_{orifice} x_v \left(\sqrt{\frac{2}{\rho} (P_s - p_1)} \right) \text{sign}(P_s - p_2) \\
 Q_2 = C_d A_{orifice} x_v \left(\sqrt{\frac{2}{\rho} (p_2 - P_r)} \right) \text{sign}(p_2 - P_r)
 \end{cases}
 \quad x_v < 0$$

(2.4-2)

Where:

P_r, P_s : Return pressure and supply pressure

Q_1, Q_2 : Fluid volume flow rates to chamber 1 and chamber 2

p_1, p_2 : Pressures in chamber 1 and chamber 2

x_v : Valve spool displacement

ρ : Hydraulic oil density

C_d : Orifice coefficient of discharge

$A_{orifice}$: Orifice area gradient

Furthermore, using continuity equations and assuming compressibility of the hydraulic fluid, we can obtain a relationship between chamber pressure, their flows and the piston velocity. The flows of the chambers may be expressed as:

$$\begin{aligned}
Q_1 &= A_1 \dot{x} + \frac{A_1 x + V_h}{\beta} \dot{p}_1 \\
Q_2 &= A_2 \dot{x} - \frac{A_2(L-x) + V_h}{\beta} \dot{p}_2
\end{aligned} \tag{2.4-3}$$

Where:

\dot{x} : Actuator velocity

L : Maximum piston displacement

V_h : Volume of the fluid inside a hose that connects the servo-valve to the actuator

β : Effective bulk modulus of the fluid

p_1, p_2 : Pressures in chamber 1 and chamber 2

A_1, A_2 : Effective piston areas of chamber 1 and chamber 2

Equations (2.4-2) and (2.4-3) are combined to eliminate the flow parameters,

resulting in the following equations:

$$\dot{p}_1 = \begin{cases} \frac{\beta}{A_1 x + V_h} \left[C_d A_{orifice} x_v \sqrt{\frac{2}{\rho} (p_1 - P_r)} - A_1 \dot{x} \right] & x_v \geq 0 \\ \frac{\beta}{A_1 x + V_h} \left[C_d A_{orifice} x_v \sqrt{\frac{2}{\rho} (P_s - p_1)} - A_1 \dot{x} \right] & x_v < 0 \end{cases} \tag{2.4-4}$$

$$\dot{p}_2 = \begin{cases} -\frac{\beta}{A_2(L-x) + V_h} \left[C_d A_{orifice} x_v \sqrt{\frac{2}{\rho} (P_s - p_2)} - A_2 \dot{x} \right] & x_v \geq 0 \\ -\frac{\beta}{A_2(L-x) + V_h} \left[C_d A_{orifice} x_v \sqrt{\frac{2}{\rho} (p_2 - P_r)} - A_2 \dot{x} \right] & x_v < 0 \end{cases} \tag{2.4-5}$$

Modeling of dynamic systems with stick-slip friction phenomenon has been the subject of nonlinear dynamics as considered by numerous researchers in the field of hydraulic systems [16-20]. Due to the complexity of nonlinear friction and difficulty in its modeling, researchers have come up with approximated and semi empirical

expressions to represent friction in dynamic modeling [2]. Friction is usually modeled as a function of velocity, and in particular sign of the velocity (i.e., direction of motion). Cylinders in hydraulic actuators need to be sealed properly due to the existence of high pressures in its chambers. It is needed as well to minimize the friction between the seals and the sliding components. Due to the significant effect of friction on the dynamics of a system, in 1985 Karnopp [21] proposed a stick-slip friction model in which a straightforward method for representing and simulating friction effects is presented. True zero velocity sticking was also represented without equation reformulation or the introduction of numerical stiffness problems. Later in 1996, Laval [22] proposed a similar method which improved Karnopp's model for friction inside a hydraulic cylinder. Friction is particularly noticeable at low velocities, and then smoothly varies with the piston velocity. This friction force combines two major effects: Coulomb friction and stiction, due to seals, bearings and the effect of oil viscosity. Estimating these parameters is not straightforward because of the existing nonlinearities in the components. To estimate these friction parameters simultaneously, the following expression was proposed by Laval [22]:

$$f_f = \begin{cases} [f_{st} - (f_{st} - f_{sl})(1 - e^{-C_b|\dot{x}|})] \text{sign}(\dot{x}) + d\dot{x} & \dot{x} \neq 0 \\ f_{st} & \dot{x} = 0 \end{cases} \quad (2.4-6)$$

Where:

f_{st} : Static friction

f_{sl} : Slip friction

C_b : Lubrication coefficient

d : Effective damping ratio

To express the position of the flow controlling valve as a function of the drawn current, the following quadratic equation can be written:

$$K_{sp}u = \ddot{x}_v + 2\omega_n d_m \dot{x}_v + \omega_n^2 x_v \quad (2.4-7)$$

Where:

K_{sp} : Spool valve position variable

ω_n : Natural frequency of the valve

u : Valve input current

d_m : Damping ratio

In order to use this dynamic model in our study, the system parameters must be known either by direct measurement or some previously known data specifications provided by the manufacturers. However, sometimes due to difficulties associated with unspecified data and information, none of the above methods can be used and some alternative methods must be considered. For the present research, experiments are implemented to determine these parameters through system states.

Friction parameters need a series of experiments for their determination. To approximate the static friction f_{st} , assuming that the set-up is stationary and the initial acceleration is ignored at start, the input current to the system is increased slowly until the actuator starts to move. At that instance, the required force to move the actuator is equivalent to the static force of friction. For the purpose of accuracy and minimizing the experimental errors, the experiment is repeated in three different locations along the cylinder for both extension and retraction. The average value for the total calculated

static force for each trial is considered to represent the estimated static friction force, which is 369 N.

To approximate the slip friction parameter f_{sl} , the actuator is run at several velocities with reasonably good precision, assuming that there is no acceleration or deceleration during these runs (except at start and stop). As shown in Figure 2.8, the actuator force undergoes some change for the first few seconds until it reaches the velocity of 0.05 m/s. For the velocity above this point, the actuator force for both extension and retraction directions stays constant and steady throughout the runs and it converges to a value of 285 N and 271 N respectively. It is also observed that the average velocity of 0.07 m/s is reached by the actuator. In order to estimate the slip friction parameter from the analysis, the average steady value between the extension and the retraction processes is taken, which is 278 N.

Besides the slip and static friction parameters in the friction dynamic equation 2.4-6, there are two other parameters that need to be determined: lubrication coefficient (C_b) and effective damping ratio (d). In order to estimate these two parameters, the friction equation is plotted for different values of C_b and d and fitted to the experimental model plotted in Figure 2.8, in a trial and error approach. Using the best fitted curve, the best values for these state-space model parameters are chosen and are as follows: $C_b = 58$ s/m and $d = 127$ N.s/m .

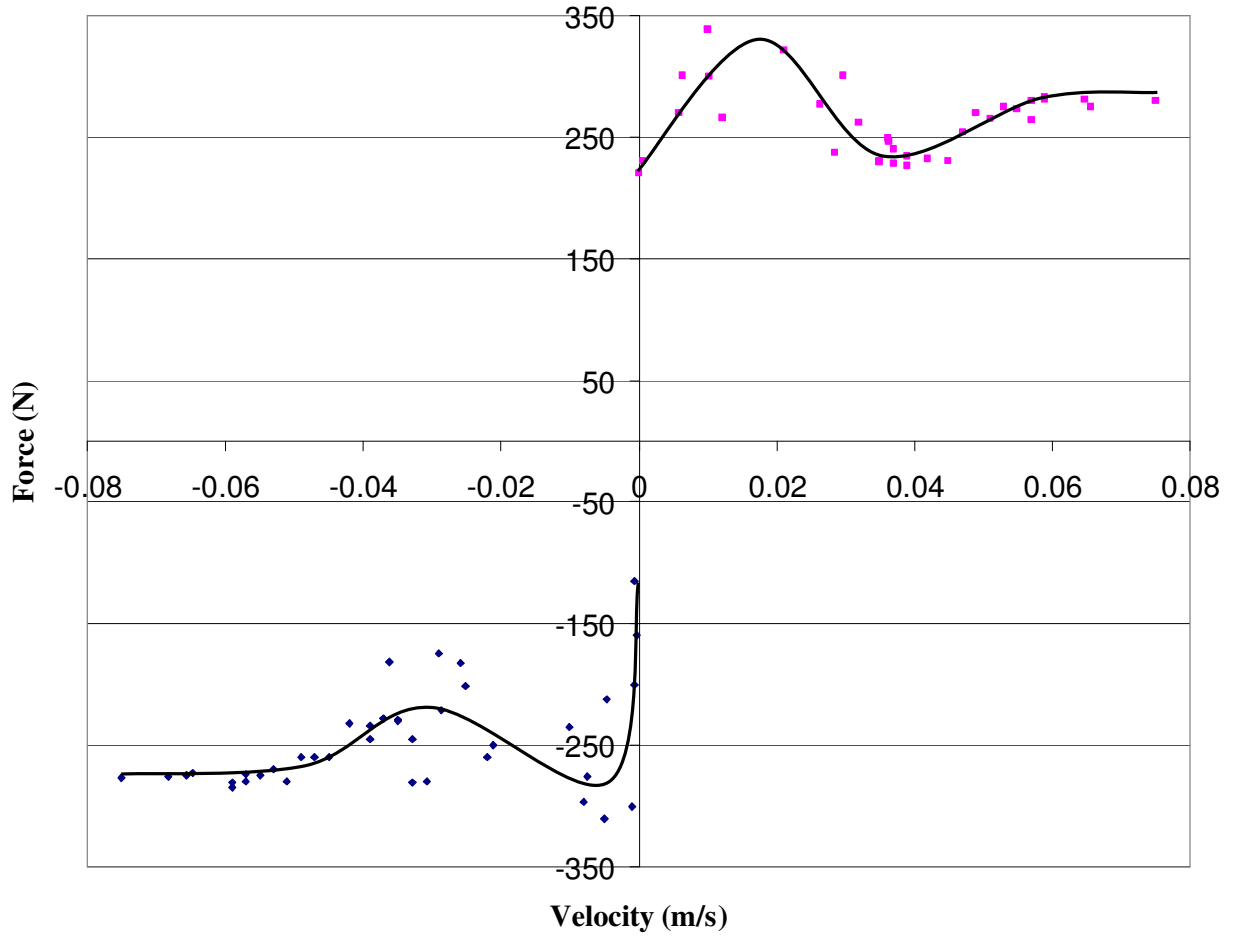


Figure 2.8: Slip Friction Experimental Result

As mentioned before, some parameters are provided by the manufacturers, some are obtained by experimentation, and some by parameter tuning methods. Table 2.1 gives all the required parameters of the state-space model.

Table 2.1: Dynamic Parameters of the Hydraulic System

$A_1 = 1.144 \times 10^{-3} m^2$	$f_{st} = 369 \text{ N}$	$V_h = 8.50 \times 10^{-5} m^3$
$A_2 = 0.633 \times 10^{-3} m^2$	$f_{sl} = 278 \text{ N}$	$A_{orifice} = 0.04 m^2 / m$
$L = 0.0508 \text{ m}$	$C_b = 58 \text{ s/m}$	$\beta = 8.90 \times 10^8 Pa$
$d = 127 \text{ N.s/m}$	$K_{sp} = 3.80 \times 10^{-3} \text{ s/m}$	$\rho = 857 \text{ kg/m}^3$
$M_Y = 55.7 \text{ kg}$	$\omega_n = 126 \text{ rad/s}$	$P_s = 20.7 \text{ MPa}$
$C_d = 3.604 \times 10^{-2}$	$d_m = 1.2$	$P_r = 0$
$v_0 = 0.001$		

2.4.2 State-Space Model

A state space representation is a mathematical model of a physical system as a set of inputs and state variables related by first-order differential equations, and an algebraic output equation related to the state variables. To abstract from the number of inputs, outputs and states, the variables are expressed as vectors, and the differential and algebraic equations are written in the vector-matrix form. Having expressed the appropriate system dynamic equations in the previous section, now they are converted into the state-space form, by introducing the following six state variables of the state vector:

$$\dot{x} = [x_1 \quad x_2 \quad x_3 \quad x_4 \quad x_5 \quad x_6]^T = [x \quad \dot{x} \quad P_1 \quad P_2 \quad x_v \quad \dot{x}_v]^T \quad (2.4-8)$$

By definition and from the previous physical dynamic equations, the state equations of the hydraulic system are expressed next. First, by definition we have:

$$\dot{x}_1 = x_2 \quad (2.4-9)$$

It should be mentioned that in numerical computations, generally a threshold such as v_0 is introduced for zero in the friction equations. Keeping this in mind, using equations 2.4-1 and 2.4-9 to express \ddot{x} , the second state equation is obtained as:

$$\dot{x}_2 = \frac{1}{M} [A_1 x_3 - A_2 x_4 - f_f] \quad (2.4-10)$$

Where:

$$f_f = \begin{cases} [f_{st} - (f_{st} - f_{sl})(1 - e^{-C_b |x_2|})] \text{sign}(x_2) + dx_2 & |x_2| > v_0 \\ f_{st} & |x_2| \leq v_0 \end{cases} \quad (2.4-11)$$

Equations 2.4-4 and 2.4-5 are used to obtain the third and the fourth state equations, for \dot{x}_3 and \dot{x}_4 , as follows:

$$\dot{x}_3 = \begin{cases} \frac{\beta}{A_1 x_1 + V_h} \left[C_d A_{orifice} x_5 \sqrt{\frac{2}{\rho} (x_3 - P_r)} - A_1 x_2 \right] & x_5 \geq 0 \\ \frac{\beta}{A_1 x_1 + V_h} \left[C_d A_{orifice} x_5 \sqrt{\frac{2}{\rho} (P_s - x_3)} - A_1 x_2 \right] & x_5 < 0 \end{cases} \quad (2.4-12)$$

$$\dot{x}_4 = \begin{cases} -\frac{\beta}{A_2 (L - x_1) + V_h} \left[C_d A_{orifice} x_5 \sqrt{\frac{2}{\rho} (P_s - x_4)} - A_2 x_2 \right] & x_5 \geq 0 \\ -\frac{\beta}{A_2 (L - x_1) + V_h} \left[C_d A_{orifice} x_5 \sqrt{\frac{2}{\rho} (x_4 - P_r)} - A_2 x_2 \right] & x_5 < 0 \end{cases}$$

Similar to 2.4-9, by definition, we can write the fifth state equation, which expresses the spool valve displacement:

$$\dot{x}_5 = x_6 \quad (2.4-13)$$

By using equation 2.4-7 for \ddot{x}_v and in view of equation 2.4-13, we have the sixth state equation:

$$\dot{x}_6 = K_{sp}u - 2\omega_n d_m x_6 - \omega_n^2 x_5 \quad (2.4-14)$$

This completes the state space model.

2.4.3 Model Validation

The developed mathematical model of the hydraulic system needs to be validated experimentally with respect to actual measurements from the experimental system in order to validate the model under various operating conditions. This process also will determine the uncertainty parameter values. According to literature [4, 10-11], the amount of acceptable threshold allowed for signals simulated from a model is about 10% of the measurement from the actual system. This 10% error may be attributed to model uncertainty, for example incorporated in the disturbances of the Kalman filter algorithm (see Chapter 3).

In the present research, for calculating the error signals between the model and actual measurement, the method of *moving average error* (MAE) is used, as suggested in [4, 10-11]. In this method, the average of a certain number of error data points, between simulation and measurement, is taken at every k^{th} time step and then these average points are plotted against time. The following expression is used for calculating the MAE at each k^{th} time step in this research:

$$\mathcal{E}_k = \frac{\sum_{j=k-n}^k |\mathcal{E}_j|}{n} \quad (2.4-15)$$

Where:

\mathcal{E}_i = Error data between measured and simulated values at j^{th} time step

n = Number of error data used in calculating the average

In this research, a value of 100 is assigned for n based on the sampling time of 50 ms, and the reference signal frequency of 0.4π as mentioned in section 2.3. By choosing n as 100, MAE can be calculated for a complete motion which consists of the full retraction and full extension of the piston.

The reason for implementing the MAE scheme in our analysis is to make the difference error data smoother as it minimizes the effect of unwanted added noise and transient errors in the data.

2.4.4 Experimental Results

It is essential to establish that the model is sufficiently accurate. This means that the model can be satisfactorily represent the real system for experimentation and analysis purposes. To validate the state space model developed in this research, a low frequency reference signal of $r = 0.025 + 0.0125\sin(0.4\pi t)$ m is applied for both the experimental test rig and the state space model in the simulations, during a period of 30 seconds. Figure 2.9, Figure 2.10, and Figure 2.11 show characteristic and MAE plots for chamber 1, chamber 2, and the actuator displacement, respectively. Figures 2.9-2.11 (a), illustrate the relative accuracy of the state space model with respect to the measured values. Figures 2.9-2.11 (b) show the moving average error between the simulated and the measured values for the corresponding state as each state converges to a reasonable and acceptable value. By inspection, it can be observed that the pressures in chamber 1 and chamber 2 are about 2 MPa and 4 MPa with an MAE value of around 0.23 MPa and 0.24 MPa, respectively. The error value for actuator displacement has a steady-state value of approximately 2 mm as shown in Figure 2.11 (b).

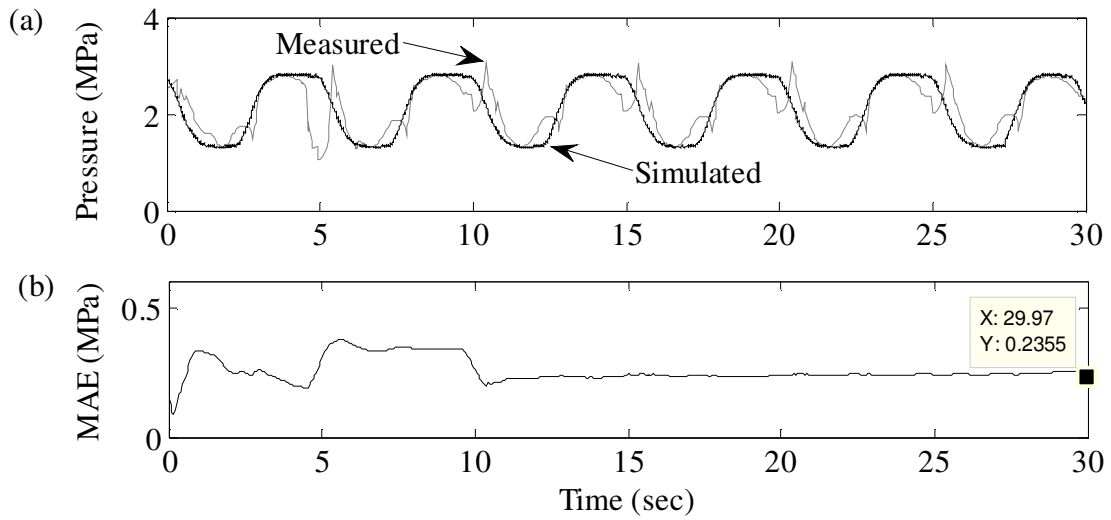


Figure 2.9: (a) Characteristic Plots for Simulated versus Measured Pressure in Chamber 1, (b) Plot of MAE between Simulated and Measured Pressures

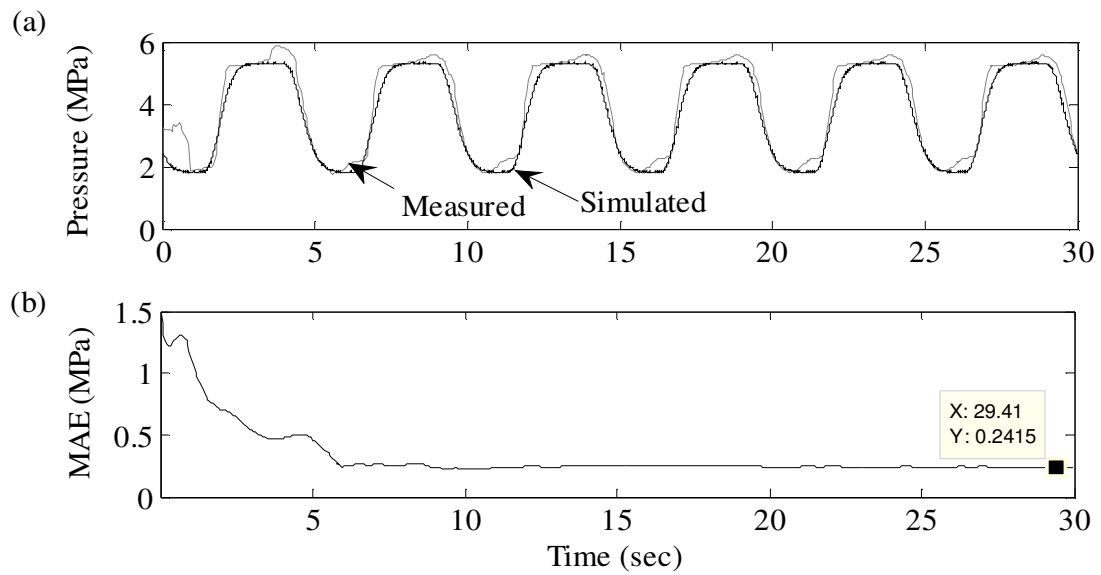


Figure 2.10: (a) Characteristic Plots for Simulated versus Measured Pressure in Chamber 2, (b) Plot of MAE between Simulated and Measured Pressures

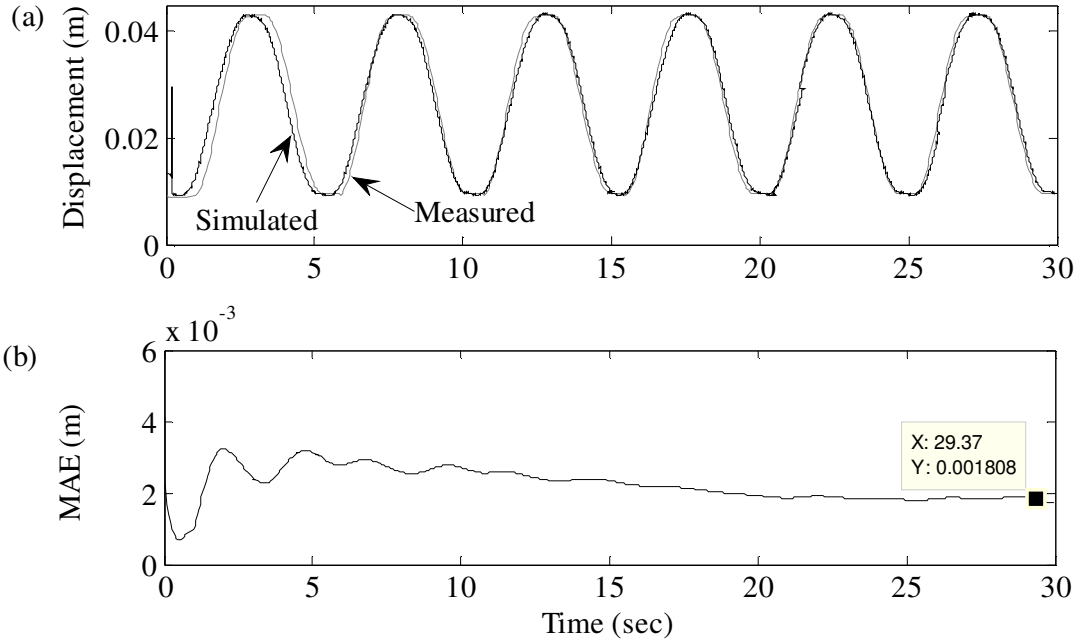


Figure 2.11: (a) Characteristic Plots of Actuator Displacement- Simulated and Measured Results, (b) Plot of MAE between Simulated and Measured Results

As mentioned in the previous sections, the target of model validation is that the MAE value of the signals from the model stays within 10% of the measured ones. From the MAE curves it is evident that all the simulated signals have converged to satisfactory values as needed.

2.4.5 Frequency Range

In this part of experimentation, a sinusoidal time varying frequency with a constant-amplitude position reference signal of $r = 0.025 + 0.0125 \sin\left(0.3\left(1 + \frac{t}{4}\right) t\right)$ is applied to both the state-space model and the actual hydraulic test-rig. The differences in signals between the measured and simulated results are shown in Figures 2.12 to 2.14.

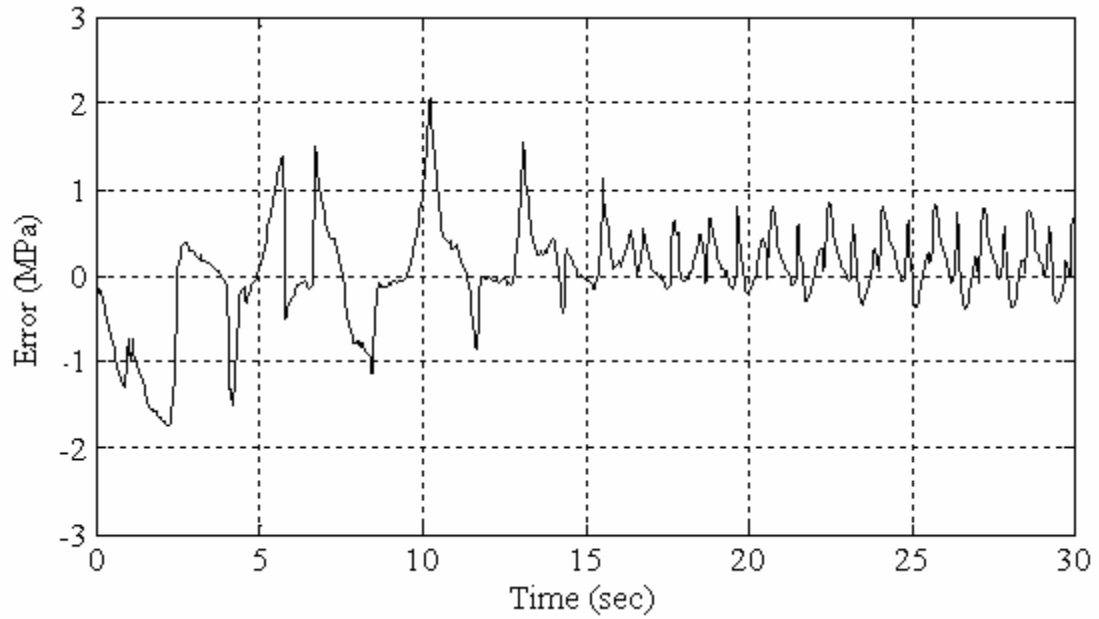


Figure 2.12: Error in Chamber 1 Pressure between Measured and Simulated Signals

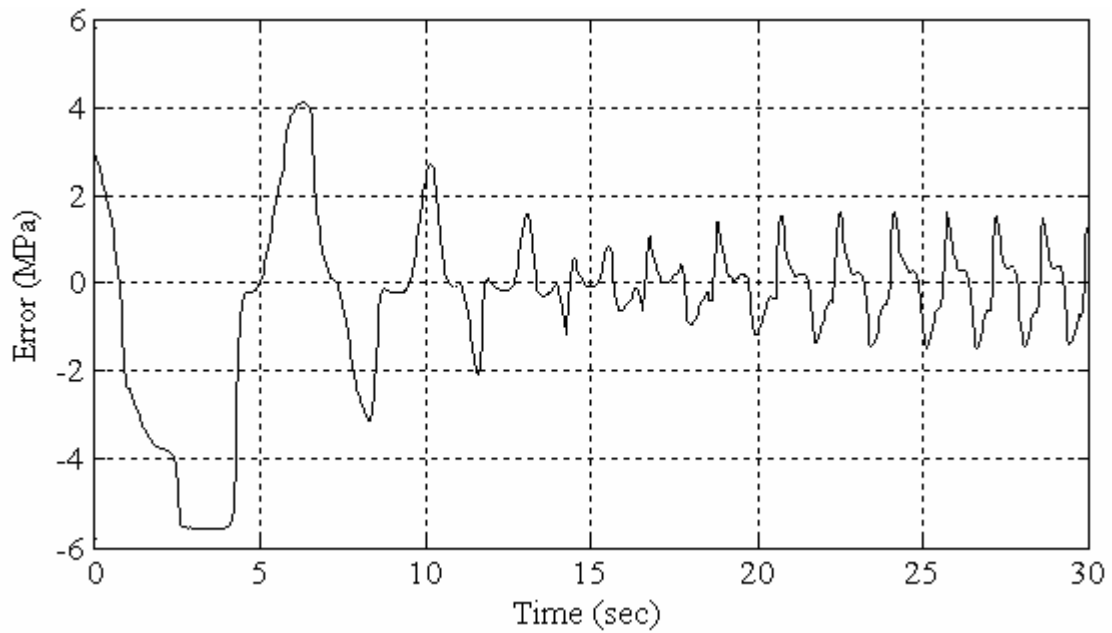


Figure 2.13: Error in Chamber 2 Pressure between Measured and Simulated Signals

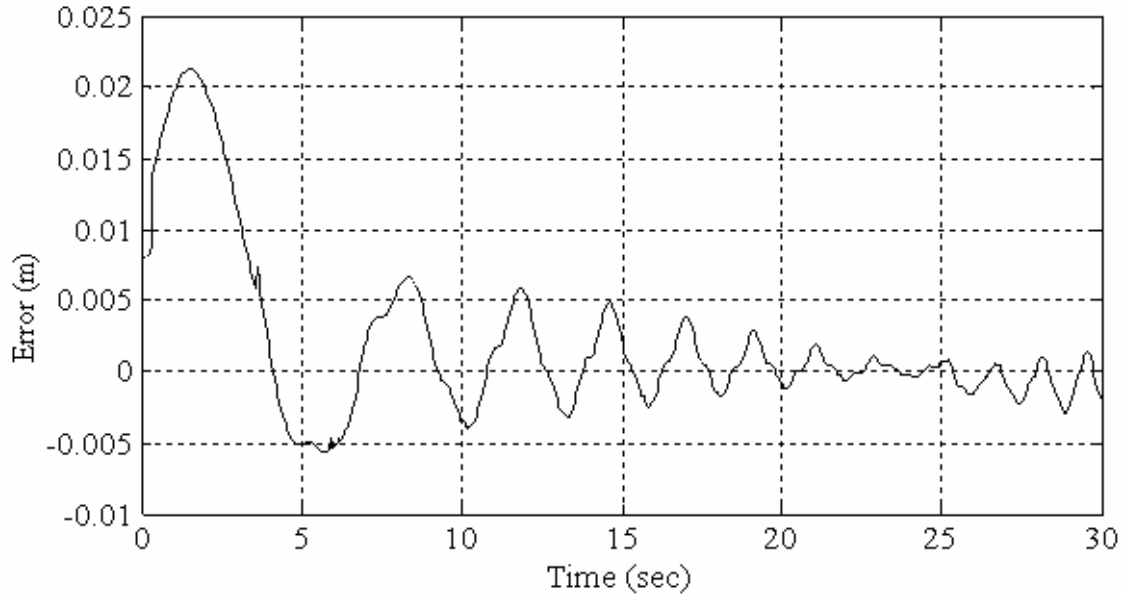


Figure 2.14: Error in Displacement between Measured and Simulated Signals

For the hydraulic system under study in the present research, the typical ranges of practical operating frequencies are between 0.05 Hz to 0.5 Hz. As shown in the above figures, the signal errors have attained stable and constant amplitude and stayed within a satisfactory boundary. This is due to the fact that as time (t) increases, the frequency increases and the amplitude of both state-space model and the measured signals decrease at the same rate. As seen in these curves, in the first few seconds of the run, the actuator had to be brought to the midpoint and as the result there is an increase in the amplitude. However, as the actuator reaches the center point, the amplitude reduces to the desired and bounded value. In this work, all experiments are carried out at the frequency of 0.2 Hz.

2.4.6 Repeatability of Experiments

In the present experimentation it is desired to have a constant operating condition (e.g., the same environment, fluid temperature, supply pressure, oil viscosity, instruments and equipment) throughout the process in every experiment. Failure to meet this requirement may make the obtained data unreliable non-comparable. The temperature of the environment was measured to be about 17°C and the operating supply pressure was around 20.7 MPa. In order to illustrate these desired conditions, as an example, a curve is plotted for the repeatability of the pressure in chamber 1, as given in Figure 2.15.

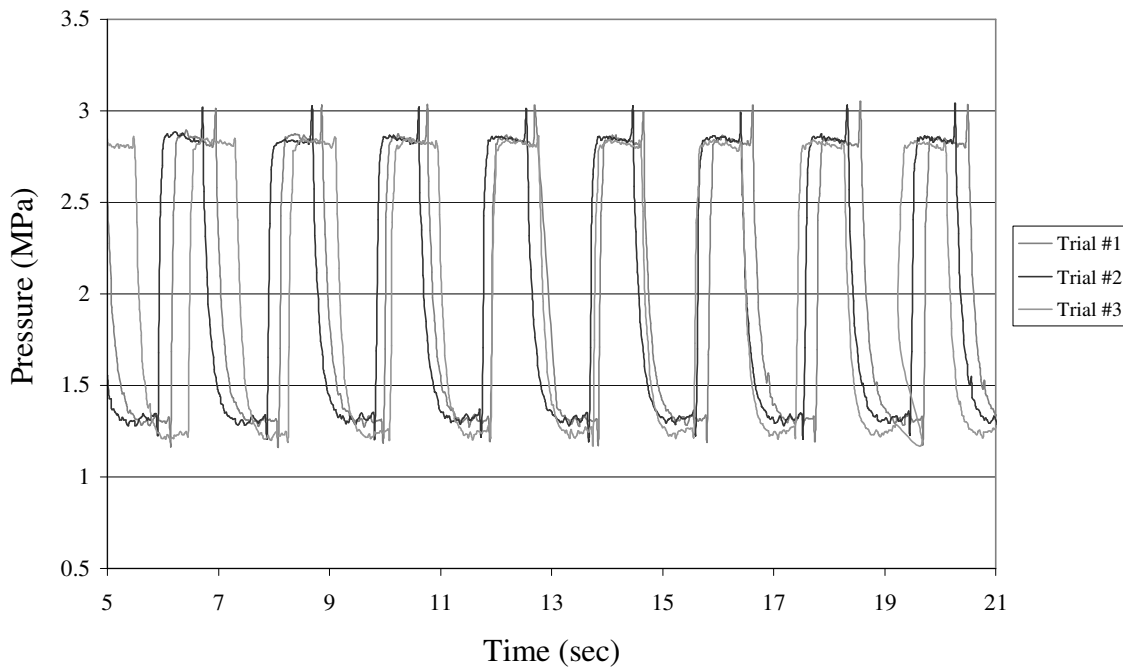


Figure 2.15: Pressure Repeatability Data for Chamber 1

The test rig is run at three different times of the day (morning, noon and evening) and three sets of measurements are taken under the same operating conditions. Visually it is verified that the data for all three trials are practically the same, following a similar trend and having almost the same magnitude and the time period.

Chapter 3

Implementation of UKF in Fault Monitoring Scheme

3.1 Introduction

The term “fault” in a system refers to an unwanted deviation of at least one feature of a system property from the acceptable, standard and usual condition [23]. This can lead to a “failure” which is a permanent disruption of a system’s ability to perform the required function under specific operating conditions.

For the improvement of reliability, safety and efficiency, advanced methods of monitoring, fault-detection and fault diagnosis become increasingly important. This holds especially for safety related processes like aircraft, trains, automobiles, power plants and chemical plants. In some cases, such as in aircraft and vehicles, the control task, reliability and safety depend heavily on the correct functioning of all process parts such as actuators, sensors and related hardware. Failure in such systems must be removed immediately to avoid catastrophic damages and possible loss of human life.

Classical approaches of fault detection are limited to trend checking of some measurable output variables and thus, they do not give a deeper insight and usually do not allow a proper fault diagnosis. With this simple method, typically the faults are detected with much delay and a detailed fault diagnosis not possible. Methods of modern systems theory enable the systematic use of mathematical models of processes and signals, and methods of identification and estimation. These advanced methods allow development of fault detection and diagnosis techniques [24].

In this chapter, schemes of condition monitoring that are relevant to the current study are indicated in some detail. Specifically, the Unscented Kalman Filtering (UKF) is investigated with respect to detecting and diagnosing faults in a hydraulic system. The organization of the material in this chapter is as follows: in section 3.2 classifications of techniques in fault monitoring are discussed. This is followed by explaining the Kalman filter algorithm for linear systems, in section 3.3. Introduction of UKF and its applications in the present study are discussed in sections 3.4 and 3.5.

3.2 General Techniques of Fault Monitoring

Methods of fault diagnosis are usually categorized based on the usage of *a priori* knowledge—the relation between the failure and the observations. For instance, in order to accurately design a controller, sufficient knowledge about the plant (e.g., accurate dynamic model). This may come from the physics and the fundamentals of the system, experience and experimentation. Fault diagnosis schemes can be categorized into two groups: *model-based* and *signal-based* schemes [25-26]. In a model-based scheme, the fault monitoring system requires a dynamic model of the plant that is being monitored. In some cases, due to system complexity, unknowns, and modeling difficulties, a signal-based scheme may be advantageous in system monitoring and fault diagnosis. These two approaches are each classified into two subgroups: *quantitative based* and *qualitative based*.

3.2.1 Model-based Fault Diagnosis Approach

The following sections discuss various techniques that can be used in monitoring and fault diagnosis of a system using the model-based approach.

3.2.1.1 Quantitative Approach

In the qualitative approach, an in-depth understanding of the exact system behavior and the reasons that govern such behavior are gathered qualitatively. However, in quantitative approaches, they rely mostly on previously available data and information. More emphasis has been traditionally placed upon quantitative approaches of model-based fault diagnosis, and these rely on detailed knowledge of a dynamic model of the system. A model will provide details about the changes in system dynamics. The major emphasis in the field of quantitative model-based fault diagnosis has been placed upon methods of detecting and isolating faults rapidly and accurately [26].

Most studies done in the quantitative model-based approach rely on forming residual errors from a state-space model. This approach uses state equations (state-space model), state observers and parity space relations. Next these classifications are discussed in detail.

1) Physical Equations

In general, a complete model of a system can be directly obtained from physical equations [27]. These models are generated on the basis of the understanding of the physical system and they describe the relationships that exist between the process

variable. Typically they allow detecting faults of small size. The drawback to this method is that the development of an accurate model using physical equations can be extremely difficult and sometimes impossible for many systems. The parameter identification also adds another difficulty into this technique.

2) State Equations of Linear Systems

A dynamic stationary linear system that has “ b ” inputs and “ c ” outputs can be described in continuous time by following equations:

$$\begin{aligned}\dot{x}(t) &= Ax(t) + Bu(t) \\ y(t) &= Cx(t) + Du(t)\end{aligned}$$

These state equations are the basis for residual generation and the design of diagnostic observers [28].

3) State Observers

Design of an observer in control systems makes it possible to generate residuals which can be used to express the state variables of a dynamic system based on the actual input and output signals as obtained from sensors. A popular technique in this field is the Kalman Filter. The prediction of errors by Kalman filter can be used as a fault detection residual. Then, a zero mean residual will represent a no fault condition in the system and a non-zero mean residual will indicate the presence of a fault.

4) Parity Space Relations

Parity space fault diagnosis techniques are used to detect abnormal operation of dynamic processes and diagnose sensor and actuator faults. Parity relations can be

defined as balance equations that are based on the input-output data of the system. First, the process model between the plant inputs and plant outputs is developed. Then the parity residuals are formed to examine the consistency of the model with sensor data and known system input [29].

3.2.1.2 Qualitative Approach

Qualitative model-based approaches are mostly classified into diagraphs, fault trees and qualitative physics. This classification is discussed next.

1) Signed Graphs

Signed digraphs (SDG), which can describe target systems as qualitative network models with nodes and branches, provide a new approach to describe large-scale systems. In this formulation, the propagation principle of fault evolution in a complicated system can be explored and the inference can be applied to accomplish hazard and risk assessment or fault diagnosis. The SDG concept and method for fault diagnosis were first presented by Iri et al. in 1979 [30]. The SDG method can save time, manpower, and cost, and it is known to possess good maturity and in-depth reasoning ability.

2) Fault Trees

Fault Tree Analysis (FTA) can model and analyze failure processes of engineering systems. FTA is basically composed of logic diagrams that display the state of the system and is constructed using graphical design techniques. FTA can be used as a valuable design tool, can identify potential accidents, and can eliminate costly design

changes. It can also be used as a diagnostic tool, predicting the most likely system failure in a system breakdown. FTA is used in safety engineering and in major fields of engineering.

3) Qualitative Physics Classes

In fault diagnosis approaches, qualitative physics mostly concern the behavior of the physical system based on reasoning using artificial intelligence [4]. This technique deals with qualitative equations which are derived using knowledge and experience.

3.2.2 Signal-based Fault Diagnosis Approach

These methods of faults diagnosis do not use a mathematical model of the plant and they range from physical redundancy and special sensors through limit-checking and spectrum analysis to logic reasoning. Next, these methods are discussed in point form rather than in detail for the sake of introducing the existing approaches, pointing out that the signal-based approach is not the main objective of the present research. More information is found in [3], which discusses fault monitoring in engineering systems.

1) Physical Redundancy

In this approach, the same physical quantity is measured using multiple sensors installed on the machine. Any serious discrepancy between measurements indicates a sensor fault.

2) Special Sensors

Special sensors are designed specifically for designated task, such as measurement of pressure (pressure transducers), temperature and vibration, which can perform limit checking in hardware.

3) Limit Checking

In this approach, once the signals are received by the hardware, the thresholds are compared to the preset limits, and fault situations are identified if any of the thresholds are exceeded. Various methods of warning are used in industries, and can vary from pre-warning to emergency warning, which may shut down the entire operation. This capability has made the approach popular and widely used in industry.

4) Spectrum Analysis

This method is based on measuring the frequency spectrum of the variables of the operational plant. Each variable has a typical frequency spectrum and any deviation may indicate a fault in the system.

5) Neural Network Models

Artificial neural networks (ANN) can be applied to model complex and nonlinear dynamic systems and can be trained using measurement data. ANN are made up of interconnecting artificial neurons that mimic the properties of biological neurons. They may be used to solve artificial intelligence problems without necessarily creating an analytical model of the system. The important advantages of ANN are the ability of

modeling nonlinearities, high robustness to disturbance, and the ability to generalizing knowledge contained from the network. More discussion on this topic can be found in [31].

6) Expert System

As discussed by de Silva [32], an expert system attempts to reproduce the performance of one or more human experts, most commonly in a specific problem domain, and is a traditional application and/or subfield of artificial intelligence. Expert systems have a common element in that once the system is developed it is proven by being placed in the same real world problem solving situation. Typically it can be used as an aid to human workers or experts or a supplement to an information system.

3.3 Kalman Filtering in Fault Diagnosis

There are also many examples in engineering where filtering is desirable. Radio communication signals are often corrupted with noise. A good filtering algorithm can remove the noise from electromagnetic signals while still retaining the useful information. Many countries require in-home filtering of power line voltages before supplying them to personal computers and peripherals. Without filtering, the power fluctuations would drastically shorten the lifespan of these devices.

The Kalman filter is a recursive estimator. This means that only the estimated state from the previous time step and the current measurement are needed to compute the estimate for the current state. Kalman filtering was developed in the 1960s and has been applied in areas as diverse as aerospace, marine navigation, nuclear power plant instrumentation, demographic modeling, manufacturing, and many others.

3.3.1 Fundamentals of Kalman Filter

Kalman filter is based on a linear dynamical system, and it may be discretised in the time domain. Its future state depend only on the present state, and not on the past state. The state of the system is represented as a vector of state variables. At each discrete time increment, a linear operator is applied to the state to generate the new state, where noise is included. Another linear operator generates the outputs from the hidden state vector, including additive noise. Inputs to the algorithm are the model, noise parameters, and measurements from the system. Two types of noises are used in Kalman

Filters: measurement noise, which disrupts the response of the system during measurement, and process noise or disturbances that exist at the system input.

In order to use the Kalman filter to estimate the internal state of a process, given a sequence of noisy observations, one must model the process in accordance with the framework of the Kalman filter. The Kalman filter model in discrete-time assumes that the true state at time $k+1$ is evolved from the state at (k) according to:

$$x_{k+1} = Ax_k + Bu_k + w_k \quad (3.1)$$

Here A and B are the matrices of the state space model, as discussed in Chapter 2, but properly discretized with respect to time.

Process noise may not always have direct physical meaning, and may represent model uncertainties. The Kalman filter formulation requires that the measurements be linearly related to the states according to:

$$y_k = Hx_k + v_k \quad (3.2)$$

Here H is the output/measurement matrix. Also, x is the state vector, y is the system output, u is the system input, w is the process/input noise and v is the measurement noise which are all expressed as vectors. There is a process noise covariance matrix Q corresponding to the process noise vector according to:

$$Q_k = E[w_k w_k^T] \quad (3.3)$$

The measurement noise covariance matrix R is related to the measurement noise vector v according to:

$$R_k = E[v_k v_k^T] \quad (3.4)$$

Since the filter state estimation is done on the basis of predicted-corrected approach, before proceeding further, the two important key equations must be defined: a

priori (predicted) and *a posteriori* (corrected) state estimate vector. The predicted (*a priori*) state estimate vector equation at time step (k) uses the corrected (*a posteriori*) state estimate vector from the previous time step ($k-1$) and the known system input to write the following “time update” equation:

$$\hat{x}_k^- = A\hat{x}_{k-1} + Bu_k \quad (3.5)$$

Using the information from the current observation and the given residual, which is the difference between the measured and predicted outputs, the corrected (*a posteriori*) state estimate vector equation written in the following form:

$$\hat{x}_k = \hat{x}_k^- + K_k (y_k - H\hat{x}_k^-) \quad (3.6)$$

Where:

$(y_k - H\hat{x}_k^-)$: State residual

K_k : Kalman filter gain

It is appropriate to discuss few points observed in equation 3.6. In real-time fault diagnosis y_k is the output from the sensors. However, for simulation purposes, equation 3.2 should be used for calculating y_k . Accurate state estimation is desired here and therefore it is desirable to have *a posteriori* state vector equal to the *a priori* state vector, $\hat{x}_k = \hat{x}_k^-$ resulting in a zero residual or $(y_k - H\hat{x}_k^-) = 0$. In order to minimize the error for the filter estimation in both stages of prediction and correction, the Kalman gain function is defined as:

$$K_k = P_k^- H^T (HP_k^- H^T + R)^{-1} \quad (3.7)$$

Where:

P_k^- = Minimized *a priori* estimate error covariance

P_k = Minimized *a posteriori* estimate error covariance

Covariance is a measure of how much two variables are related. In these equations, covariance matrices P_k^- and P_k represent errors in the state estimates before and after an update, respectively. The equations are as follows:

$$P_k^- = AP_{k-1}A^T + Q \quad (3.8)$$

$$P_k = (I - K_k H)P_k^- \quad (3.9)$$

At the start of the operation, the Kalman filter algorithm requires some initial estimates for state variable values, x_k , and *a posteriori* estimate of the error covariance, P_0 , since these estimates are needed in the first step which is “Time Update” stage. Zarchan and Musoff [33] gives the details of Kalman filtering and its practical approach. Zheng et al. [34] have constructed different Kalman filters for a networked control system according to different system faults. Respective residues were generated and a fault detection and isolation (FDI) approach was introduced. Pirmoradi et al. [35] in 2007 developed a new scheme for fault detection and diagnosis in spacecraft Attitude Determination (AD) sensors. In their work, measurement data from all sensors are fused by a linearized Kalman filter, and fault isolation is performed through Extended Kalman Filters (EKF). Xue et al. [36] implemented a robust Kalman filter and a bank of Kalman filters in fault detection and isolation (FDI) of sensors and actuators of an aircraft gas turbine engine. The block diagram given in Figure 3.1 [4] illustrates the structure of a working Kalman filter.

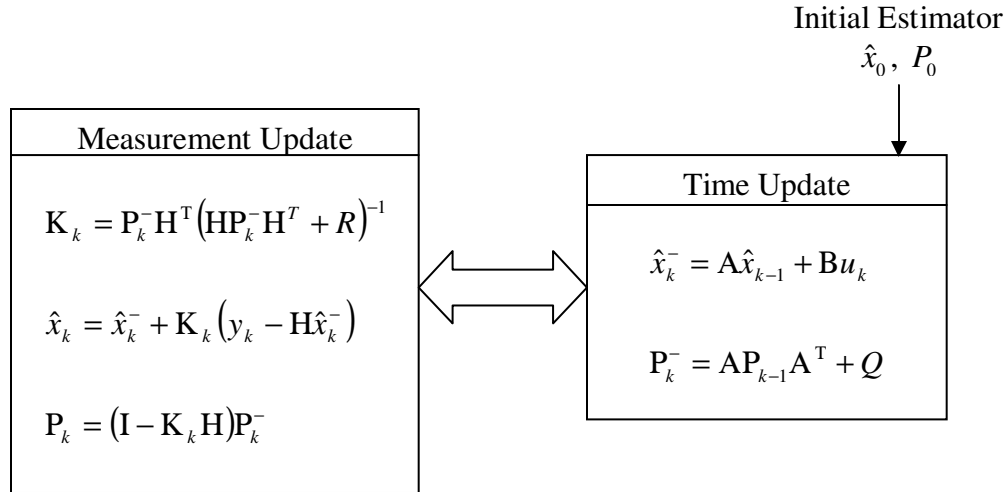


Figure 3.1: Block Diagram of Working Kalman Filter

3.3.2 Extended Kalman Filter

In the previous section we discussed how a linear Kalman filter is designed, when the system is described by linear differential equations expressed in the state-space form and when the measurements are linear functions of the states. However, in most engineering problems, nonlinearities are unavoidable. The Extended Kalman Filter (EKF) has become a standard technique for nonlinear estimation and machine learning applications [37]. These include estimating the state of a nonlinear dynamic system, and estimating parameters for nonlinear system identification where both states and parameters are estimated simultaneously. In EKF, the covariance is determined by linearizing the dynamic equations at each time step around the last state or the current estimate, and then determining the posterior covariance matrices analytically for the linear system; i.e., performing the “Time Update” and “Measurement Update.”

Unlike its linear counterpart, the extended Kalman filter in general is not an optimal estimator (it is optimal if the measurement and the state transition model are both

linear) [38, 39]. If the initial estimate of the state is wrong, or if the process is modeled incorrectly, the filter may quickly diverge, owing to its linearization. Another problem with the extended Kalman filter lies in the estimation of the covariance matrices. It is likely that the estimated state for a real system vary from the actual current state of the system (i.e., estimated covariance matrix tends to underestimate the true covariance matrix). This difference may lead to instability of the procedure. In this case it is common to add an external signal, stabilizing noise, to the system in order to overcome this instability.

Linearization that is needed in EKF generates unreliable estimates in highly nonlinear systems. When one applies an EKF to a complex system, a major problem arises in the computation of the state transition matrix which calls for calculation of the Jacobian matrix (a matrix of partial derivatives). This process essentially linearizes the nonlinear function around the current estimate. Besides being a computationally expensive operation, there is no universal and robust numerical way to carry it out.

Due to the reasons of difficulty in implementing and linearization error, it is agreed that EKF is only reliable for first order system derivatives which are not highly nonlinear. The second order filters provide better estimation performance. However, the implementation is more difficult and derivatives should be calculated analytically. In many applications second order derivatives will not be available analytically and approximations will inevitably be subjected to error. The solution to this problem is the use of unscented transformation (UT) which is discussed in the next section.

3.4 Unscented Kalman Filter

When the state transition and observation models, which are the predicting and updating functions in equations 3.1 and 3.2, are highly nonlinear, the extended Kalman filter can give particularly poor performance. This is because in that approach the nonlinear states and parameters are approximated. In 1997, Julier and Uhlmann [37] introduced Unscented Kalman Filtering (UKF) which employs an unscented transformation (UT) to pick a minimal set of sample points (called sigma points) around the mean. These sigma points are then propagated through nonlinear functions, from which the mean and covariance of the estimate are then recovered.

3.4.1 Unscented Transformation

As mentioned, the unscented Kalman filter (UKF) uses the unscented transformation to pick sigma points around the mean. These sigma points are then propagated through nonlinear functions, from which the mean and covariance of the estimate are then recovered. The result is a filter which more accurately captures the true mean and covariance. In addition, this technique removes the requirement to explicitly and precisely calculate Jacobians, which for complex functions can be a difficult and time consuming task, requiring complicated derivatives if done analytically or having a high computational cost if done numerically. Julier and Uhlmann [38, 40-41] introduced unscented transformation which uses sampled data to calculate the mean and the covariance. It is founded on the intuition that it is easier to approximate a Gaussian distribution than it is to approximate an arbitrary nonlinear function. The approach is

illustrated in Figure 3.2. A set of point (sigma points) are chosen whose sample mean and sample covariance are \bar{x} and P_{xx} , respectively. The nonlinear function, $y = h(x)$, is applied to each point to yield a cloud of statistically transformed points \bar{y}_u and P_u .

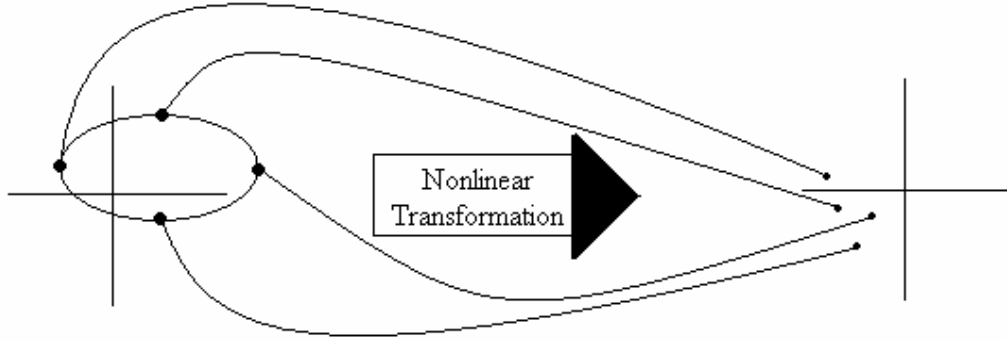


Figure 3.2: Unscented Transformation Scheme.

The following algorithm is used for the nonlinear transformation by forming a vector of $2n$ sigma points:

$$\begin{aligned}
 \tilde{x}^{(i)} &= \left(\sqrt{nP}\right)_i^T & i &= 1, \dots, n \\
 \tilde{x}^{(i+n)} &= -\left(\sqrt{nP}\right)_i^T & i &= 1, \dots, n \\
 \tilde{x}^{(i)} &= \bar{x} + \tilde{x}^{(i)} & i &= 1, \dots, 2n
 \end{aligned} \tag{3.10}$$

where $\left(\sqrt{nP}\right)$ is the matrix square root of nP , which is defined as $\left(\sqrt{nP}\right)^T \sqrt{nP} = nP$ and $\left(\sqrt{nP}\right)_i$ is the i^{th} row of the $\left(\sqrt{nP}\right)$. No linearization is used in this method. In the next step, the calculated sigma points are propagated through the nonlinear function of $y^{(i)} = h(x^{(i)})$ for the range $i = 1, \dots, 2n$. The statistically transformed points \bar{y}_u and P_u are obtained using the following equations:

$$\begin{aligned}\bar{y}_u &= \frac{1}{2n} \sum_{i=1}^{2n} y^{(i)} \\ P_u &= \frac{1}{2n} \sum_{i=1}^{2n} (y^{(i)} - \bar{y}_u)(y^{(i)} - \bar{y}_u)^T\end{aligned}\tag{3.11}$$

3.4.2 Performance Comparison between UT and EKF

From the previous sections it is seen that the unscented algorithm is able to partially incorporate information of higher order in nonlinearity, leading to greater accuracy than what is possible with EKF. A study is done by Simon on UT characteristics and accuracy against EKF [42]. He compared the exact, linearized and unscented mean and covariance of randomly generated points as shown in Figure 3.3.

In this experiment, sensors measure and sample two motion variables (polar coordinates) r and θ at each time step and the points are then transformed and converted into rectangular (Cartesian) coordinate Y_1 and Y_2 using following familiar equations:

$$\begin{aligned}Y_1 &= r \cdot \sin \theta \\ Y_2 &= r \cdot \cos \theta\end{aligned}\tag{3.12}$$

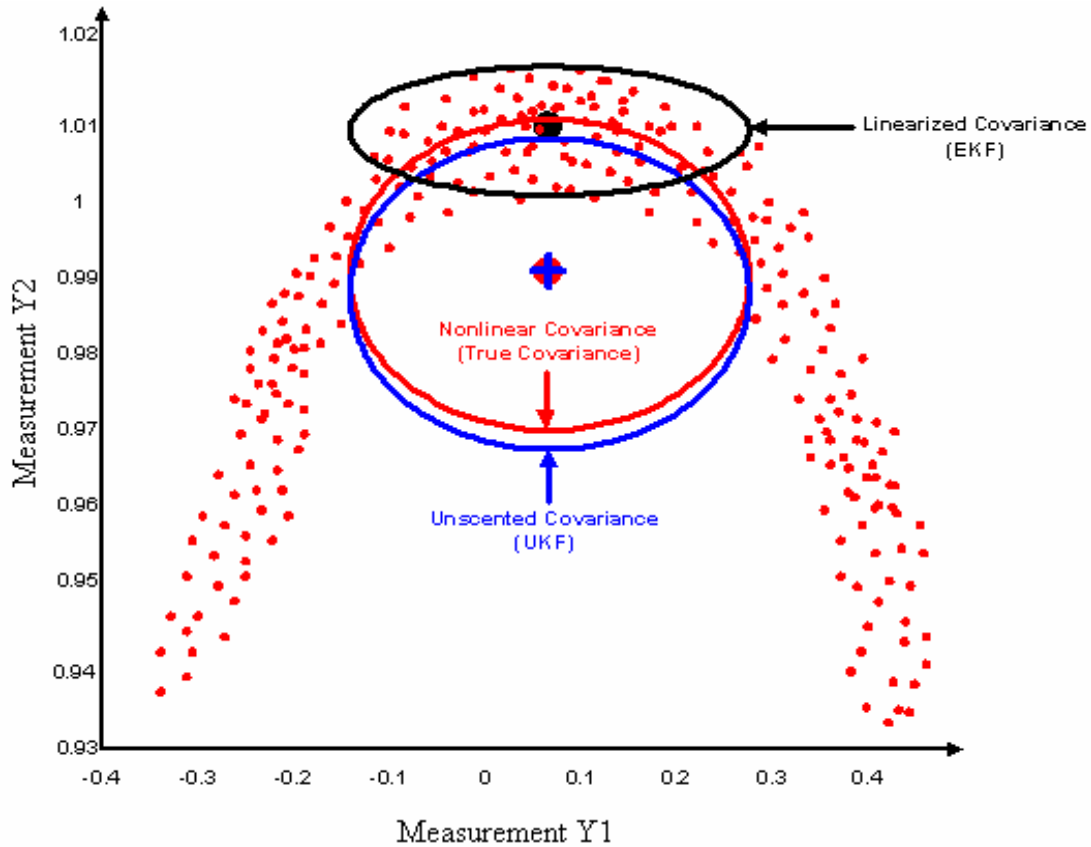


Figure 3.3: Comparison between UT and EKF

As observed in the above figure, the unscented covariance calculated using UT is much closer to the actual nonlinear covariance than that calculated using EKF. In particular, the mean computed using UT virtually coincides with the actual mean of the nonlinear data whereas with EKF, the mean falls far away from the desired location. Therefore, it is concluded that the UT is better suited than a first-order linearization method. As it is reasoned out in [37, 43], EKF is good only for predicting mean and covariance with first order accuracy. However, a filter that uses the unscented transform will have the estimates closer to real values due to the higher order accuracy for Gaussian inputs.

3.4.3 Unscented Kalman Filter (UKF) Algorithm

The UKF algorithm tries to propagate the mean and covariance of a system using time-update and measurement update. The transformation process is similar to the ordinary Kalman filter which includes the following:

- 1) Predict the new state of the system and its associated covariance taking into account the effect of observation noise
- 2) Predict the expected observation and the improved covariance taking into account the effect of observation noise
- 3) Predict the cross-correlation matrix

In recent years a new technique of UKF has been used by researchers to estimate the state of nonlinear systems, which minimizes the prediction errors, for application in the field of fault diagnosis [38-43]. The following equations explain the algorithm used in the UKF which is an extension to UT:

- 1) Consider an n -state discrete-time nonlinear system at step k , with f and h representing the nonlinear state function and the measurement function, respectively, given by

$$\begin{aligned}x_{k+1} &= f(x_k, u_k, t_k) + w_k \\y_k &= h(x_k, t_k) + v_k \\w_k &\approx (0, Q_k) \\v_k &\approx (0, R_k)\end{aligned}\tag{3.13}$$

- 2) Initialize the filter using the following equations:

$$\begin{aligned}\hat{x}_0 &= E(x_0) \\P_0 &= E[(x_0 - \hat{x}_0)(x_0 - \hat{x}_0)^T]\end{aligned}\tag{3.14}$$

The next step uses the “Time Update” equations which propagate the state estimate and covariance from one measurement time to the next.

3) Initially choose a set of sigma points to propagate from time step $(k-1)$ to k :

$$\begin{aligned}\tilde{\mathbf{x}}^{(i)} &= \left(\sqrt{n\mathbf{P}_{k-1}}\right)_i^T & i &= 1, \dots, n \\ \tilde{\mathbf{x}}^{(i+n)} &= -\left(\sqrt{n\mathbf{P}_{k-1}}\right)_i^T & i &= 1, \dots, n \\ \tilde{\mathbf{x}}_{k-1}^{(i)} &= \hat{\mathbf{x}}_{k-1} + \tilde{\mathbf{x}}^{(i)} & i &= 1, \dots, 2n\end{aligned}\quad (3.15)$$

4) Transform the Sigma points into the $\hat{\mathbf{x}}_k^i$ vector and combine to obtain the *a priori* state estimate $\hat{\mathbf{x}}_k^-$ and its predicted error covariance (by taking process noise into account) \mathbf{P}_k^- , at time k :

$$\hat{\mathbf{x}}_k^{(i)} = f\left(\hat{\mathbf{x}}_{k-1}^{(i)}, \mathbf{u}_k, t_k\right) \quad (3.16)$$

$$\hat{\mathbf{x}}_k^- = \frac{1}{2n} \sum_{i=1}^{2n} \hat{\mathbf{x}}_k^{(i)} \quad (3.17)$$

$$\mathbf{P}_k^- = \frac{1}{2n} \sum_{i=1}^{2n} \left(\hat{\mathbf{x}}_k^{(i)} - \hat{\mathbf{x}}_k^-\right) \left(\hat{\mathbf{x}}_k^{(i)} - \hat{\mathbf{x}}_k^-\right)^T + \mathbf{Q}_{k-1} \quad (3.18)$$

Now the “Measurement Update” has to be implemented since the “Time Update” step has been completed. However, to save the computational effort, instead of generating a new set of sigma points, the same sigma points generated in the “Time Update” step are used. Accordingly, as before, the predicted observation vector $\hat{\mathbf{y}}_k$ and its predicted covariance \mathbf{P}_y are obtained using following equations:

$$\hat{\mathbf{y}}_k^{(i)} = h\left(\hat{\mathbf{x}}_k^{(i)}, t_k\right) \quad (3.19)$$

$$\hat{\mathbf{y}}_k = \frac{1}{2n} \sum_{i=1}^{2n} \hat{\mathbf{y}}_k^{(i)} \quad (3.20)$$

$$P_y = \frac{1}{2n} \sum_{i=1}^{2n} (\hat{y}_k^{(i)} - \hat{y}_k) (\hat{y}_k^{(i)} - \hat{y}_k)^T + R_k \quad (3.21)$$

5) To estimate the similarities between \hat{x}_k^- and \hat{y}_k , the cross covariance matrix is calculated using the following expression:

$$P_{xy} = \frac{1}{2n} \sum_{i=1}^{2n} (\hat{x}_k^{(i)} - \hat{x}_k^-) (\hat{y}_k^{(i)} - \hat{y}_k)^T \quad (3.22)$$

6) In the concluding step of the algorithm, we calculate the filter gain K_k , the final updated state estimate \hat{x}_k^- , and the covariance P_k . The equations are as follows:

$$K_k = P_{xy} P_y^{-1} \quad (3.23)$$

$$\hat{x}_k = \hat{x}_k^- + K_k (y_k - \hat{y}_k) \quad (3.24)$$

$$P_k = P_k^- - K_k P_y K_k^T \quad (3.25)$$

The schematic block diagram shown in Figure 3.4 gives the structure of the UKF algorithm.

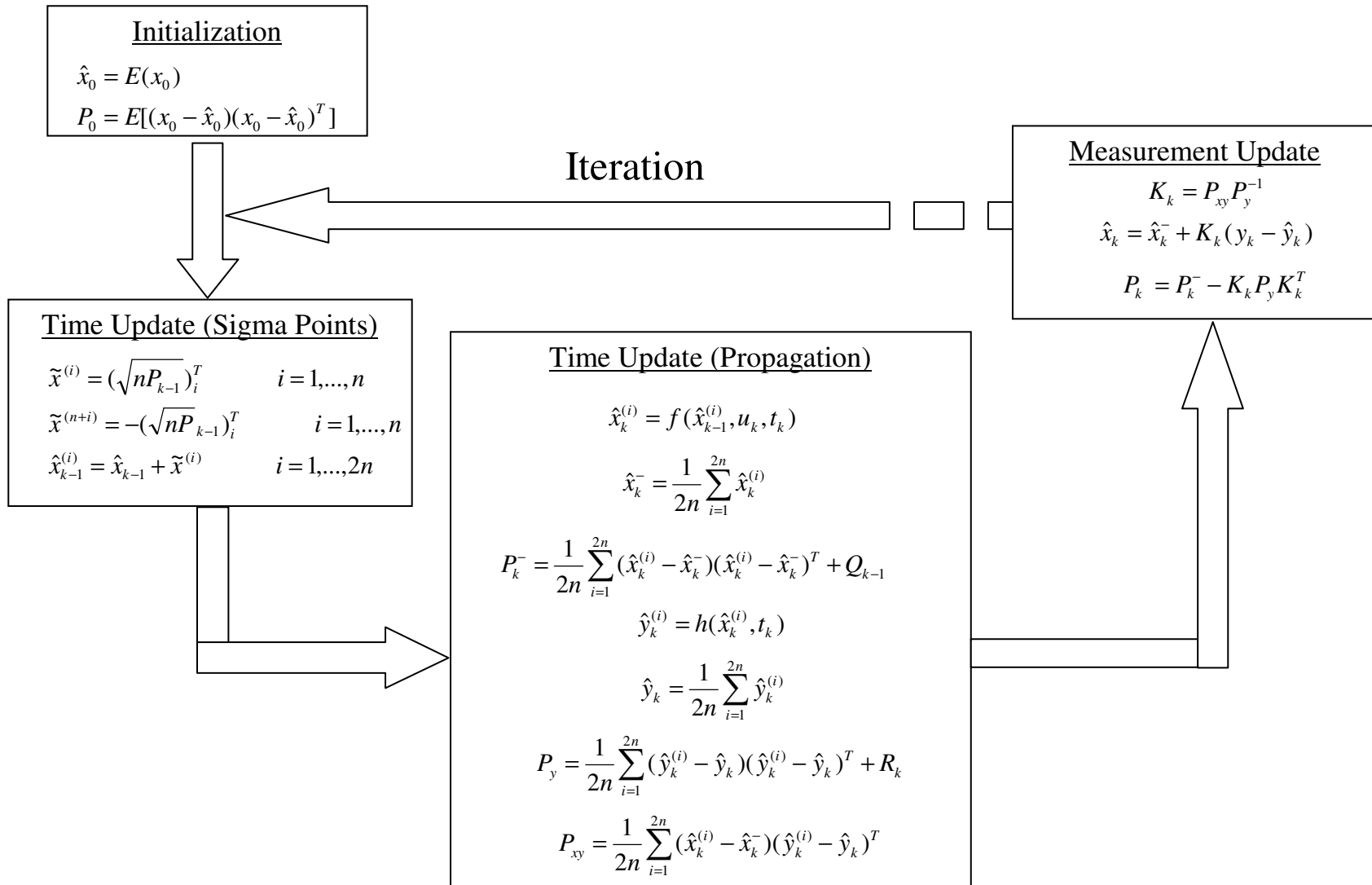


Figure 3.4: Schematic Block Diagram of UKF

3.5 UKF Application in Hydraulic System

The state space model of the dynamic system (hydraulic actuator system) as developed and validated in Chapter 2 is used now to implement and evaluate the Unscented Kalman Filter algorithm.

3.5.1 Discretised Dynamic Model

The state space model developed in Chapter 2 is discretised with respect to time using the sampling time T and the process time step k for implementation in the discrete-time UKF algorithm. Specifically, using the forward difference method, we have:

$$x_1(k+1) = Tx_2(k) + x_1(k)$$

$$x_2(k+1) = \frac{T}{M_y} (A_1x_3(k) - A_2x_4(k) - f_f(k)) + x_2(k)$$

Where:

$$f_f = \begin{cases} [f_{st} - (f_{st} - f_{sl})(1 - e^{-C_b|x_2(k)|})] \text{sign}(x_2(k)) + dx_2(k) & |x_2(k)| > v_0 \\ f_{st} & |x_2(k)| \leq v_0 \end{cases}$$

$$x_3(k+1) = \begin{cases} \frac{T\beta}{A_1x_1(k) + V_h} \left[C_d A_{orifice} x_5(k) \sqrt{\frac{2}{\rho} (x_3(k) - P_r)} - A_1x_2(k) \right] + x_3(k) & x_5(k) > 0 \\ \frac{T\beta}{A_1x_1(k) + V_h} \left[C_d A_{orifice} x_5(k) \sqrt{\frac{2}{\rho} (P_s - x_3(k))} - A_1x_2(k) \right] + x_3(k) & x_5(k) < 0 \end{cases}$$

$$x_4(k+1) = \begin{cases} -\frac{T\beta}{A_2(L-x_1(k))+V_h} \left[C_d A_{orifice} x_5(k) \sqrt{\frac{2}{\rho}(P_s-x_4(k))} - A_2 x_2(k) \right] + x_4(k) & x_5(k) > 0 \\ -\frac{T\beta}{A_1(L-x_1(k))+V_h} \left[C_d A_{orifice} x_5(k) \sqrt{\frac{2}{\rho}(x_4(k)-P_r)} - A_2 x_2(k) \right] + x_4(k) & x_5(k) < 0 \end{cases}$$

$$x_5(k+1) = T x_6(k) + x_5(k)$$

$$x_6(k+1) = T \left[K_{sp} u(k+1) - 2\omega_n d_m x_6(k) - \omega_n^2 x_5(k) \right] + x_6(k)$$

(3.26)

3.5.2 Matrix Specification

It is important to identify the shape and form of the matrices which are used in the present implementation. The measurement matrix (or H-matrix) having the linear form of $y = Hx$ is one of the three matrices to be determined through experimentation using the three outputs that we measure: chamber one pressure (x_3), chamber two pressure (x_4) and actuator displacement (x_1). As in equations 3.27 and 3.28, the following expressions represent the form of the H matrix and the y vector:

$$H = \begin{bmatrix} 0 & 0 & 1 & 0 & 0 & 0 \\ 0 & 0 & 0 & 1 & 0 & 0 \\ 1 & 0 & 0 & 0 & 0 & 0 \end{bmatrix}_{3 \times 6} \quad (3.27)$$

$$y = \begin{bmatrix} P_1 \\ P_2 \\ x_y \end{bmatrix}_{3 \times 1} \quad (3.28)$$

The other matrices to be determined are the process noise matrix Q and the measurement noise matrix R , both of which are diagonal. Recalling the preliminary

experimental results in section 2.5.1, the MAE values for all three measurable states between the measured and the model-based data, are calculated and summarized in Table 3.1.

Table 3.1: The MAE Value of the Three Measured States

State	Actuator Displacement	Pressure in Chamber 1	Pressure in Chamber 2
Uncertainty Value (MAE)	2.00 mm	0.23 (MPa)	0.24 (MPa)

By examining these uncertainty values (MAE value of the state), the three components of the process noise matrix for the three measurable states can be determined keeping in mind that the covariance value is always square of the uncertainty value of the state. Values for the other components of the matrix are assigned based on the physical characteristic of the related states. The following expression represents the Q-matrix in SI unit:

$$Q = \begin{bmatrix} 10^{-6} & 0 & 0 & 0 & 0 & 0 \\ 0 & 10^{-6} & 0 & 0 & 0 & 0 \\ 0 & 0 & 10^{10} & 0 & 0 & 0 \\ 0 & 0 & 0 & 10^{10} & 0 & 0 \\ 0 & 0 & 0 & 0 & 10^{-8} & 0 \\ 0 & 0 & 0 & 0 & 0 & 10^{-8} \end{bmatrix}_{6 \times 6} \quad (3.29)$$

In order to determine the measurement noise matrix, it is necessary to know the accuracy of the sensors that are used. The SENSOTEC pressure transducer has an accuracy of 1.05×10^5 Pa, and the accuracy of the Temposonics linear displacement transducer (LDT) is calculated to be 2.08×10^{-5} m. Since there are no major sources of noise near

the experimental set-up, the noise level is assumed low. Hence, the following expression is written in SI unit to represent the measurement noise matrix:

$$R = \begin{bmatrix} 10^{10} & 0 & 0 \\ 0 & 10^{10} & 0 \\ 0 & 0 & 10^{-10} \end{bmatrix} \quad (3.30)$$

Before implementing the UKF algorithm on the hydraulic system, according to the block diagram in Figure 3.4, we must initialize the state \hat{x}_0 and the covariance P_0 . The initial state of \hat{x}_0 is defined as a 6th order column vector whose first component value should stay within the range of maximum and minimum values of the actuator displacement $[0, L]$. Accordingly, the third and the fourth components should be within the range of chamber pressures $[P_r, P_s]$. Defining P_0 as a positive-definite matrix, the following expressions are written in SI unit:

$$\hat{x}_0 = [0.025 \quad 0 \quad 9.5 \times 10^6 \quad 10 \times 10^6 \quad 0 \quad 0]$$

$$P_0 = \text{diag}[10^{-10} \quad 10^{-10} \quad 10^{10} \quad 10^{10} \quad 10^{-8} \quad 10^{-8}] \quad (3.31)$$

Now that all the required matrices are defined, the UKF algorithm can be implemented in MATLAB[®] and a trial simulation is run to test the performance of the filter. The results of the residual errors in the system state estimation are presented in Figure 3.5. These plots show the errors in the estimates made by the UKF and the associated plus and minus values of the theoretical standard deviation bounds of the measurements. If the filter has acceptable performance for our nonlinear system, the error should lie within the bounds $[4, 33, 40]$ 68% of the time. By visual inspection, it can be verified that the errors in the UKF consistently lie well within two standard

deviations, and it is concluded that the UKF has satisfactory performance for our nonlinear system.

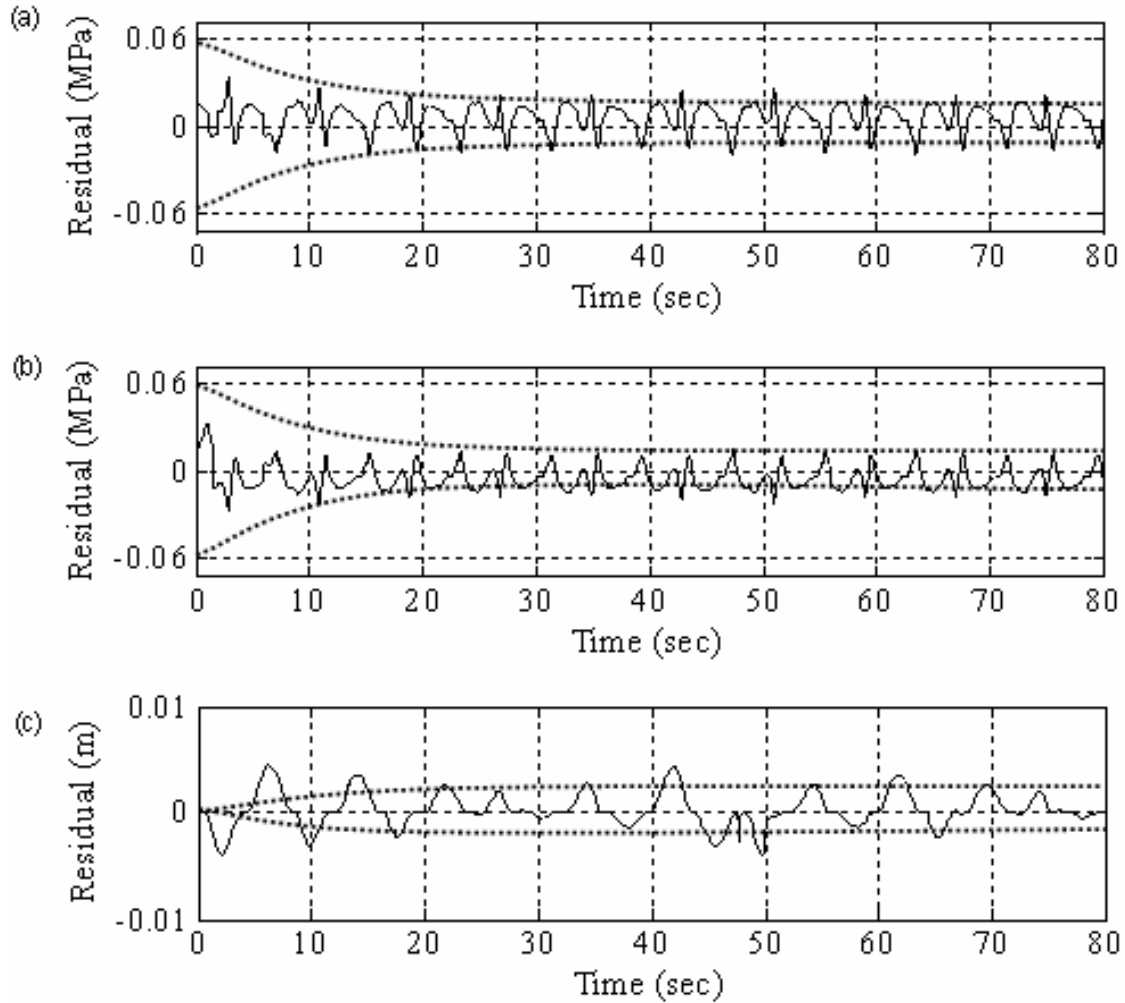


Figure 3.5: System Estimation Error for (a) Pressure in Chamber 1, (b) Pressure in Chamber 2, (c) Actuator Position

Now that all the required matrices are defined, the UKF algorithm can be implemented into the experimental hydraulic system in order to detect and diagnose the system faults. The corresponding experimental results are presented and discussed in the next chapter.

Chapter 4

UKF and Fault Monitoring in Hydraulic Systems

4.1 Introduction

Industries aim to reduce costs associated with operation and maintenance of their machinery and equipment. Cost reductions may be achieved by reducing down time and repair costs and improving the quality of products and services. Use of on-line condition monitoring for detection and diagnosis of faults and malfunctions, leading to condition-based maintenance rather than scheduled (i.e., time-based) maintenance will significantly contribute in achieving this objective. With the evolution of monitoring systems, maintenance and operation personnel are able to concentrate their activities on other tasks with high added value and demand. In particular, continuous on-line monitoring of hydraulic systems provides the means to evaluate the current conditions of the equipment and detect abnormality. It allows corrective measures to be taken to prevent impending failure, and enables proper response to normal and emergency conditions.

Continuous monitoring of a hydraulic system will identify potential problem areas that can lead to substantial equipment damage. Correlation between the pressure measurement and the actuator position would allow abnormal conditions to be identified, which in return would notify operation and maintenance personnel of existence of a potential problem. Further deterioration of the condition could lead to a recommendation to take the equipment out of service for repair and maintenance. The real value of the on-

line monitoring is not in setting off multiple alarms but rather in triggering the maintenance events leading to a true condition-based on maintenance, and providing key answers to implementing the plant assets management.

The four procedures associated with process monitoring are: fault detection, fault identification, fault diagnosis, and process recovery. *Fault detection* means determining whether a fault has occurred. Early detection may provide invaluable warning on emerging problems with appropriate actions to be taken to avoid serious process upset. *Fault identification* is identifying the observation variables most relevant to diagnosing the fault. The purpose of this procedure is to shift the attention of the plant operators and engineers to the subsystems most related to the diagnosis of the fault, so that the effect of the fault could be eliminated in a more efficient manner. *Fault diagnosis* is determining the details of the fault that has occurred (i.e., what component and what possible cause) and *process recovery* is removing the effect of the fault.

In this chapter we present some results obtained through implementation of a UKF filter on the experimental hydraulic system for detection and diagnosis of a set of artificially introduced faults as discussed in Chapter 2. The performance of the developed procedure is studied using these results.

4.2 Experimental Results

In order to carry out fault monitoring experiments using UKF on the hydraulic test rig, a sinusoidal position reference signal $r = 0.025 + 0.0125 \sin(0.4 \pi t)$ is used as in the model discussed in Chapter 2. We have shown using this sinusoidal reference input

signal that the simulated response of the state-space model closely follows that of the actual experimental test rig, under normal operating conditions. However, using the UKF filter, we are able to estimate the state of the system with high precision, enabling fault detection and diagnosis. The overall duration of each test is about 110 seconds and each fault is initiated in the set-up after 50 seconds of the normal machine run and is maintained until the end of the test.

In the present study we monitor the effect of four hydraulic faults in real time. These faults consist of one internal leakage, two external leakages, and frictional build up on the cutter table (carriage). In the following sections, the experimental results of the induced faults are presented and discussed.

4.2.1 Actuator Leakage Faults

In this section experimental results of the internal and external actuator leakage faults will be studied and discussed. The severity of the introduced leakage faults in this study is proportional to the level of opening of the control needle valve, which is categorized into low, medium and high as indicated in Table 4.2-1.

Table 4.1: Severity Categorization of the Leakage Faults

Severity of the Leakage	Number of Opening Turns of Needle Valve
Low	$\frac{1.5}{10}$
Medium	$\frac{3}{10}$
High	$\frac{5}{10}$

4.2.1.1 Actuator External Leakage at Chamber 1

The external leakage occurs at chamber 1 due to either hosing rapture or poor hosing connections, which result in loss of hydraulic fluid. This fault is emulated using a needle vale that returns a portion of the supply pressure from chamber 1 back to the hydraulic tank. The severity of this fault is manually adjusted by turning the knob of the needle valve as specified in Table 4.1. The occurrence of this fault in the system will drop the pressure in chamber 1 and that will create a bigger pressure difference across the chambers 1 and 2. Due to pressure loss in chamber 1 during extraction, the required force to withhold the piston and push it back towards chamber 2 will be reduced. Therefore, the piston will have a shift of few millimeters of towards chamber 1 depending on the severity of the leakage, as shown in Figure 4.1. Due to the existence of a closed-loop controller, the shifting stops after about one cycle and it remains consistent for the entire run of the experiment. A similar outcome is observed for all the three levels of leakage; however, for brevity, only the medium level leakage is discussed in more detail.

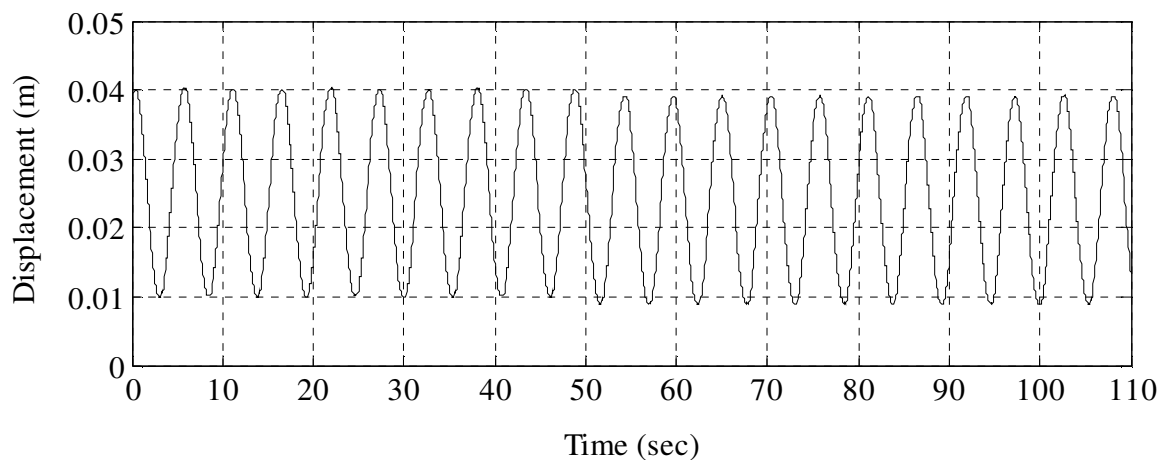


Figure 4.1: Actuator Displacement with Moderate External Leakage at Chamber 1

According to the generated residual error, this pressure drop creates a bigger difference between the actual pressure of the state and the estimated pressure from UKF for chamber 1 than for chamber 2. This phenomenon will become more apparent as the leakage level increases from low to medium and to high. Figures 4.2 to 4.4 show the residual errors calculated for each level of leakage.

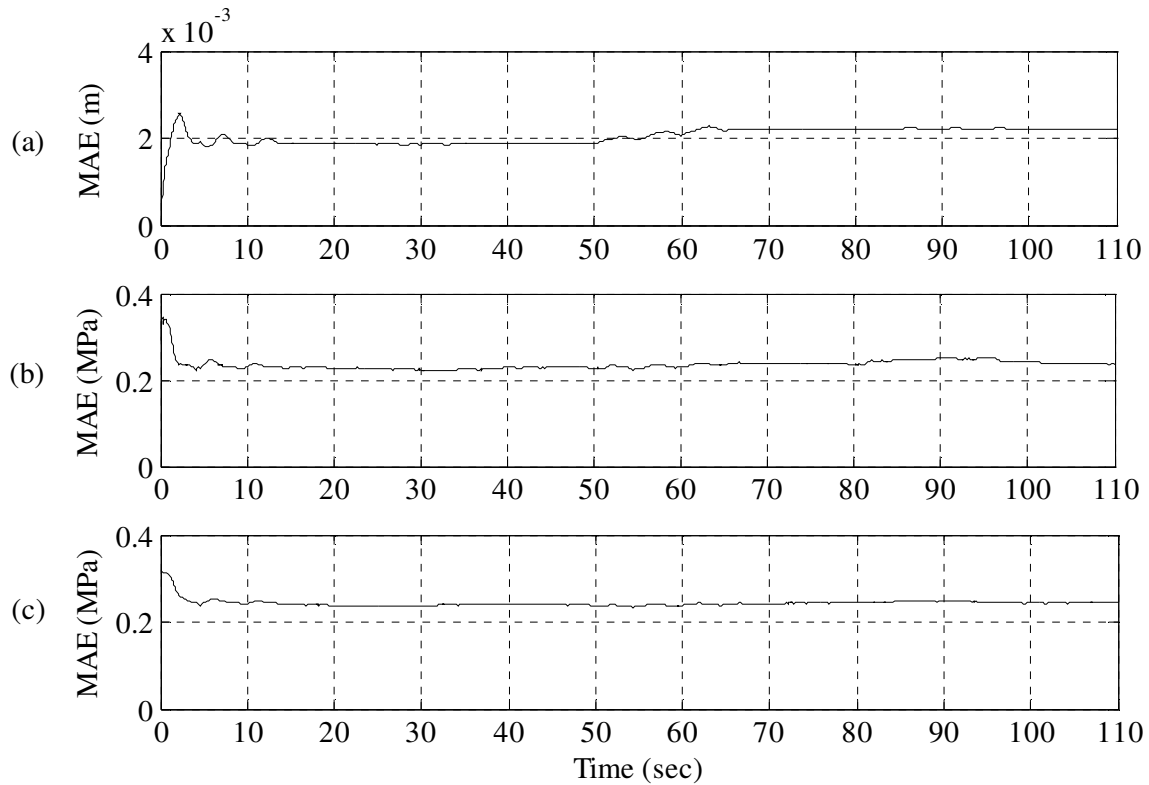


Figure 4.2: Residual Error for Low Leakage at Chamber 1; (a) Actuator Displacement (b) Pressure in Chamber 1; (c) Pressure in Chamber 2

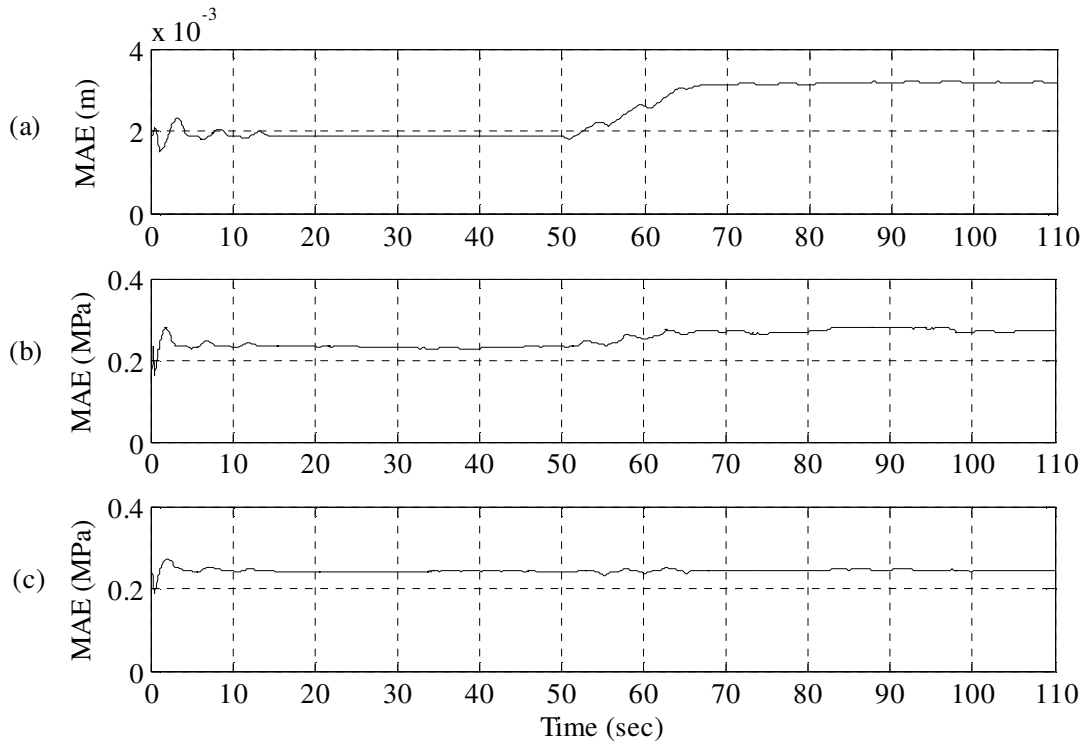


Figure 4.3: Residual Error for Moderate Leakage at Chamber 1; (a) Actuator Displacement (b) Pressure in Chamber 1; (c) Pressure in Chamber 2

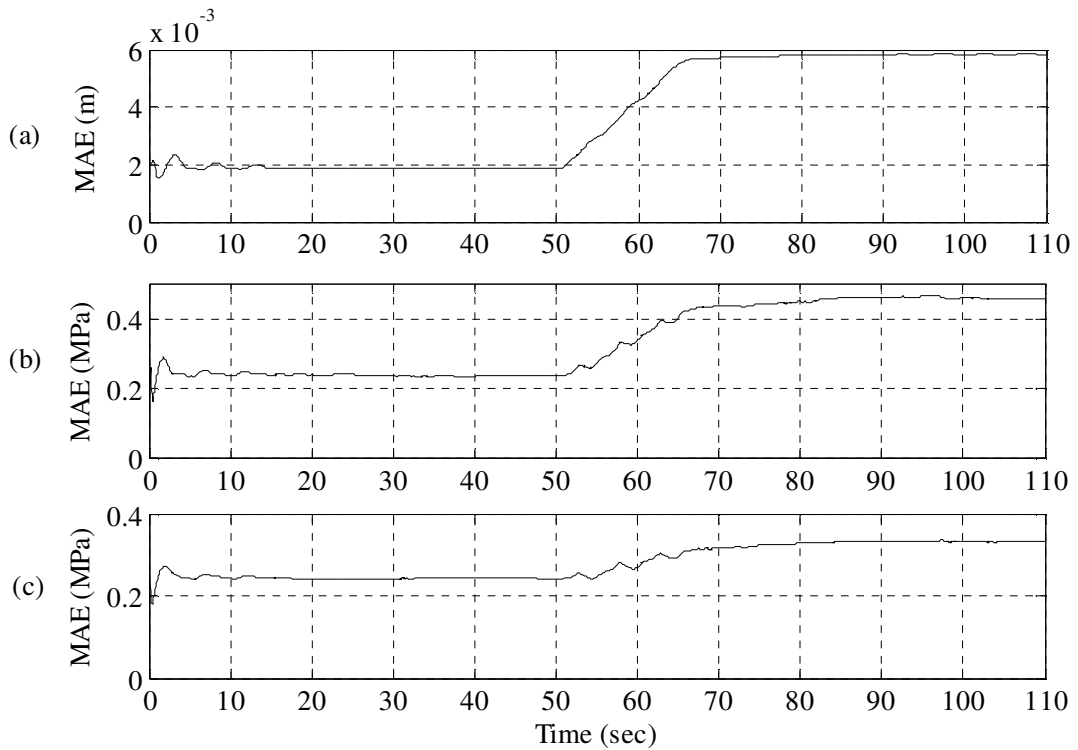


Figure 4.4: Residual Error for High Leakage at Chamber 1; (a) Actuator Displacement (b) Pressure in Chamber 1; (c) Pressure in Chamber 2

For simplicity and clarity of observation and comparison, the results for the corresponding variation of residual MAEs are summarized in Table 4.2. It can be observed that the increase in external leakage at chamber 1, increases the residual error for chamber 1 compared to that of chamber 2. This difference in value increases as the level of leakage increases from low to high.

Table 4.2: External Leakage at Chamber 1 and the Change in MAEs

Fault \ Measurand	Pressure in Chamber 1 (MPa)	Pressure in Chamber 2 (MPa)	Actuator Position (mm)
Leakage at Chamber 1 (low)	0.0169	0.0027	0.33
Leakage at Chamber 1 (medium)	0.0371	0.0028	1.20
Leakage at Chamber 1 (high)	0.220	0.0897	3.95

4.2.1.2 Actuator External Leakage at Chamber 2

In this section the external leakage at chamber 2 is considered. The reasons behind the occurrence of this common fault in hydraulic system are similar to that of the chamber 1 leakage; specifically, hose rupture or loss piping connections. As before, the external leakage fault is emulated by using the connecting hoses and the needle valve mounted on chamber 2 which take the hydraulic fluid back to the tank. Again, the severity of the leakage is manually adjusted by using the designated knob of the needle valve. Due to the characteristic similarities for all three levels of leakage and for brevity, the medium level leakage is discussed in more detail in this section. Figure 4.5 illustrates the hydraulic actuator displacement while a medium level external leakage occurs in chamber 2. As this external leakage occurs during retracting period, chamber 2 sees a

pressure drop and will not have sufficient power to push the piston back towards chamber 1. As a result, a shifting towards chamber 2 is observed. For the same reason as mentioned in previous section, shifting of the piston is completed after about one cycle due to the existence of the closed-loop controller, and the piston remains consistent for the entire run. Comparing Figure 4.1 and Figure 4.5, it can be concluded that the effect of the external leakage at chamber 2 is felt more by the actuator due to the greater shifting that takes place in this chamber. This phenomenon is expected as the pressure in chamber 2 is much greater than that of chamber 1. As a result, more fluid will exit the chamber and back to the tank, at a faster rate.

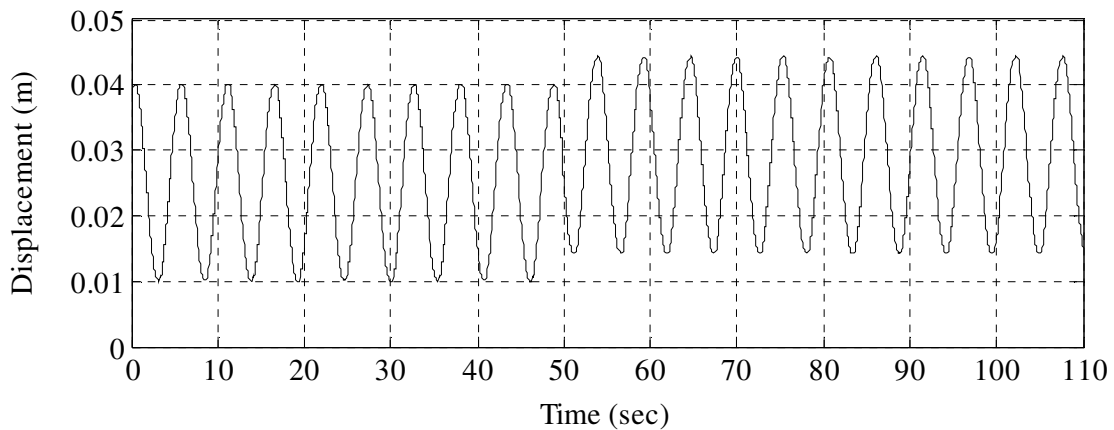


Figure 4.5: Actuator Displacement with Moderate External Leakage at Chamber 2

For further study of the leakage at chamber 2, Figure 4.6 to 4.8 illustrate the changes in residual error that takes place for chambers 1 and 2 as well as the actuator displacement error in three levels of leakage of low, medium and high. From these figures it can be concluded that the leakage at chamber 2 results in greater pressure difference across its chamber compared to that of the pressure difference taking place at chamber 1.

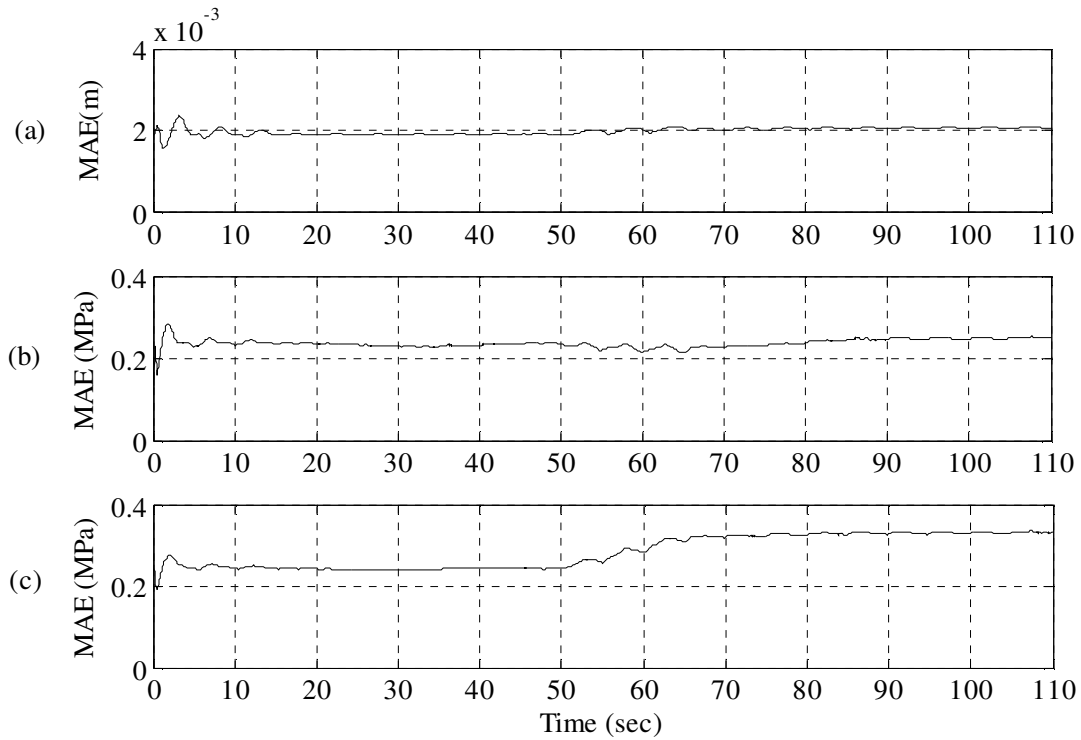


Figure 4.6: Residual Error for Low Leakage at Chamber 2; (a) Actuator Displacement (b) Pressure in Chamber 1; (c) Pressure in Chamber 2

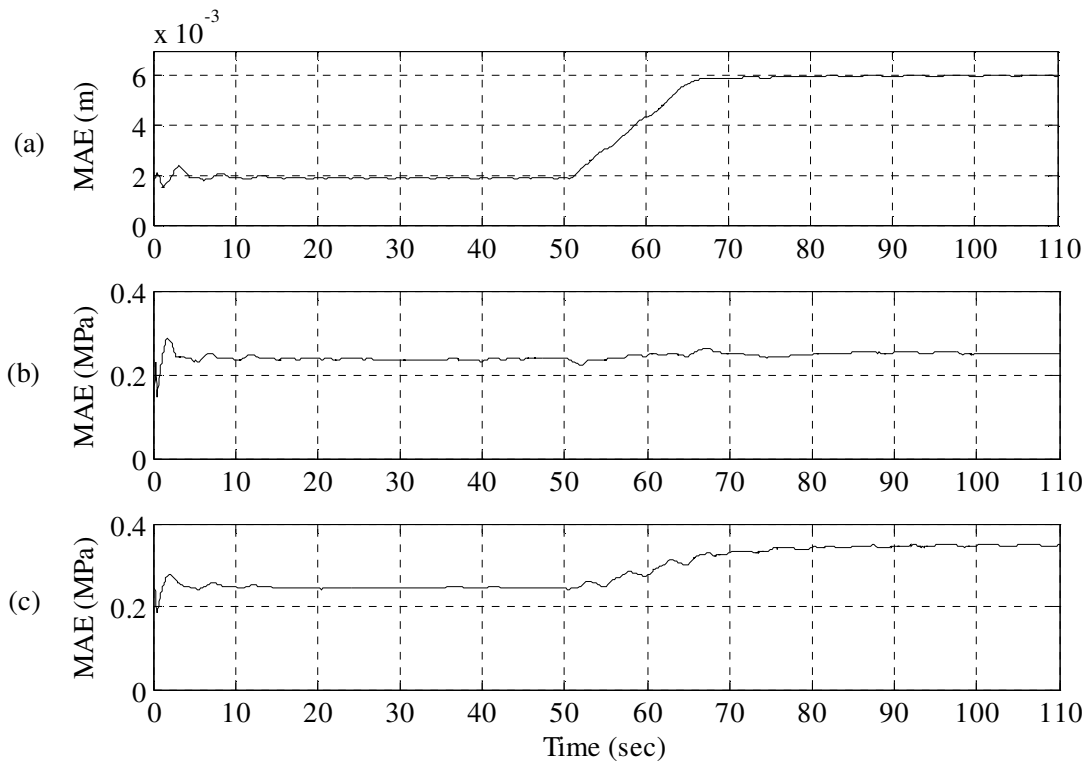


Figure 4.7: Residual Error for Moderate Level Leakage at Chamber 2; (a) Actuator Displacement (b) Pressure in Chamber 1; (c) Pressure in Chamber 2

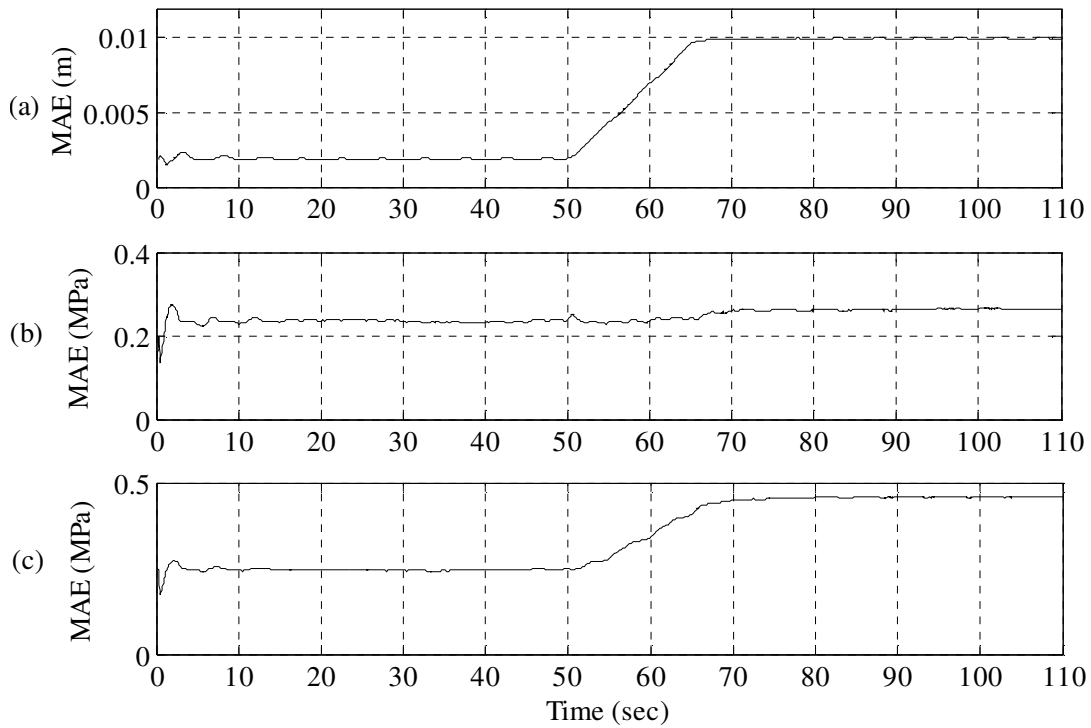


Figure 4.8: Residual Error for High Leakage at Chamber 2; (a) Actuator Displacement (b) Pressure in Chamber 1; (c) Pressure in Chamber 2

Table 4.3 summarizes the results for the corresponding variation of residual MAEs. It can be observed that the occurrence of the external leakage at chamber 2 increases the residual error for this chamber compared to that of chamber 1. This difference in value increases as the level of leakage increases from low to high.

Table 4.3: External Leakage at Chamber 2 and the Change in MAEs

Fault \ Measurand	Pressure in Chamber 1 (MPa)	Pressure in Chamber 2 (MPa)	Actuator Position (mm)
Leakage at Chamber 2 (low)	0.0166	0.088	0.22
Leakage at Chamber 2 (medium)	0.0172	0.106	4.20
Leakage at Chamber 2 (high)	0.0240	0.2170	8.10

4.2.1.3 Actuator Internal Leakage

In this section, the effect of internal leakage on the hydraulic actuator and the necessary steps required to detect the fault using UKF are discussed. There are potential causes that lead to internal leakage of a hydraulic cylinder which essentially leads to improper operation or malfunctioning of the hydraulic actuator. Excessive leakage is a result of the fluid leaking through a piston seal. Damaged or weakened sealant used to seal the piston which prevents the hydraulic fluid from leaking across the chambers as a result of either a worn seal or a worn cylinder barrel, may be the reason. In fact, the most common cause of internal leakage is wear of component surfaces during normal operation. Leakage can also result from poor system design, incorrect component selection, and poor quality control tolerances during the manufacturing of a component, and incorrect overhaul of rebuilt components. Degraded system performance and reliability, and increased operating temperatures are the first visual signs of internal leakage. In hydraulic cylinders, drift or creep in the cylinder rod and the cylinder's inability to hold the designed load will result from increase in leakage.

In this experiment, the severity of the internal leakage is adjusted manually by turning the knob of the designated valve of the hose connecting chamber 1 and 2. As before, the experiment is carried out for the three levels of leakage: low, medium and high by making the corresponding number of turns of the knob. Again due to the similarity in the characteristics of the three leakage levels and for brevity, only the medium leakage level is discussed in more detail. Figure 4.9 illustrates the actuator displacement while a medium internal leakage takes place. This case has similar behavior to that of chamber 2. Upon the occurrence of the internal leakage, the piston

shifts more towards chamber 2 which has a higher pressure. Internal leakage reduces the pressure difference between the two chambers. The chamber with more effective area (chamber 1) exerts greater force on the piston and consequently, it shifts towards the other chamber with a lower effective area (chamber 2). For the same reason as mentioned in previous sections, the shifting of the piston is completed after about one cycle due to the existence of the closed-loop controller, and it remains consistent for the entire run.

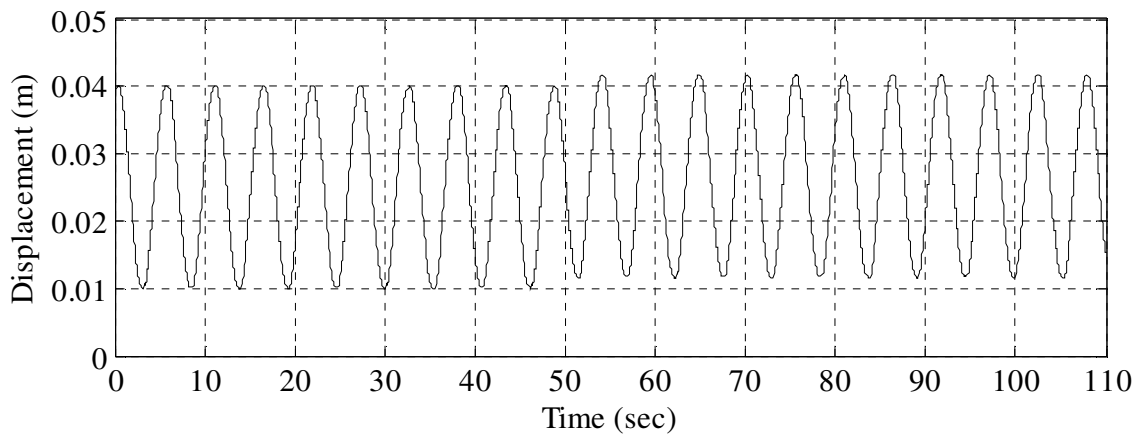


Figure 4.9: Actuator Displacement with Moderate Internal Leakage

Figure 4.10 to 4.12 illustrate the changes in the residual error for chambers 1 and 2 as well as the actuator displacement error at low, medium and high levels of leakage. From these figures it can be concluded that the internal leakage results in an increase in MAEs of all the measurements. In addition, the change in MAE of the actuator displacement is more than the change in MAE of the chamber pressure.

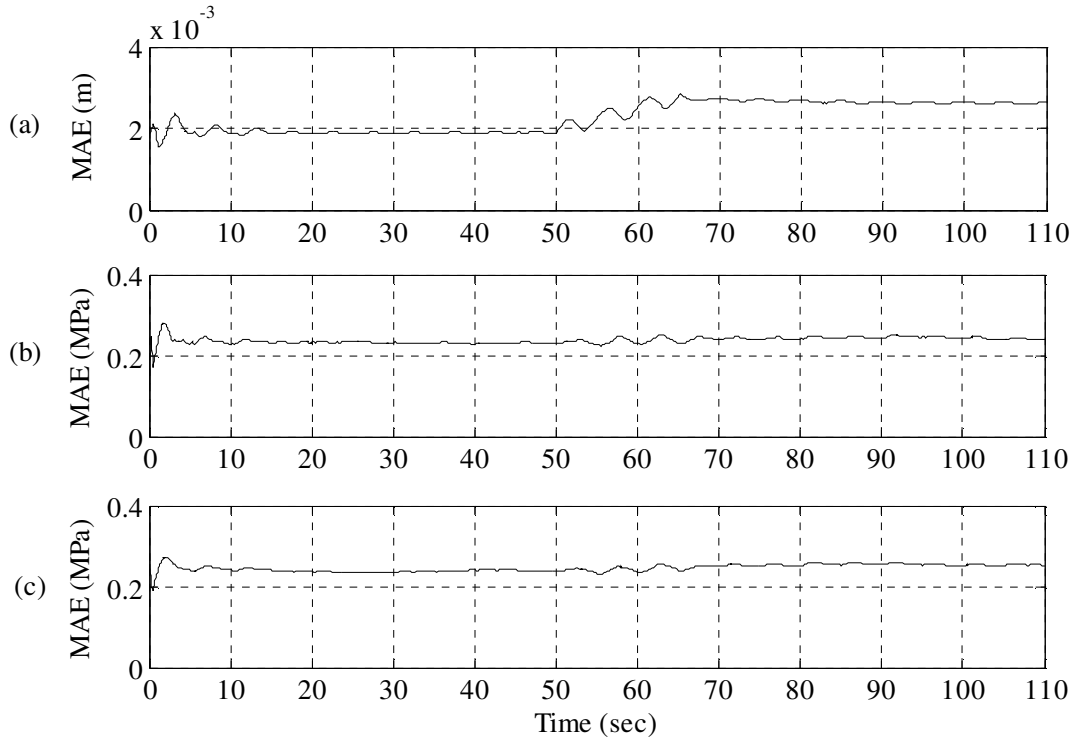


Figure 4.10: Residual Error for Low Internal Leakage; (a) Actuator Displacement (b) Pressure in Chamber 1; (c) Pressure in Chamber 2

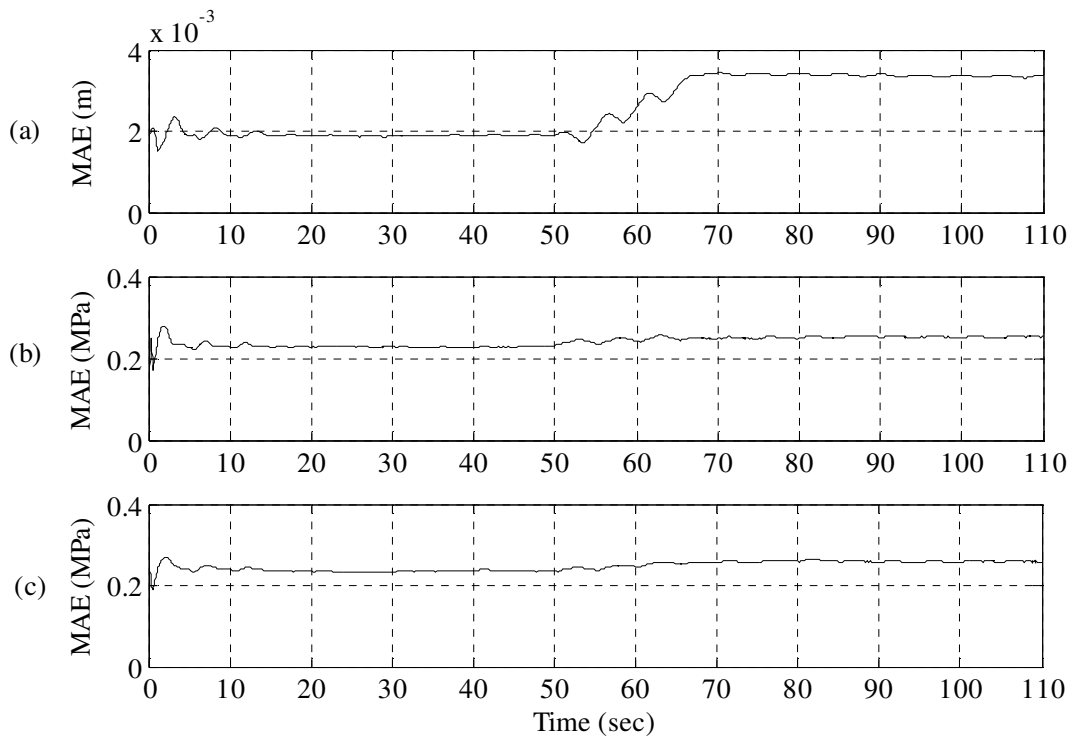


Figure 4.11: Residual Error for Moderate Internal Leakage; (a) Actuator Displacement (b) Pressure in Chamber 1; (c) Pressure in Chamber 2

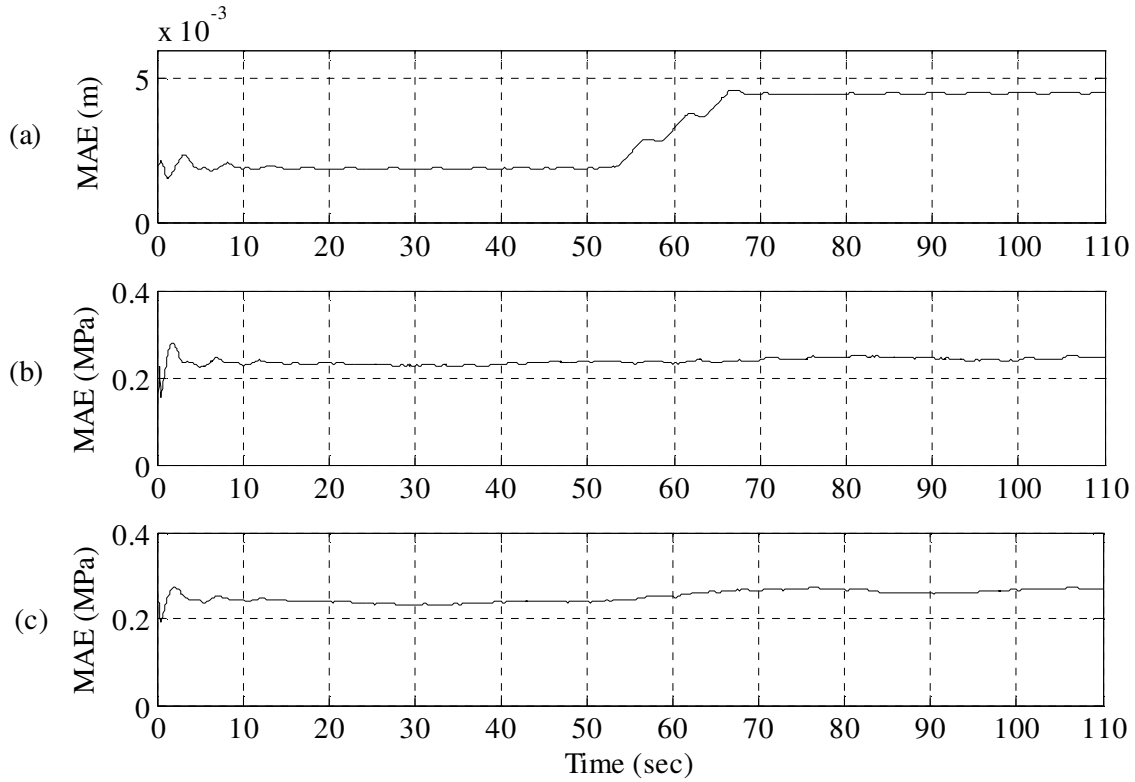


Figure 4.12: Residual Error for High Internal Leakage; (a) Actuator Displacement (b) Pressure in Chamber 1; (c) Pressure in Chamber 2

Table 4.4 summarizes the results for the corresponding variation of residual MAE. Note that the increase in MAEs of chambers 1 and 2 are always within the same order of magnitude. The MAE for actuator position increases as the leakage level increases from low to high. Therefore, the amount of displacement occurring can determine the leakage severity.

Table 4.4: Internal Leakage and the Change in MAEs

Measurand Fault	Pressure in Chamber 1 (MPa)	Pressure in Chamber 2 (MPa)	Actuator Position (mm)
Internal Leakage (low)	0.015	0.012	0.78
Internal Leakage (medium)	0.028	0.024	1.51
Internal Leakage (high)	0.020	0.025	2.60

4.2.1.4 Dry Friction of the Cutter Table

One of the challenges with our industrial machine is the necessary and adequate lubrication of the moving surfaces of the cutter table, which is important for accurate response to the cutting control signals. If adequate lubrication is not present at the sliding surface of the cutter carriage, the cutter table may not reach the correct position at the correct time for cutting the fish head. A positioning delay of a fraction of a second can cause serious problems in the cutting operation. For example, the cut will take place at different parts of the fish body, resulting in meant wastage or degraded product quality. If the system can detect inadequate lubrication and resulting friction build-up on the cutter table surface, it can inform the operator for corrective action. It is important to detect this problem as soon as possible in order to prevent excessive heat generation and material wear, as the heavy table slides on top of the metal plate underneath it.

For this study, an experiment is carried using the implemented UKF, with lubrication-free surface of the cutter table. For the first 50 seconds, the table is run under normal conditions. From then on, the table is maintained in a lubrication-free (dry) condition until the end of the run.

Figure 4.13 illustrates the hydraulic actuator displacement while the dry friction build up takes place on the surface of the cutter table. Due to this, the actuator movement is restricted and it falls short of reaching the designated location which is the gill of the fish.

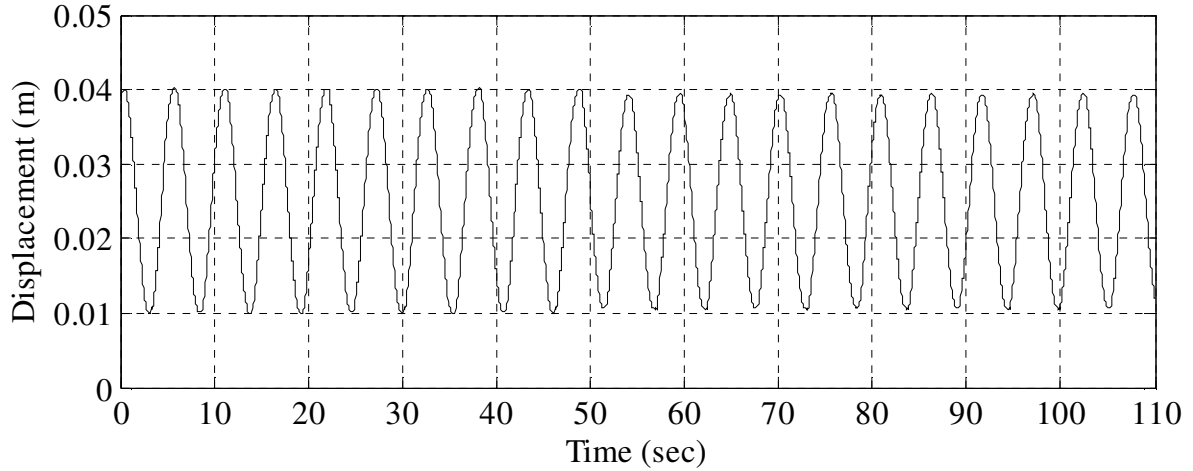


Figure 4.13: Actuator Displacement with Dry Friction Build-up

Figure 4.14 shows the residual error signals due to the dynamic friction load. It can be visually observed that the residual error of the actuator position increases much more than that of the pressures in chambers 1 and 2.

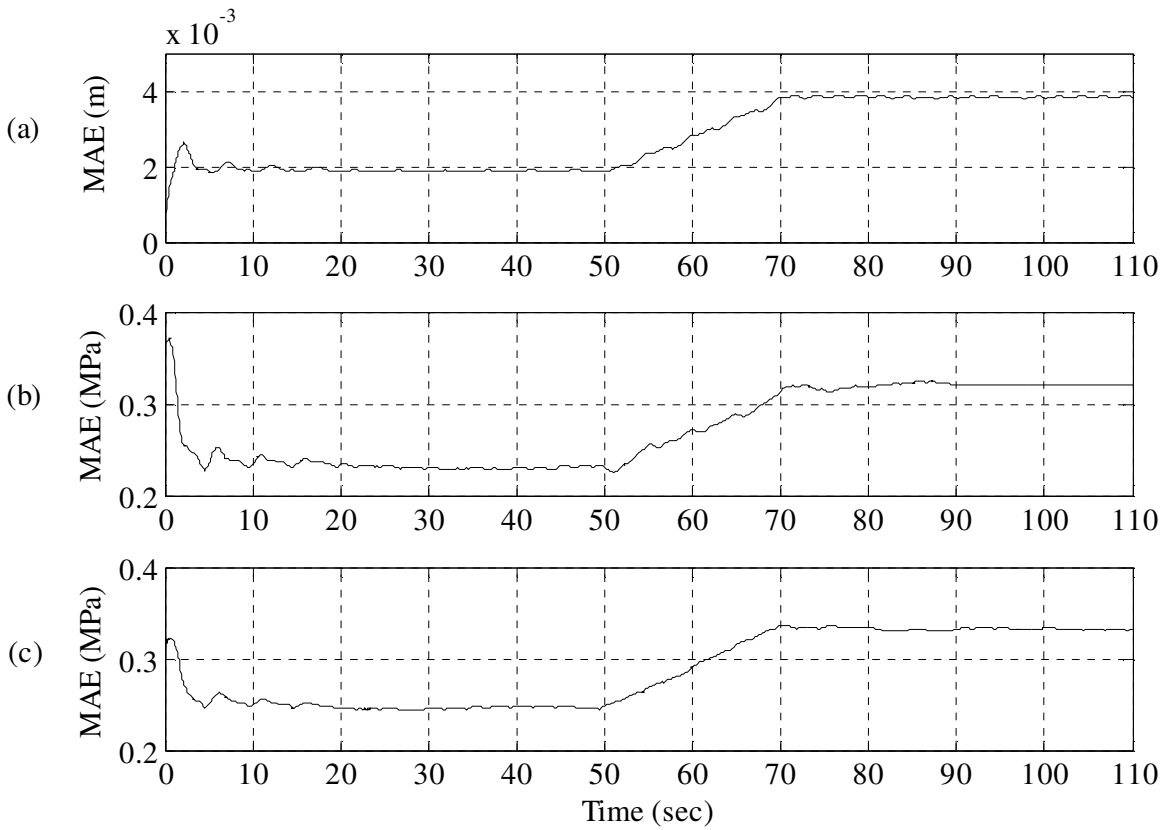


Figure 4.14: Residual Error for Dry Friction Build-up; (a) Actuator Displacement (b) Pressure in Chamber 1; (c) Pressure in Chamber 2

Figure 4.5 presents the variation of the residual MAEs. It can be seen that both pressure residual errors are increased and have stayed within the same order of magnitude. Also the increase in actuator displacement MAE is the largest among the three.

Table 4.5: Dry Friction Build-up and the Change in MAEs

Measurand Fault	Pressure in Chamber 1 (MPa)	Pressure in Chamber 2 (MPa)	Actuator Position (mm)
Dry Friction	0.092	0.085	1.98

4.3 Fault Diagnosis and Discussion

In section 4.2, the proposed UKF was implemented in the hydraulic system of the industrial machine for on-line monitoring fault detection and diagnosis of the system. The experimental results were presented for two external leakages, one internal leakage, and dry friction fault in the cutter carriage. In order to accurately diagnose the occurring fault in the system, there are three main factors that should be considered. These factors are the change in the residual MAEs of chamber pressures and actuator displacement. In this section each fault is discussed individually and a method of drawing a conclusion on whether that particular fault is taking place is introduced. Table 4.6 summarizes the measurements obtained from our fault monitoring scheme, which was introduced in section 4.2, for the industrial machine.

Table 4.6: Summary of the Increase in MAEs due to Fault Occurrence

Fault \ Measurand	Pressure in Chamber 1 (MPa)	Pressure in Chamber 2 (MPa)	Actuator Position (mm)
Leakage at Chamber 1 (low)	0.0169	0.0027	0.33
Leakage at Chamber 2 (low)	0.0166	0.088	0.22
Internal Leakage (low)	0.015	0.012	0.78
Leakage at Chamber 1 (medium)	0.0371	0.0028	1.20
Leakage at Chamber 2 (medium)	0.0172	0.106	4.2
Internal Leakage (medium)	0.028	0.024	1.51
Leakage at Chamber 1 (high)	0.22	0.0897	3.95
Leakage at Chamber 2 (high)	0.0240	0.2170	8.10
Internal Leakage (high)	0.020	0.025	2.60
Dry Friction	0.092	0.085	1.98

Leakage at Chamber 1

From Table 4.6 it can be concluded that for any level of leakage at chamber 1, the increase in MAE of the pressure in chamber 1 is much greater than that of chamber 2. The estimated difference between the values for these two chambers is almost three times

in the case of low leakage and this difference increases with the severity of the leakage. In particular, in case of external leakage at chamber 1, an increase in MAE of the pressure in chamber 1 is always at least 14 KPa higher than the increase in MAE of the pressure in chamber 2. In addition, the MAE increases for actuator displacement by about 3 times that for the previous level, for successively higher levels of leakage. Therefore, the intensity of the leakage at chamber 1 can be estimated by considering all these increases in MAEs and by observing the amount of residual error increments.

Leakage at Chamber 2

From Table 4.6 and comparing the increase in MAEs for the leakage at chamber 2, it can be concluded that regardless of any other criterion of variation, in the case of having a leakage at chamber 2, the MAE increase in pressure in chamber 2 is almost five times greater (70 KPa) than the MAEs increase in pressure in chamber 1. For instance, consider a medium leakage at chamber 2. It is evident that increase in MAE of the pressure in chamber 2 is about 89 KPa greater (about 6 times) than the MAE of the pressure in chamber 1. Comparing the change in MAEs of the actuator, the increase in displacement is about 4 mm as we move up from low to medium and to high levels of leakage at chamber 2. If the residual MAEs for chamber 2 is greater and that an increase in MAE of the actuator is taking place, the operator should be able to detect and estimate the leakage at chamber 2 by observing the residual error increments.

Internal Leakage and Dry Friction

Referring to Table 4.6, in the event of an internal leakage or dry friction build-up, the MAEs for both pressures in chambers 1 and 2 grow identically and stay within a same order. In view of this, it is hard for the operator to distinguish between which fault is occurring in the system; therefore, further criteria are needed.

In section 4.2.1.3 we discussed that in the case of internal leakage, the actuator movement has a shift towards chamber 2 due to having less effective area and thus a smaller force is exerted on the piston. Additionally, as shown in Figure 4.15, the pressure transducers will detect a decrease in pressures for both chambers 1 and 2. By considering these three criteria: MAEs of pressures for both chambers grow equally, actuator shifts towards chamber 2, and chamber pressures drop; the occurrence of an internal leakage in the system should be detectable. However, the severity of the leakage should be estimated based on the MAE of the actuator displacement, which increases by about 1 mm with each increasing level of leakage from low to medium to high.

As for detecting a dry friction build-up, recalling section 4.2.1.4, the actuator displacement plot reduces in magnitude due to restricted movement caused by friction build-up on the surface of the table. To compensate for the external force, higher pressures are applied on the actuator as shown in Figure 4.16. For easier examination of the increase in pressure of chambers, a close-up plot is shown in Figure 4.17. It follows that, increase in chamber pressures, reduce in displacement magnitude, and equal increase in MAEs of pressure for both chambers, will enable the operator to detect a fault of dry friction.

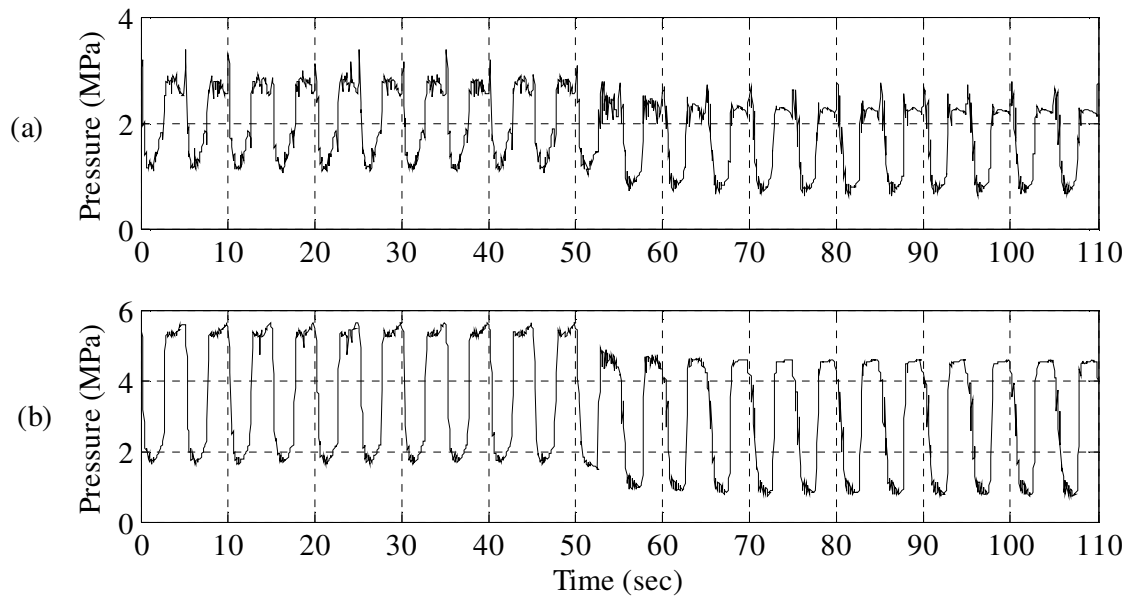


Figure 4.15: Chambers Pressure Characteristics under High Internal Leakage; a) Pressure in Chamber 1, and b) Pressure in Chamber 2

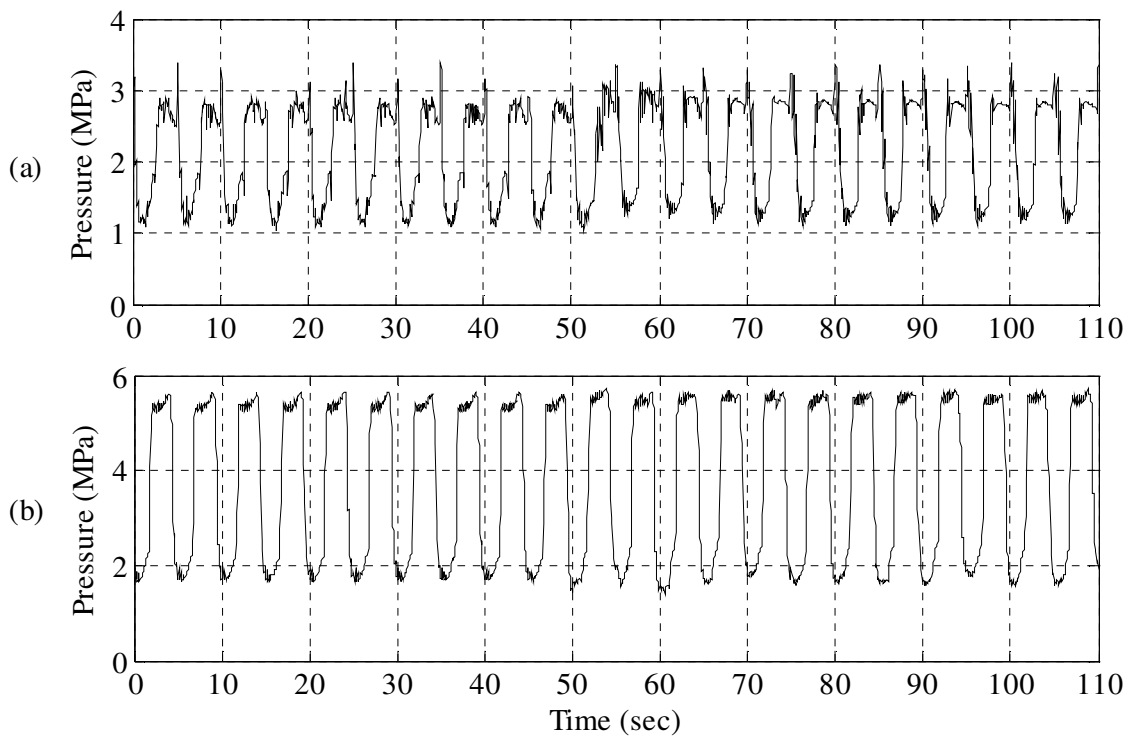


Figure 4.16: Chambers Pressure Characteristics under Dry Friction; a) Pressure in Chamber 1, and b) Pressure in Chamber 2

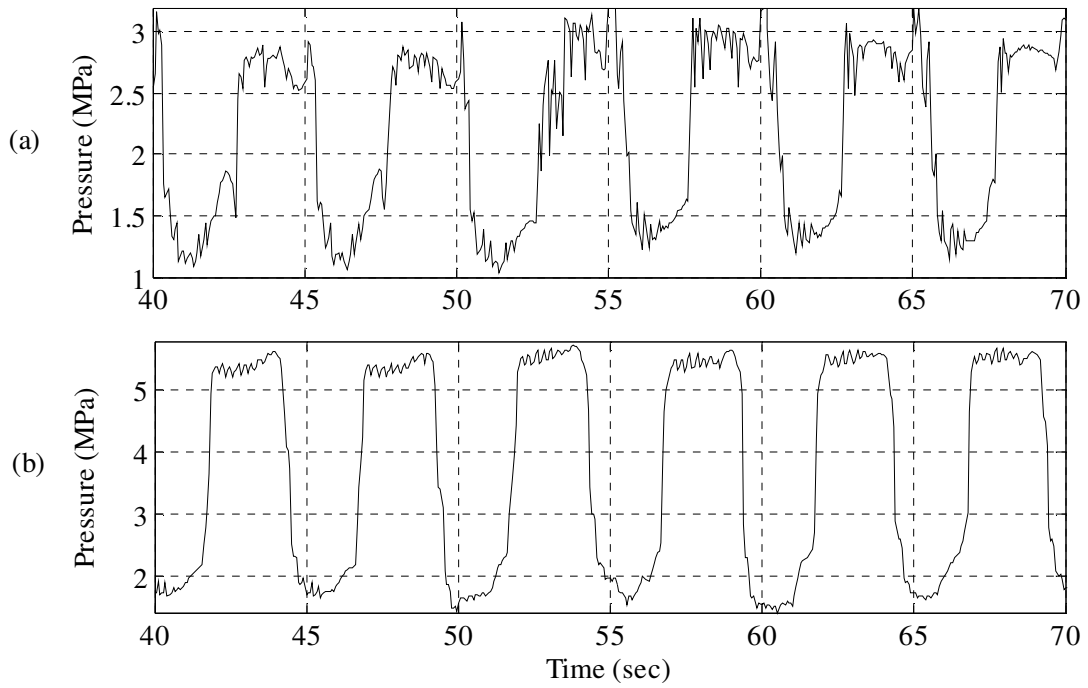


Figure 4.17: Zoomed-in Chamber Pressure Characteristics Plot under Dry Friction; a) Pressure in Chamber 1, and b) Pressure in Chamber 2

Chapter 5

Conclusion

5.1 Summary

In this thesis, a model-based online condition monitoring scheme using Unscented Kalman Filter (UKF) was developed, implemented on the hydraulic system of an automated industrial fish processing machine, and tested. The hydraulic test rig and its subsystem components were described. A nonlinear state-space model of the system was developed and validated through experimentation. Based on an extensive literature review, four common hydraulic actuator faults were chosen and artificially introduced to the system. Tests were carried out and based on the results, it was indicated how the faults could be diagnosed.

A requirement for the method developed in the present work is an accurate model of the system. Therefore the system was carefully inspected and a 6th order nonlinear state-space model was derived for use in the UKF algorithm. The six state variables are the actuator displacement and velocity, pressures in chambers 1 and 2, and the displacement and velocity of the servo-valve spool. The state-space model had both known and unknown parameters. The known parameters were chosen from either previously available information on the machine or by direct measurement. The unknown parameters were determined by carrying out a sequence of experiments. The state-space model was then validated by comparing the simulated response to the actual

response measured directly from the machine, for a sinusoidal position reference signal. The validation results showed that under normal operating conditions the state-space model closely represented the actual system as it converged to the corresponding set-up features.

In general, the thesis described important contributions of Kalman filtering in fault monitoring and diagnosis. The general algorithms of Kalman filter and Extended Kalman Filter (EKF) were described and some of their draw backs were discussed, which lead led to the introduction of the need for UKF. It was shown that UKF was more reliable and provided better performance over EKF in estimating the states of a nonlinear system.

The faults studied in the thesis are:

- 1) External leakage at chamber 1 of hydraulic cylinder
- 2) External leakage at chamber 2 of hydraulic cylinder
- 3) Internal leakage inside the hydraulic cylinder
- 4) Dry friction build-up on the surface of the cutter table (carriage)

The developed UKF methodology for fault monitoring system was tested in the physical hydraulic system of the automated fish cutting machine, for each of the four faults. Leakage faults were introduced using externally mounted needle valves, at three different levels of leakage from low to medium to high. The UKF scheme correctly identified the state of the system and generated a residual error given by the difference between the measured and the predicted outputs. The three outputs measured in this experiment were, the pressures in chambers 1 and 2 and the actuator displacement. For observation and presentation of the data trend, the moving average error (MAE) for each measurement

was calculated. It was shown that in order to draw the best possible conclusion on which fault was occurring and its level of severity, three criteria had to be taken into account. These criteria were the residual MAEs of the chamber pressures and the actuator displacement, the change in pressure in chambers 1 and 2, and characteristics of the actuator displacement.

The main contributions of the thesis, which have an impact on the field of fault monitoring and diagnosis of industrial hydraulic systems, are summarized below:

- A nonlinear state-space model was developed for the hydraulic positioning system of an industrial fish cutting machine, and was validated through experimentation. The response of the model converged within 10% of the actual measurements.
- A UKF scheme was developed and successfully implemented on the automated fish processing machine for online condition monitoring.
- The UKF scheme was able to accurately distinguish between different types of leakage faults (external and internal leakages at chambers 1 and 2) and the level of their severities.
- Detecting dry friction build-up in industrial machines is a rather challenging task. The UKF scheme developed in the present work was able to successfully and reliably detect this fault in a hydraulic positioning system

5.2 Suggestions for Future Work

Fault diagnosis of nonlinear systems using model-based techniques is a vast area of research in the field of control and automation. The following suggestions may be considered as possible future work for the improvement of fault diagnosis of the fish processing machine.

- To be able to accurately diagnose faults in the automated industrial machine, the developed UKF scheme should be extended to other parts of the system. This will require accurate modeling of the entire system with appropriate estimation of their parameters (in particular, the entire hydraulic system including hydraulic pump, motor and hosing).
- There are many other faults that may be introduced into the system to examine the effectiveness of the developed condition monitoring scheme. It is essential to develop a technique that is able to distinguish between different faults when considering the entire hydraulic system.
- This UKF scheme should be further improved for accurate diagnosing of multiple faults occurring simultaneously in the system.
- The present UKF scheme detects and diagnoses faults in the hydraulic positioning system of the automated fish cutting machine. An expert system may be designed and implemented in order to select the most appropriate action to resolve the occurring faults. For system maintenance, this expert

system should be able to make decisions based on the history of the previous repair done on the machine.

References

- [1] Merritt, H.E., 1967, *Hydraulic Control Systems*, John Wiley and Sons Inc, New York, NY.
- [2] Tafazoli, S., 1997, "Identification of Frictional Effects and Structural Dynamics for Improved Control of Hydraulic Manipulators," PhD Dissertation, University of British Columbia, Vancouver, Canada, pp. 1-41.
- [3] Gertler, J., 1998, *Fault Detection and Diagnosis in Engineering Systems*, CRC Press, Boca Raton, FL.
- [4] Sepasi, M., 2007, "Fault Monitoring in Hydraulic Systems using Unscented Kalman Filter," MSc Dissertation, University of British Columbia, Vancouver, Canada.
- [5] Manring, N., 2005, *Hydraulic Control Systems*, John Wiley and Sons Inc, Hoboken, NJ.
- [6] Stringer, J., 1976, *Hydraulic Systems Analysis: An Introduction*, John Wiley & Sons, New York, NY.
- [7] de Silva, C.W., 2007, *Sensors and Actuators: Control Systems Instrumentation*, Taylor & Francis, CRC Press, Boca Raton, Florida.
- [8] Majumdar, S.R., 2002, *Oil Hydraulic Systems: Principles and Maintenance*, McGraw-Hill Publishing Company, New York, NY.
- [9] Henke, R., 1987, "Hydraulic System Trends: PART IX Leakage Control: Practice & Product," *Diesel Progress North American*, 53(12), pp. 36-39.

[10] An, L. and Sepehri, N., 2008, "Leakage Fault Detection in Hydraulic Actuators Subject to Unknown External Loading," *International Journal of Fluid Power*, 9(2), pp. 15-25.

[11] An, L. and Sepehri, N., 2006, "Hydraulic Actuator Leakage Quantification Scheme Using Extended Kalman Filter and Sequential Test Method," *Proc. 2006 American Control Conference*, Institute of Electrical and Electronics Engineers, Inc, Piscataway, NJ, pp. 4424-4429.

[12] Werlefors, M., and Medvedev, A., 2008, "Observer-based Leakage Detection in Hydraulic Systems with Position and Velocity Feedback," *Proc. 17th IEEE International Conference on Control Applications*, Institute of Electrical and Electronics Engineers Inc, New York, NY, pp. 948-953.

[13] Zhang, Z., Fu, Z., and Chen, Z., 1998, "Leakage Fault Diagnosis of the Hydraulic System Based on the BP Neural Network," *Mechanical Science and Technology*, 17(1), pp. 116-118.

[14] El-Betar, A., Abdelhamed, M. M., El-Assal, A., 2006, "Fault Diagnosis of a Hydraulic Power System using an Artificial Neural Network," *JKAU: Eng. Sci.*, 17(1), pp. 117 - 137.

[15] Vossoughi, R. and Donath, M., 1992, "Dynamic Feedback Linearization for Electrohydraulically Actuated Servosystems," *Proc. 1992 Japan - USA Symposium on Flexible Automation*, Part 1, San Francisco, CA, USA, July 1992, ASME, New York, NY, pp. 595-606.

[16] Armstrong-Helouvry, B., Dupont, P., and Wit, C. D., 1994, "Survey of Models, Analysis Tools and Compensation Methods for the Control of Machines with Friction," *Automatica*, 30(7), pp. 1083-1138.

[17] Acho, L., Iurian, C., Ikhouane, F., 2007, "Robust-Adaptive Control of Mechanical Systems with Friction: Application to an Industrial Emulator," *American Control Conference*, July 2007, Institute of Electrical and Electronics Engineers Inc, New York, NY, pp. 5970-5974.

[18] de Wit, C. C., Olsson, H., Astrom, K. J., 1995, "New Model for Control of Systems with Friction," *IEEE Transactions on Automatic Control*, 40(3) pp. 419-425.

[19] Bonchis, A., Corke, P. I., and Rye, D. C., 1999, "Pressure-Based, Velocity Independent, Friction Model for Asymmetric Hydraulic Cylinders," *Proc. IEEE International Conference on Robotics and Automation*, Detroit, MI, pp. 1746-1751.

[20] Kitching, R. and Gleaves, J. S., 1968, "Static Friction between a Cup Leather Seal and a Cylinder Wall," *International Journal of Mechanical Sciences*, 10(10) pp. 783-784, IN1-IN4, 785-801.

[21] Karnopp, D., 1985, "Computer Simulation of Stick-Slip Friction in Mechanical Dynamic Systems," *Journal of Dynamic Systems, Measurement and Control*, Transactions of the ASME, 107(1), pp. 100-103.

[22] Laval, L., M'Sirdi, N. K., and Cadiou, J., 1996, "H-infinity Force Control of a Hydraulic Servo-actuator with Environmental Uncertainties," Part 1 (of 4), *Robotics and Automation*, Minneapolis, MN, April 1996, IEEE, New York, NY, pp. 1566-1571.

[23] Isermann, R., 2006, *Fault-Diagnosis Systems: An Introduction from Fault Detection to Fault Tolerance*, Springer, New York, NY, pp. 475.

[24] Isermann, R., 1995, "Model-Base Fault Detection and Diagnosis Methods," *Proc. American Control Conference*, Seattle, WA, June 1995, pp. 1605-1609.

[25] Patton, R. J., 1997, "Fault Tolerant Control Systems: The 1997 Situation," *Proc. IFAC Symposium on Fault Detection Supervision and Safety for Technical Processes*, Hull, UK, pp. 1033-1054.

[26] Patton, R. J. and Chen, J., 1996, "Robust Fault Detection and Isolation (FDI) systems", *Control and Dynamic Systems*. C. Leondes, Ed., pp. 171-224, Mita Press, Hull, U.K.

[27] De Silva, C.W., 2009, *Modeling and Control of Engineering Systems*, Taylor & Francis, CRC Press, Boca Raton, FL.

[28] Chow, E. Y. and Willsky, A. S., 1984, "Analytical Redundancy and the Design of Robust Failure Detection Systems," *IEEE Transactions on Automatic Control*, 29(7), pp. 603-614.

[29] Kosebalaban, F. and Cinar, A., 2001, "Integration of Multivariate SPM and FDD by Parity Space Technique for a Food Pasteurization Process," *Computers and Chemical Engineering*, 25(2-3), pp. 473-491.

[30] J. Shiozaki, H. Matsuyama, E. O'Shima, and M. Ira, 1979, "An Algorithm for Diagnosis of System Failures in the Chemical Process". *CACE '79*, Switzerland, pp. 489-493.

[31] Karray, F and de Silva, C.W., 2004, *Soft Computing and Intelligent Systems Design*, Addison-Wesley, New York, NY.

[32] De Silva, C.W., 1995, *Intelligent Control: Fuzzy Logic Applications*, CRC Press, Boca Raton, FL.

[33] Zarchan, P. and Musoff, H., 2005, *Fundamentals of Kalman Filtering: A Practical Approach*, AIAA, Reston, VA, pp. 129-140.

[34] Zheng, Y., Fang, H., and Wang, Y., 2004, "Kalman filter based FDI of networked control system," *Proc. Fifth World Congress on Intelligent Control and Automation*, Hangzhou, China, June 2004, Institute of Electrical and Electronics Engineers Inc, New York, Y., pp. 1330-1333.

[35] Pirmoradi, F., Sassani, F., and De Silva, C. W., 2007, "An Efficient Algorithm for Health Monitoring and Fault Diagnosis in a Spacecraft Attitude Determination System," *Proc. IEEE International Conference on Systems, Man, and Cybernetics*, Montreal, QC, Canada, October 2007, Institute of Electrical and Electronics Engineers Inc, New York, NY, pp. 4024-4030.

[36] Xue, W., Guo, Y., and Zhang, X., 2007, "A Bank of Kalman Filters and a Robust Kalman Filter Applied in Fault Diagnosis of Aircraft Engine Sensor/Actuator," *2nd International Conference on Innovative Computing, Information and Control*,

Kumamoto, Japan , September 2007, Institute of Electrical and Electronic Engineers, New York, NY, pp. 10-11.

[37] Julier, S. J. and Uhlmann, J. K., 1997, "New Extension of the Kalman Filter to Nonlinear Systems," *Proc. Signal Processing, Sensor Fusion, and Target Recognition*, April 1997, Society of Photo-Optical Instrumentation Engineers, Orlando, FL, pp. 182-193.

[38] Julier, S. and Uhlmann, J., 2004, "Unscented Filtering and Nonlinear Estimation," *Proceedings of the IEEE*, 92(3), pp. 401-422.

[39] Romanenko, A. and Castro, J. A. A. M., 2004, "The Unscented Filter as an Alternative to the EKF for Nonlinear State Estimation: A Simulation Case Study," *Computers and Chemical Engineering*, 28(3), pp. 347-355.

[40] Julier, S. J. and Uhlmann, J., 2000, "New Method for the Nonlinear Transformation of Means and Covariances in Filters and Estimators," *IEEE Transactions on Automatic Control*, 45(3), pp. 477-482.

[41] Julier, S. J., Uhlmann, J., and Durrant-Whyte, H., 1995, "A New Approach for Filtering Nonlinear Systems," *Proc. American Control Conference*, Seattle, WA, pp. 1628-32.

[42] Simon, D., 2006, *Optimal State Estimation: Kalman, H-Infinity, and Nonlinear Approaches*, Wiley-Interscience, Hoboken, NJ, pp. 433-458.

[43] Wan, E. and Van der Merwe, R., 2001, *The Unscented Kalman Filter*, John Wiley and Sons, New York, NY.